Auxiliary Space Preconditioners for SIP-DG Discretizations of H(curl)-elliptic Problems with Discontinuous Coefficients

Blanca Ayuso de Dios[*], Ralf Hiptmair[†], Cecilia Pagliantini[‡]

Abstract

We propose a family of preconditioners for linear systems of equations arising from a piecewise polynomial symmetric Interior Penalty Discontinuous Galerkin (IP-DG) discretization of $\mathrm{H}(\mathbf{curl}, \Omega)$-elliptic boundary value problems on conforming meshes. The design and analysis of the proposed preconditioners relies on the auxiliary space method (ASM) employing an auxiliary space of $\mathrm{H}(\mathbf{curl}, \Omega)$-conforming finite element functions together with a relaxation technique (local smoothing). On simplicial meshes, the proposed preconditioner enjoys asymptotic optimality with respect to mesh refinement. It is also robust with respect to jumps in the coefficients ν and β in the second and zeroth order parts of the operator, respectively, except when both coefficients are discontinuous and the problem is curl-dominated in some regions and reaction dominated in others. On quadrilateral/hexahedral meshes our ASM may fail, since the related $\mathrm{H}(\mathbf{curl}, \Omega)$-conforming finite element space does not provide a spectrally accurate discretization.

1 Introduction

This work was inspired by the development of *discontinuous Galerkin* (DG) methods for the magnetic advection-diffusion equations of resistive magneto-hydrodynamics (MHD), see [56]. In each timestep of a partly implicit time-stepping scheme we have to solve a $\mathrm{H}(\mathbf{curl}, \Omega)$-elliptic boundary value problem, which, in abstract form, reads

$$\begin{cases} \nabla \times (\nu \nabla \times \boldsymbol{u}) + \beta \boldsymbol{u} = \boldsymbol{f} & \text{in } \Omega, \\ \boldsymbol{u} \times \mathbf{n} = 0 & \text{on } \partial\Omega. \end{cases} \tag{1.1}$$

Here $\Omega \subset \mathbb{R}^3$ is a bounded domain with Lipschitz boundary $\partial\Omega$, $\boldsymbol{f} \in L^2(\Omega)^3$, and $\nu(\mathbf{x})$ and $\beta(\mathbf{x})$ are possibly discontinuous coefficients, which are assumed to be positive and bounded functions in Ω. They represent properties of the medium or material: ν is typically the inverse of the magnetic permeability and β is proportional to the ratio of electrical conductivity and the time step. For the sake of simplicity, we confine ourselves to domains Ω with *trivial topology.*

The boundary value problem (1.1) allows an $\mathrm{H}(\mathbf{curl}, \Omega)$-elliptic variational formulation, which reads: find $\boldsymbol{u} \in \mathrm{H}_0(\mathbf{curl}, \Omega)$ such that

$$a(\boldsymbol{u}, \boldsymbol{v}) := (\nu \nabla \times \boldsymbol{u}, \nabla \times \boldsymbol{v})_{0,\Omega} + (\beta \boldsymbol{u}, \boldsymbol{v})_{0,\Omega} = (\boldsymbol{f}, \boldsymbol{v})_{0,\Omega} \qquad \forall \boldsymbol{v} \in \mathrm{H}_0(\mathbf{curl}, \Omega). \tag{1.2}$$

We have used the standard notations for the Hilbert spaces

$$\mathrm{H}(\mathbf{curl}, \Omega) := \{\boldsymbol{v} \in L^2(\Omega)^3 : \ \nabla \times \boldsymbol{v} \in L^2(\Omega)^3\}$$
$$\mathrm{H}_0(\mathbf{curl}, \Omega) := \{\boldsymbol{v} \in \mathrm{H}(\mathbf{curl}, \Omega) : \mathbf{n} \times \boldsymbol{v} = \mathbf{0} \text{ on } \partial\Omega\}$$

[*]Dipartimento di Matematica, Università di Bologna, Piazza di Porta San Donato 5, Bologna, Italy
[†]Seminar for Applied Mathematics, ETH Zürich, Rämistrasse 101, Zürich, Switzerland
[‡]Seminar for Applied Mathematics, ETH Zürich, Rämistrasse 101, Zürich, Switzerland

endowed with the graph norm

$$\|\boldsymbol{v}\|^2_{\mathrm{curl},\Omega} := \|\boldsymbol{v}\|^2_{0,\Omega} + \|\boldsymbol{\nabla} \times \boldsymbol{v}\|^2_{0,\Omega}\,.$$

The assumptions $\nu > 0$, $\beta > 0$ in Ω ensure existence and uniqueness of solutions of (1.2).

In MHD simulations the rationale for using DG is to cope with (locally) dominating transport. We are not interested in the capability of DG to accommodate rather general meshes; the methods are considered on *standard conforming finite element meshes* and this will be the setting of the present paper. We acknowledge an extension of our approach to more general meshes is an open problem.

Our contribution. Based on the *auxiliary space method* (ASM), explained in Section 3, we derive a family of preconditioners for a symmetric Interior Penalty Discontinuous Galerkin (IP-DG) discretization of (1.1) by means of piecewise polynomials on conforming meshes, see Section 2. Specifically, we address the influence of possible discontinuities in the "diffusivity" ν and/or in the "reaction coefficient" β on the asymptotic performance of the preconditioners. Throughout,

> we take for granted the availability of a (direct) solver for any standard $\mathrm{H}(\mathbf{curl},\Omega)$-conforming Galerkin discretization of (1.2).

Under this assumption we aim to determine the precise dependence of the performance of the ASM preconditioners on both the mesh width and the coefficients in Section 4. The main result is Theorem 4.1, which asserts that, in a broad range of situations, the ASM approach provides a preconditioner that does not degrade on fine meshes and in the presence of large jumps of the coefficients. The latter statement has to be qualified, since a particular combination of discontinuities of ν and β is not captured by our estimates (yet?).

Related work for DG. Over the last fifteen years a considerable effort has been devoted to the development of efficient and robust preconditioning techniques for discontinuous Galerkin (DG) discretizations. Most analysis and especially convergence results have dealt with DG approximations of simple (mostly second order) elliptic problems.

The first efforts were focused on the development and analysis of classical domain decomposition methods: overlapping Schwarz methods were studied in [50, 51, 27] for Interior Penalty (IP) DG approximations of second and fourth order problems, whilst simple Schwarz methods with no overlap were introduced and proved to be convergent (unlike to the conforming case) in [50, 2, 3] for all the DG methods considered in [10]. The analysis in the works mentioned above uses an augmented version of classical Schwarz theory in order to deal with the non-conformity of the finite element spaces. Simultaneously, first attempts to design and analyze efficient multigrid solvers in [53, 28] followed the classical multigrid theories of [21] and [20, 22], respectively. Nowadays, there is still active research in these directions trying to harness classical theories. In particular, Schwarz preconditioners [6, 18, 26, 5, 37] and multigrid methods [24, 23, 73, 40, 7] have been investigated for newly introduced DG discretizations and for *hp*-DG approximations of elliptic problems.

Furthermore, more sophisticated non-overlapping domain decomposition preconditioners of substructuring type have been recently studied for DG for elliptic second order problems in two dimensions. In [45, 46, 47, 4] non-overlapping BDDC, N-N, FETI-DP and substructuring methods have been introduced and analyzed for a Nitsche-type approximation. BDDC preconditioners are also studied in [25] for a weakly penalized IP method; for the *p*-version of a hybrid DG method in [81]; and in [36] for *hp*-IP-DG spectral methods. While different approaches have been considered in the analysis, all the above works provide quasi-optimality results (with respect to the mesh size and in [36, 4] also with respect to the polynomial degree) and robustness of the preconditioners with respect to possible high variations or jumps in the diffusion coefficient.

The evolution of domain decomposition and multigrid preconditioners has been paralleled by the design and analysis of other subspace correction methods (for two and three dimensional problems), erected on the construction of suitable splittings of DG finite element spaces. At least two main approaches, based on different principles, have been pursued: the use of a suitable subspace and the construction of orthogonal splittings. Optimal multilevel preconditioners based on an orthogonal space decomposition of the DG space, were introduced in [16] for symmetric and non-symmetric piecewise linear IP approximations of elliptic problems. This technique has been adapted and extended to deal with a larger family of problems including elliptic problems with jumping coefficients [14], linear elasticity [13] and convection dominated problems corresponding to drift-diffusion models for the transport of species [15].

A different direction was followed in [41] and [32, 33], where the authors introduced two-level and multilevel preconditioners, respectively, for the Interior Penalty (IP) DG methods. There is a close relationship with our work, because the conceptual foundation behind both works (although in the first is not explicitly mentioned) is the Fictitious Space Lemma and the ASM, with an auxiliary finite element space (piecewise constants and conforming linear finite elements, respectively) in which preconditioning techniques are available. The ASM has been further exploited recently in [12] to construct optimal preconditioners for a family of $\mathrm{H}(\mathbf{div},\Omega)$-DG discretizations of the Stokes problem, and in [31] to develop optimal multilevel preconditioners for spectral DG discretizations (see also [36] where these results are used for designing a BDDC preconditioner). In particular, the analysis in [12] requires a suitable extension of the Fictitious Space Lemma.

There is also a relatively big body of work on DG discretizations for boundary values problems like (1.1). Different varieties of DG for different extended and regularized versions of (1.1) have been presented in, among others, [34, 35, 64, 78]. By and large it seems that numerical analysis has entirely focused on a priori and a posteriori error estimate and no attention has been paid to the design and analysis of preconditioners. Apparently, the present paper is the first study to address this.

Work on preconditioners for conforming finite element methods. Subspace correction preconditioners in the context of conforming Galerkin finite element discretizations of $\mathrm{H}(\mathbf{curl},\Omega)$-elliptic variational problems are well established both in the form of multigrid [57, 59, 11, 63] and domain decomposition methods [60, 84]. The authors prove uniform performance with respect to mesh refinement, but their analyses do not take into account discontinuities in the coefficients. However, in [57] numerical evidence hints that multigrid methods in $\mathrm{H}(\mathbf{curl},\Omega)$ are affected by jumping coefficients in a similar way as their scalar counterparts.

For conforming and non-conforming discretizations of scalar second order elliptic problems, the design preconditioning strategies, that can be proven to be robust with respect to the jumps in the diffusion coefficient has received a lot of attention. However, in presence of two different coefficients (i.e. a reaction-diffusion problem or one resulting upon time discretization of a parabolic model), the asymptotic convergence of multilevel solvers for conforming discretizations has only been recently addressed in [72]. The authors show that robustness can only be achieved when one of the two coefficients is constant, or if both coefficients have the same pattern distribution.

Much less progress has been made in the context of $\mathrm{H}(\mathbf{curl},\Omega)$-elliptic problems with two variable coefficients. In spite of the relevance of the problem, the bulk of contributions is largely restricted to conforming finite element approximations of the two dimensional problem. Non-overlapping domain decomposition methods of substructuring type are studied in [88, 42], Neumann-Neumann methods in [83], and FETI and FETI-DP in [79] and [86], respectively. Besides the work in [42], where the authors used non standard coarse spaces based on energy minimization, all other mentioned works reflect a dependence on the coefficients in the asymptotic convergence that predicts deterioration of the preconditioner in the mass-dominated regime.

For the three dimensional $\mathrm{H}(\mathbf{curl},\Omega)$-elliptic problem with two variable coefficients, there are even less works. This is certainly related to the significant challenges that emerge in the three dimensional continuous problem but it is also due to the much intricate construction of the finite element discretizations. FETI-DP algorithms for conforming approximations were introduced in [85] and the analysis reveals explicit dependence on the ratio between the reaction and the **curl** coefficients, as appeared in all first works for the two dimensional case. Other significant contributions are contained in [67, 68], where the authors further extended the research from [70, 69]. In [67] a novel mortar method for H(**curl**, Ω)-conforming finite element discretizations is introduced and analyzed. A weighted (with respect to the reaction coefficient) Helmholtz decomposition is derived in [68] and applied to the analysis of the substructuring preconditioner introduced in [70] applied to the problem with variable coefficients. The assumptions on the distribution of the coefficients seems however quite restrictive, ruling out many cases of interest. More recently in [43], the authors have devised a non-overlapping BDDC algorithm able to improve the dependence on the quotient H/h between the coarse and fine meshes by saving two logarithmic factors. Nevertheless, their analysis still reflects the same dependence on the coefficients as in [85].

Remark. The asymptotic analysis and estimates derived in the remainder of this work, require to introduce constants. With a small abuse of notation, by C we will denote a generic positive constant whose value may vary among different occurrences, but, unless otherwise specified, will be independent of the mesh width and the coefficients of the problem and may only depend on the polynomial degree, the shape regularity and the connectivity of the mesh partition.

2 Interior Penalty discontinuous Galerkin discretization: abstract setting

This section is devoted to the derivation of a symmetric Interior Penalty discontinuous Galerkin discretization of the model problem (1.1). First, we fix the basic notation and introduce assumptions on the mesh partition of the domain together with the finite element spaces of interest for the method. Then the discretization approach is presented and its basic properties discussed.

2.1 Mesh Partition and Jump operators

Let $\mathcal{T}_h$ be a shape regular partition of the computational domain Ω into disjoint tetrahedra (d- simplices with $d = 3$) or axis-parallel hexahedral elements such that $\overline{\Omega} = \cup_{T\in\mathcal{T}_h}\overline{T}$. Moreover, the partition $\mathcal{T}_h$ is assumed to be conforming, locally quasi-uniform, and affine. Let h_T denote the diameter of $T \in \mathcal{T}_h$; we set $h := \max_{T\in\mathcal{T}_h} h_T$ to represent the mesh width of $\mathcal{T}_h$. The local mesh sizes are of bounded variation, that is, there exists a constant $\rho > 0$ depending only on the shape regularity of the mesh, such that every neighboring elements T and T' satisfy $\rho h_T \leq h_{T'} \leq \rho^{-1} h_T$.

An interior face $f = \partial T_1 \cap \partial T_2$ is the intersection of the boundary of two neighboring elements $T_1, T_2 \in \mathcal{T}_h$, while a boundary face $f = \partial T \cap \partial\Omega$ is given by the intersection of the boundary with a boundary element $T \in \mathcal{T}_h$. Each interior face is equipped with an intrinsic orientation and the boundary faces are by convention assumed to be oriented such that the normal vector points inward. We denote by $\mathcal{F}_h$ the set of all faces of the partition ($d-1$-dimensional cells of the partition), and by $\mathcal{F}_h^o$ and $\mathcal{F}_h^\partial$ the collection of all interior and boundary faces, respectively. Trivially, $\mathcal{F}_h = \mathcal{F}_h^o \cup \mathcal{F}_h^\partial$. Similarly, $\mathcal{E}_h$ will refer to the set of all edges of the skeleton of $\mathcal{T}_h$ ($d-2$-dimensional cells of the partition), and by $\mathcal{E}_h^o$ and $\mathcal{E}_h^\partial$ we denote the collection of all interior and boundary edges, respectively.

In order to define the trace operators (see e.g. [78, Section 3]), let $f \in \mathcal{F}_h^o$ be an interior face shared by two elements T^+ and T^- and let $\mathbf{n}^+$ and $\mathbf{n}^-$ denote the unit normal vectors on f pointing outwards from T^+ and T^-, respectively. For a piecewise smooth vector-valued function $\boldsymbol{v}$, we denote by $\boldsymbol{v}^\pm$ the traces of $\boldsymbol{v}$ taken from within $T^\pm$. We define the average and tangential jump across $f \in \mathcal{F}_h^o$ by

$$\{\!\{\boldsymbol{v}\}\!\} := \frac{\boldsymbol{v}^+ + \boldsymbol{v}^-}{2}, \qquad [\![\, \boldsymbol{v} \,]\!]_{\boldsymbol{\tau}} := \mathbf{n}^+ \times \boldsymbol{v}^+ + \mathbf{n}^- \times \boldsymbol{v}^-,$$

and on a boundary face $f \in \mathcal{F}_h^\partial$, we set $\{\!\{\boldsymbol{v}\}\!\} := \boldsymbol{v}$ and $[\![\, \boldsymbol{v} \,]\!]_{\boldsymbol{\tau}} := \mathbf{n} \times \boldsymbol{v}$.

Throughout the paper we will use the following sets of mesh cells:

$$\begin{aligned} \mathcal{T}(e) &:= \{T \in \mathcal{T}_h : e \subset \partial T\}\,; \qquad & \mathcal{E}(T) &:= \{e \in \mathcal{E}_h : e \in \partial T\}\,; \\ \mathcal{F}(T) &:= \{f \in \mathcal{F}_h : f \in \partial T\}\,; \qquad & \mathcal{F}(e) &:= \{f \in \mathcal{F}_h : e \in \partial f\}\,. \end{aligned}$$

2.2 Finite Element Spaces and local representation

We introduce the (family of) finite element spaces

$$\boldsymbol{V_h} = \{\boldsymbol{v} \in L^2(\Omega)^3 : \ \boldsymbol{v} \in \mathcal{M}(T),\, T \in \mathcal{T}_h\}\,, \tag{2.1}$$

where $\mathcal{M}(T)$ is a local space of vector-valued polynomials which, for a fixed degree k, satisfy $\mathcal{M}(T) \subseteq \mathbb{P}_k(T)^3$ if T is a simplex or $\mathcal{M}(T) \subseteq \mathbb{Q}_k(T)^3$ if T is an hexahedron. The corresponding $\mathrm{H}_0(\mathbf{curl}, \Omega)$-conforming finite element spaces are

$$\boldsymbol{V_h^c} := \boldsymbol{V_h} \cap \mathrm{H}_0(\mathbf{curl}, \Omega) = \{\boldsymbol{v} \in \mathrm{H}_0(\mathbf{curl}, \Omega) : \ \boldsymbol{v} \in \mathcal{M}(T),\, T \in \mathcal{T}_h\}.$$

Throughout, the local space $\mathcal{M}(T)$ will be defined as one of the following:
1. Nédélec elements of the second family on simplicial meshes: Full polynomial space

$$\mathcal{M}(T) = \mathcal{N}^{II}(T) := \mathbb{P}_k(T)^3, \qquad k \geq 1. \tag{2.2}$$

2. Nédélec elements of the first family on simplicial meshes: For an integer $k \geq 0$, we define

$$\mathcal{M}(T) = \mathcal{N}^{I}(T) := \mathbb{P}_k(T)^3 \,\oplus\, \left(\mathbf{x} \times \mathbb{H}_k(T)^3\right), \qquad k \geq 0, \tag{2.3}$$

where $\mathbb{H}^k(T)$ denotes the space of homogeneous polynomials of degree k.
3. Nédélec elements of the first family on cubical meshes [75]*:* The polynomial space:

$$\mathcal{M}(T) = \mathcal{N}_q^{I}(T) := \mathbb{Q}_{k,k+1,k+1}(T) \times \mathbb{Q}_{k+1,k,k+1}(T) \times \mathbb{Q}_{k+1,k+1,k}(T), \qquad k \geq 0, \tag{2.4}$$

where $\mathbb{Q}_{\ell,m,n}(T)$ is the local space of polynomials of degree at most ℓ, m, n in each vector component. For hexahedral and cubical meshes our analysis is restricted to local spaces of Nédélec elements of the first family. However, a thoughtful discussion on the possible use of other local elements and the failure of the corresponding theory is provided in Remark 4.18 and in the numerical experiments in Section 6.

For each of the above spaces, the local degrees of freedom (dofs) are the normalized moments on edges, faces and elements (see [74, Definition 5.30] and [19, Sections 2.3.2 and 2.4.4] for details). An important property of the spaces $\mathcal{M}(T)$ is that they (and their dofs) are invariant under the action of a covariant transform in case of affine mappings. In fact, the construction, implementation and analysis of the proposed preconditioners heavily relies on the use of the local spaces $\mathcal{M}(T)$ together with the corresponding choice of degrees of freedom. In particular, denoting by $\boldsymbol{v}_{e,T} = \{v_{e,T}^i\}_{i=1}^{N_e}$, $\boldsymbol{v}_{f,T} = \{v_{f,T}^i\}_{i=1}^{N_f}$ and $\boldsymbol{v}_T = \{v_T^i\}_{i=1}^{N_b}$ the moments of $\boldsymbol{v} \in \mathcal{M}(T)$ (corresponding to the particular choice of $\mathcal{M}(T)$), the following representation holds,

$$\boldsymbol{v}(\mathbf{x}) = \sum_{e \in \mathcal{E}(T)} \sum_{i=1}^{N_e} v_{e,T}^i\, \boldsymbol{\varphi}_{e,T}^i(\mathbf{x}) + \sum_{f \in \mathcal{F}(T)} \sum_{i=1}^{N_f} v_{f,T}^i\, \boldsymbol{\varphi}_{f,T}^i(\mathbf{x}) + \sum_{i=1}^{N_b} v_T^i\, \boldsymbol{\varphi}_T^i(\mathbf{x})\,, \quad \forall\, \mathbf{x} \in T \tag{2.5}$$

where $\{\boldsymbol{\varphi}_{e,T}^i\}_{i=1}^{N_e}$, $\{\boldsymbol{\varphi}_{f,T}^i\}_{i=1}^{N_f}$ and $\{\boldsymbol{\varphi}_T^i\}_{i=1}^{N_b}$ refer to the basis functions of $\mathcal{M}(T)$ (dual to the degrees of freedom relative to $\mathcal{M}(T)$). Note that even if the degrees of freedom are on the edges and faces of the mesh, they are confined to a single element therefore no continuity across the mesh cells has to be imposed.

Finally we remark that for the design and analysis of the solvers it is sometimes essential to characterize the kernel of the **curl** operator in $\boldsymbol{V_h^c}$ for each choice of $\mathcal{M}(T)$, see Section 4.6. Since the domain Ω is assumed to be homotopy equivalent to a ball, the kernels are given by gradients of standard scalar Lagrangian finite element functions.

2.3 Symmetric Interior Penalty method

We propose a discretization of the problem (1.1) along the lines of [64] based on the symmetric Interior Penalty discontinuous Galerkin (SIP-DG) method introduced in [8, 89, 17] (see also [10, Section 3.4]) for second order problems. To deal with the discontinuous coefficients of the problem and provide a robust approximation method, we modify the classical SIP-DG method, similarly to [44, Section 4], where a particular choice of weighted averages of the discontinuous coefficients at the mesh interfaces is introduced. More precisely, we consider the discrete variational formulation: find $\boldsymbol{u}_h \in \boldsymbol{V_h}$ such that

$$\mathrm{a}_{\mathrm{DG}}(\boldsymbol{u}_h, \boldsymbol{v}) = (\boldsymbol{f}, \boldsymbol{v})_{\mathcal{T}_h} \qquad \forall\, \boldsymbol{v} \in \boldsymbol{V_h}\,, \tag{2.6}$$

where

$$(\boldsymbol{f}, \boldsymbol{v})_{\mathcal{T}_h} := \sum_{T\in\mathcal{T}_h} (\boldsymbol{f}, \boldsymbol{v})_{0,T}\,,$$

and the bilinear form $\mathrm{a}_{\mathrm{DG}}(\cdot,\cdot)$ is defined as

$$\begin{aligned}\mathrm{a}_{\mathrm{DG}}(\boldsymbol{u}, \boldsymbol{v}) := &\sum_{T\in\mathcal{T}_h} (\nu_T \boldsymbol{\nabla}\times\boldsymbol{u}, \boldsymbol{\nabla}\times\boldsymbol{v})_{0,T} + \sum_{T\in\mathcal{T}_h} (\beta_T \boldsymbol{u}, \boldsymbol{v})_{0,T} - \sum_{f\in\mathcal{F}_h} (\{\!\{\nu\boldsymbol{\nabla}\times\boldsymbol{u}\}\!\}_\gamma\,, [\![\,\boldsymbol{v}\,]\!]_{\boldsymbol{\tau}})_{0,f} \\ &- \sum_{f\in\mathcal{F}_h} ([\![\,\boldsymbol{u}\,]\!]_{\boldsymbol{\tau}}, \{\!\{\nu\boldsymbol{\nabla}\times\boldsymbol{v}\}\!\}_\gamma)_{0,f} + \sum_{T\in\mathcal{T}_h} \alpha_T(\nu) \sum_{e\in\mathcal{E}(T)} \sum_{f\in\mathcal{F}(e)} (s_f [\![\,\boldsymbol{u}\,]\!]_{\boldsymbol{\tau}}\,, [\![\,\boldsymbol{v}\,]\!]_{\boldsymbol{\tau}})_{0,f}\,.\end{aligned} \tag{2.7}$$

Here $\nu_T \in \mathbb{P}_0(T)$ and $\beta_T \in \mathbb{P}_0(T)$ are the restriction of the coefficients ν and β to the element $T \in \mathcal{T}_h$. We assume that the partition $\mathcal{T}_h$ resolves the coefficients: ν, $\beta \in \mathbb{P}_0(\mathcal{T}_h)$.

In (2.7), the function s_f penalizes the tangential jumps over the $(d-1)$-cells of the skeleton of the partition. Every face jump is weighted with the sum of certain coefficients $\alpha_T(\nu)$ belonging to the elements T sharing an edge of the given face. In particular, s_f is defined as [8, 55, 78]

$$s_f := c_0 h_f^{-1} \qquad \forall\, f \in \mathcal{F}_h \tag{2.8}$$

where $c_0 > 0$ is a strictly positive constant independent of the mesh size and the coefficients of the problem and depending only on the shape regularity constant of $\mathcal{T}_h$. The function h_f is defined as

$$h_f := \begin{cases} \min\{h_{T^+}, h_{T^-}\} & f \in \mathcal{F}_h^o\,, \quad f = \partial T^+ \cap \partial T^-\,, \\ h_T & f \in \mathcal{F}_h^\partial\,, \quad f = \partial T \cap \partial\Omega\,. \end{cases}$$

The coefficient function $(\alpha_T(\nu))_{T\in\mathcal{T}_h} \in \mathbb{P}_0(\mathcal{T}_h)$ is a piecewise constant function defined elementwise by

$$\alpha_T(\nu) := \max_{f\in\mathcal{F}(T)} \{\!\{\nu\}\!\}_{*,f} \qquad \text{with} \qquad \{\!\{\nu\}\!\}_{*,f} := \begin{cases} \max\limits_{\substack{T\in\mathcal{T}(e)\\ e\in\partial f}} \nu_T & f \in \mathcal{F}_h^o\,, \\ \nu_T & f \in \mathcal{F}_h^\partial\,. \end{cases} \tag{2.9}$$

Observe that in view of the above definition, the coefficient $\alpha_T(\nu)$ is taking the maximum conductivity coefficient over a patch of elements surrounding T. Moreover, in (2.7), the weighted average $\{\!\{\cdot\}\!\}_\gamma$ is defined as the plain trace for a boundary face, whereas for $f \in \mathcal{F}_h^o$,

$$\{\!\{\boldsymbol{u}\}\!\}_\gamma := \gamma_f^+ \boldsymbol{u}^+ + \gamma_f^- \boldsymbol{u}^- \qquad \text{with} \quad \gamma_f^- = 1 - \gamma_f^+\,,$$

for weights $\gamma_f^\pm$ that depend on the coefficient ν and might vary over all interior faces. More precisely, for any $f \in \mathcal{F}_h^o$ with $f = \partial T^+ \cap \partial T^-$, we take $\gamma_f^\pm$ as follows:

$$\gamma_f^\pm = \frac{\nu^\mp}{\nu^+ + \nu^-} \qquad \text{where} \qquad \nu^\pm := \nu_{|T^\pm}\,.$$

The use of the weighted average $\{\!\{\cdot\}\!\}_\gamma$ together with $\{\!\{\cdot\}\!\}_{*,f}$ and the definition of the coefficient $\alpha_T(\nu)$ is aimed at ensuring the robustness of the approximation (2.6) as well as of the preconditioners introduced in the present paper, with respect to variations of the coefficients.

In our analysis we will use the harmonic average of the coefficient ν across a face f defined as

$$\{\!\{\nu\}\!\}_{H,f} := \begin{cases} \dfrac{2\nu^+\nu^-}{\nu^+ + \nu^-} & f \in \mathcal{F}_h^o\,, \quad f = \partial T^+ \cap \partial T^-\,, \\ \nu_T & f \in \mathcal{F}_h^\partial\,, \quad f = \partial T \cap \partial\Omega\,. \end{cases} \tag{2.10}$$

Notice that $\{\!\{\nu\}\!\}_{H,f}$ is equivalent to $\min\{\nu^+,\nu^-\}$ and hence, in particular, $\{\!\{\nu\}\!\}_{H,f} \leq 2\nu^\pm$. Moreover, it satisfies the following relation with respect to the coefficient in (2.9)

$$\{\!\{\nu\}\!\}_{H,f} \leq \{\!\{\nu\}\!\}_{*,f} \qquad \forall\, f \in \mathcal{F}_h\,. \tag{2.11}$$

We finally observe that

$$\{\!\{\nu\boldsymbol{\nabla}\times\boldsymbol{v}\}\!\}_\gamma = \{\!\{\nu\}\!\}_{H,f}\,\{\!\{\boldsymbol{\nabla}\times\boldsymbol{v}\}\!\} \quad \forall \boldsymbol{v} \in \boldsymbol{V_h}\,,\ \forall f \in \mathcal{F}_h\,. \tag{2.12}$$

Note that when the variational formulation (2.6) is restricted to $\boldsymbol{V_h^c}$, the corresponding $\mathrm{H}_0(\mathbf{curl},\Omega)$-conforming discretization of (1.1) is obtained.

On $\boldsymbol{V_h}$ we introduce the seminorms

$$\|\boldsymbol{\nabla}\times\boldsymbol{v}\|^2_{0,\nu,\mathcal{T}_h} := \sum_{T\in\mathcal{T}_h} \nu_T \|\boldsymbol{\nabla}\times\boldsymbol{v}\|^2_{0,T} \qquad \forall\, \boldsymbol{v} \in \boldsymbol{V_h}\,, \tag{2.13}$$

$$|\boldsymbol{v}|^2_{*,\nu} := \sum_{T\in\mathcal{T}_h} \alpha_T(\nu) \sum_{e\in\mathcal{E}(T)} \sum_{f\in\mathcal{F}(e)} h_f^{-1} \|[\![\,\boldsymbol{v}\,]\!]_{\boldsymbol{\tau}}\|^2_{0,f} \qquad \forall\, \boldsymbol{v} \in \boldsymbol{V_h}\,,$$

and norms

$$\|\boldsymbol{v}\|^2_{0,\beta,\mathcal{T}_h} := \sum_{T\in\mathcal{T}_h} \beta_T \|\boldsymbol{v}\|^2_{0,T} \qquad \forall\, \boldsymbol{v} \in \boldsymbol{V_h}\,, \tag{2.14}$$

$$\|\boldsymbol{v}\|^2_{\mathrm{DG}} := \|\boldsymbol{\nabla}\times\boldsymbol{v}\|^2_{0,\nu,\mathcal{T}_h} + \|\boldsymbol{v}\|^2_{0,\beta,\mathcal{T}_h} + |\boldsymbol{v}|^2_{*,\nu} \qquad \forall\, \boldsymbol{v} \in \boldsymbol{V_h}\,. \tag{2.15}$$

2.4 Convergence of the approximation

We now briefly show that the bilinear form $\mathrm{a}_{\mathrm{DG}}(\cdot,\cdot)$ defined in (2.7) is continuous and coercive in $\boldsymbol{V_h}$ with respect to the $\|\cdot\|_{\mathrm{DG}}$ norm (2.15) with constants independent of the mesh size h and the coefficients of the problem. Note that, as it will be clear from the proof, the stability constant depends also on the stabilization parameter c_0 in (2.8) which therefore has to be chosen large enough in order to ensure stability of the bilinear form $\mathrm{a}_{\mathrm{DG}}(\cdot,\cdot)$ in the $\|\cdot\|_{\mathrm{DG}}$ norm.

Proposition 2.1. *Let the bilinear form $\mathrm{a}_{DG}(\cdot,\cdot)$ be defined as in* (2.7). *Then, there exist constants $C_{cont}, C_{stab} > 0$ depending only on the shape regularity of the mesh and on the polynomial degree such that*

$$|\mathrm{a}_{DG}(\boldsymbol{u},\boldsymbol{v})| \leq C_{cont}\|\boldsymbol{u}\|_{DG}\|\boldsymbol{v}\|_{DG}\,, \qquad \forall\, \boldsymbol{u},\boldsymbol{v} \in \boldsymbol{V_h}\,, \tag{2.16}$$

$$\mathrm{a}_{DG}(\boldsymbol{v},\boldsymbol{v}) \geq C_{stab}\|\boldsymbol{v}\|^2_{DG}\,, \qquad \forall\, \boldsymbol{v} \in \boldsymbol{V_h}\,. \tag{2.17}$$

Proof. We first show the coercivity (2.17). Taking $\boldsymbol{u} = \boldsymbol{v} \in \boldsymbol{V_h}$ in (2.7), results in

$$\mathrm{a}_{\mathrm{DG}}(\boldsymbol{v},\boldsymbol{v}) \geq \|\boldsymbol{\nabla}\times\boldsymbol{v}\|^2_{0,\nu,\mathcal{T}_h} + \|\boldsymbol{v}\|^2_{0,\beta,\mathcal{T}_h} + c_0|\boldsymbol{v}|^2_{*,\nu} - 2\left|\sum_{f\in\mathcal{F}_h}\int_f \{\!\!\{\nu\boldsymbol{\nabla}\times\boldsymbol{v}\}\!\!\}_\gamma \cdot [\![\,\boldsymbol{v}\,]\!]_{\boldsymbol{\tau}}\,ds\right|. \tag{2.18}$$

Cauchy-Schwarz inequality and the arithmetic-geometric inequality together with the relation (2.12) and the bound (2.11) on the harmonic average, give

$$\begin{aligned}\left|\int_f \{\!\!\{\nu\boldsymbol{\nabla}\times\boldsymbol{v}\}\!\!\}_\gamma\cdot[\![\,\boldsymbol{v}\,]\!]_{\boldsymbol{\tau}}ds\right| &\leq C\left(\frac{h_f}{\{\!\!\{\nu\}\!\!\}_{*,f}}\|\,\{\!\!\{\nu\boldsymbol{\nabla}\times\boldsymbol{v}\}\!\!\}_\gamma\,\|^2_{0,f}\right)^{1/2}\left(\{\!\!\{\nu\}\!\!\}_{*,f}\,h_f^{-1}\,\|[\![\,\boldsymbol{v}\,]\!]_{\boldsymbol{\tau}}\|^2_{0,f}\right)^{1/2}\\ &\overset{(2.12)}{\leq} C\frac{\epsilon}{\{\!\!\{\nu\}\!\!\}_{*,f}}(\{\!\!\{\nu\}\!\!\}_{H,f})^2 h_f\,\|\{\!\!\{\boldsymbol{\nabla}\times\boldsymbol{v}\}\!\!\}\|^2_{0,f} + \frac{C}{4\epsilon}\{\!\!\{\nu\}\!\!\}_{*,f}\,h_f^{-1}\,\|[\![\,\boldsymbol{v}\,]\!]_{\boldsymbol{\tau}}\|^2_{0,f}\\ &\overset{(2.11)}{\leq} C\epsilon\,\{\!\!\{\nu\}\!\!\}_{H,f}\,h_f\,\|\{\!\!\{\boldsymbol{\nabla}\times\boldsymbol{v}\}\!\!\}\|^2_{0,f} + \frac{C}{4\epsilon}\{\!\!\{\nu\}\!\!\}_{*,f}\,h_f^{-1}\,\|[\![\,\boldsymbol{v}\,]\!]_{\boldsymbol{\tau}}\|^2_{0,f}\end{aligned} \tag{2.19}$$

Now, let $f = \partial T^+ \cap \partial T^-$. The trace inequality [1, Theorem 3.10] and the inverse inequality [39, Theorem 3.2.6] together with the fact that $\{\!\!\{\nu\}\!\!\}_{H,f} \leq 2\nu_{T^\pm}$ yield

$$\{\!\!\{\nu\}\!\!\}_{H,f}\,h_f\,\|\{\!\!\{\boldsymbol{\nabla}\times\boldsymbol{v}\}\!\!\}\|^2_{0,f} \leq C(\nu_{T^+}\,\|\boldsymbol{\nabla}\times\boldsymbol{v}\|^2_{0,T^+} + \nu_{T^-}\,\|\boldsymbol{\nabla}\times\boldsymbol{v}\|^2_{0,T^-}),$$

where C depends on the shape regularity and the local polynomial space. Moreover, by the definition (2.9) it holds

$$\sum_{f\in\mathcal{F}_h}\{\!\!\{\nu\}\!\!\}_{*,f}\,\|\cdot\|_{0,f} \leq C\sum_{T\in\mathcal{T}_h}\alpha_T(\nu)\sum_{f\in\mathcal{F}(T)}\|\cdot\|_{0,f} \leq C\sum_{T\in\mathcal{T}_h}\alpha_T(\nu)\sum_{f\in\mathcal{F}(T)}\|\cdot\|_{0,f} + \sum_{T\in\mathcal{T}_h}\alpha_T(\nu)\sum_{e\in\mathcal{E}(T)}\sum_{f\in\mathcal{F}(e)\setminus\mathcal{F}(T)}\|\cdot\|_{0,f}\,.$$

Hence, summing (2.19) over all the faces yields

$$\left|\sum_{f\in\mathcal{F}_h}\int_f\{\!\!\{\nu\boldsymbol{\nabla}\times\boldsymbol{v}\}\!\!\}_\gamma\cdot[\![\,\boldsymbol{v}\,]\!]_{\boldsymbol{\tau}}ds\right| \leq C\epsilon\,\|\boldsymbol{\nabla}\times\boldsymbol{v}\|^2_{0,\nu,\Omega} + \frac{C}{4\epsilon}\sum_{T\in\mathcal{T}_h}\alpha_T(\nu)\sum_{e\in\mathcal{E}(T)}\sum_{f\in\mathcal{F}(e)}h_f^{-1}\,\|[\![\,\boldsymbol{v}\,]\!]_{\boldsymbol{\tau}}\|^2_{0,f}\,.$$

Plugging the above estimate into (2.18), results in

$$\mathrm{a}_{\mathrm{DG}}(\boldsymbol{v},\boldsymbol{v}) \geq (1-2\epsilon C)\,\|\boldsymbol{\nabla}\times\boldsymbol{v}\|^2_{0,\nu,\mathcal{T}_h} + \|\boldsymbol{v}\|^2_{0,\beta,\mathcal{T}_h} + \left(c_0 - \frac{C}{2\epsilon}\right)|\boldsymbol{v}|^2_{*,\nu}.$$

By taking the constant penalty parameter c_0 sufficiently large, coercivity (2.17) is achieved with a constant C_{stab} depending only on the shape regularity of $\mathcal{T}_h$ and the polynomial degree of $\boldsymbol{V_h}$.

Concerning the continuity (2.16), Cauchy-Schwarz inequality gives

$$\left|\sum_{T\in\mathcal{T}_h}\int_T \nu_T\boldsymbol{\nabla}\times\boldsymbol{u}\cdot\boldsymbol{\nabla}\times\boldsymbol{v} + \beta_T\boldsymbol{u}\cdot\boldsymbol{v}\right| \leq \|\boldsymbol{\nabla}\times\boldsymbol{u}\|_{0,\nu,\Omega}\|\boldsymbol{\nabla}\times\boldsymbol{v}\|_{0,\nu,\Omega} + \|\boldsymbol{u}\|_{0,\beta,\Omega}\,\|\boldsymbol{v}\|_{0,\beta,\Omega}\,,$$

$$\left|\sum_{T\in\mathcal{T}_h}\alpha_T(\nu)\sum_{e\in\mathcal{E}(T)}\sum_{f\in\mathcal{F}(e)}\int_f c_0h_f^{-1}[\![\,\boldsymbol{u}\,]\!]_{\boldsymbol{\tau}}\cdot[\![\,\boldsymbol{v}\,]\!]_{\boldsymbol{\tau}}\right| \leq C|\boldsymbol{u}|_{*,\nu}|\boldsymbol{v}|_{*,\nu} \leq C\,\|\boldsymbol{u}\|_{\mathrm{DG}}\,\|\boldsymbol{v}\|_{\mathrm{DG}}\,.$$

A similar reasoning as in (2.19) (but without using arithmetic-geometric inequality) gives

$$\left|\sum_{f\in\mathcal{F}_h}\{\!\!\{\nu\boldsymbol{\nabla}\times\boldsymbol{u}\}\!\!\}\cdot[\![\,\boldsymbol{v}\,]\!]_{\boldsymbol{\tau}}\right| \leq C\|\boldsymbol{\nabla}\times\boldsymbol{u}\|_{0,\nu,\mathcal{T}_h}\,|\boldsymbol{v}|_{*,\nu},$$

and continuity (2.16) follows from the definition (2.15) of the $\|\cdot\|_{\mathrm{DG}}$ norm. ∎

For solutions of problem (1.1) sufficiently regular, quasi-optimal error estimates in the DG-norm (2.15) for the discretization introduced in (2.6) can be derived. Since the a-priori error analysis of the DG approximation (2.6) is out of the scope of the present work, we refer the interested reader to [64, 54, 55] and references therein.

3 Auxiliary space preconditioning

In this section we present the key ideas of the abstract framework for preconditioning approaches based on fictitious or auxiliary spaces. In particular, since in the applications we have in mind, the fictitious space method is applied to finite element spaces, we will focus on finite dimensional real Hilbert spaces. The design and analysis of the proposed preconditioning technique relies on the theory of the *fictitious space method*. For this reason, following the guidelines given in [62], we provide the main steps required to apply this theory to our particular problem. Then we introduce a family of preconditioners for the IP-DG discretization of problem (1.1) presented in Section 2.3.

3.1 Fictitious space and auxiliary space method

The auxiliary space method was introduced as a technique to develop and analyze optimal multilevel preconditioners for elliptic discretizations on general unstructured meshes in [91] and for non-conforming methods in [77]. It can be interpreted as a further generalization of the fictitious space approach, based on the so-called *fictitious space Lemma* originally introduced by Nepomnyaschikh in [76]. Two main ingredients are required in the construction of a fictitious space preconditioner for the operator $\mathcal{A} : \boldsymbol{V_h} \to \boldsymbol{V_h'}$ associated to the inner product $a(\cdot,\cdot)$ and the induced norm $\|\cdot\|_{\mathcal{A}}$ on $\boldsymbol{V_h}$:

(1) Another real (and discrete or finite dimensional) Hilbert space $\overline{\boldsymbol{\mathcal{V}}}$, the *fictitious space*, endowed with the inner product $\overline{a}(\cdot,\cdot)$, induced operator $\overline{\mathcal{A}} : \overline{\boldsymbol{\mathcal{V}}} \to \overline{\boldsymbol{\mathcal{V}}}'$ and norm $\|\cdot\|_{\overline{\mathcal{A}}}$.

(2) A continuous, linear and surjective transfer operator $\Pi : \overline{\boldsymbol{\mathcal{V}}} \to \boldsymbol{V_h}$ (the so-called prolongation operator in domain decomposition and multigrid methods).

Then, the fictitious space preconditioner $\mathcal{B} : \boldsymbol{V_h'} \to \boldsymbol{V_h}$ is defined as

$$\mathcal{B} := \Pi \circ \overline{\mathcal{A}}^{-1} \circ \Pi^*. \tag{3.1}$$

Obviously, the convergence properties of $\mathcal{B}$ depend on the auxiliary space $\overline{\boldsymbol{\mathcal{V}}}$ and on $\overline{\mathcal{A}}$. Note that the fact that Π is surjective, ensures that $\mathcal{B}$ is an isomorphism, and in particular a valid preconditioner (see [62, Lemma 2.1]). The analysis of the fictitious space preconditioner is grounded on the *fictitious space Lemma*, which we recall next without proof.

Theorem 3.1. *[76, Lemma 2.2]. Assume that*

(i) Π *is surjective and bounded, i.e.* $\exists\, C_1 > 0 : \quad \|\Pi \overline{\boldsymbol{v}}\|_{\mathcal{A}}^2 \le C_1 \|\overline{\boldsymbol{v}}\|_{\overline{\mathcal{A}}}^2 \quad \forall \overline{\boldsymbol{v}} \in \overline{\boldsymbol{\mathcal{V}}}$;

(ii) $\forall \boldsymbol{v} \in \boldsymbol{V_h} \quad \exists\, \overline{\boldsymbol{v}} \in \overline{\boldsymbol{\mathcal{V}}} : \quad \boldsymbol{v} = \Pi \overline{\boldsymbol{v}}$ *and* $\exists\, C_0 > 0 : \quad \|\overline{\boldsymbol{v}}\|_{\overline{\mathcal{A}}}^2 \le C_0 \|\boldsymbol{v}\|_{\mathcal{A}}^2$.

Then

$$C_0^{-1} \|\boldsymbol{v}\|_{\mathcal{A}}^2 \le a(\mathcal{B}\mathcal{A}\boldsymbol{v}, \boldsymbol{v}) \le C_1 \|\boldsymbol{v}\|_{\mathcal{A}}^2 \quad \forall \boldsymbol{v} \in \boldsymbol{V_h}.$$

In the present work, the space $\boldsymbol{V_h}$ is as in (2.1) and it is endowed with the inner product $\mathrm{a}_{\mathrm{DG}}(\cdot,\cdot)$ given in (2.7), with induced operator $\mathcal{A} : \boldsymbol{V_h} \to \boldsymbol{V_h'}$. The coercivity and symmetry of the bilinear form $\mathrm{a}_{\mathrm{DG}}(\cdot,\cdot)$ shown in Proposition 2.1, ensure that the operator $\mathcal{A}$ is self-adjoint and positive definite. Its matrix representation, in the basis associated to the degrees of freedom (see the representation (2.5) in Section 2) will be denoted by $\mathbb{A}$ and provides a symmetric positive definite matrix. The fictitious space Theorem 3.1 provides an estimate on the spectral condition number of the preconditioned system matrix, namely

$$\kappa(\mathbb{B}\mathbb{A}) \leq C_0 C_1,$$

where $\mathbb{B}$ denotes the matrix representation of the preconditioner (3.1).

In the auxiliary space method, the fictitious space is chosen as a product space having $\boldsymbol{V_h}$ as one of its components. As observed in [91], such choice eases the construction of a *surjective* map Π, and as a consequence facilitates the analysis. In the simplest case, the fictitious space is given by $\overline{\boldsymbol{\mathcal{V}}} = \boldsymbol{V_h} \times \boldsymbol{\mathcal{W}}$, where $\boldsymbol{\mathcal{W}}$ represents the true *auxiliary space*, endowed with a symmetric positive definite bilinear form $a_{\boldsymbol{\mathcal{W}}}(\cdot,\cdot)$ and induced operator $\mathcal{A}_{\boldsymbol{\mathcal{W}}} : \boldsymbol{\mathcal{W}} \to \boldsymbol{\mathcal{W}'}$. As component of the fictitious space, the space $\boldsymbol{V_h}$ is equipped with another inner product $s(\cdot,\cdot)$ which induces an operator $\mathcal{S} : \boldsymbol{V_h} \to \boldsymbol{V_h'}$. The operator $\mathcal{S}$ is typically referred to as *smoother*. This approach can be thought of as the fictitious space technique with the inner product

$$\overline{a}(\overline{\boldsymbol{v}}, \overline{\boldsymbol{v}}) = s(\boldsymbol{v}_0, \boldsymbol{v}_0) + a_{\boldsymbol{\mathcal{W}}}(\boldsymbol{w}, \boldsymbol{w}) \qquad \forall\, \overline{\boldsymbol{v}} = (\boldsymbol{v}_0, \boldsymbol{w}), \ \ \boldsymbol{v}_0 \in \boldsymbol{V_h}, \ \boldsymbol{w} \in \boldsymbol{\mathcal{W}},$$

and the auxiliary space preconditioner operator is given by

$$\mathcal{B} = \mathcal{S}^{-1} + \Pi_{\boldsymbol{\mathcal{W}}} \circ \mathcal{A}_{\boldsymbol{\mathcal{W}}}^{-1} \circ \Pi_{\boldsymbol{\mathcal{W}}}^{*} \tag{3.2}$$

where the linear transfer operator $\Pi_{\boldsymbol{\mathcal{W}}} : \boldsymbol{\mathcal{W}} \to \boldsymbol{V_h}$ yields the surjective map

$$\Pi := \begin{pmatrix} \mathrm{Id} & \\ & \Pi_{\boldsymbol{\mathcal{W}}} \end{pmatrix} : \overline{\boldsymbol{\mathcal{V}}} \to \boldsymbol{V_h}.$$

Here, the adjoint operator $\Pi_{\boldsymbol{\mathcal{W}}}^{*} : \boldsymbol{V_h} \to \boldsymbol{\mathcal{W}}$ is defined by

$$a_{\boldsymbol{\mathcal{W}}}(\Pi_{\boldsymbol{\mathcal{W}}}^{*}\boldsymbol{v}, \boldsymbol{w}) = a(\boldsymbol{v}, \Pi_{\boldsymbol{\mathcal{W}}}\boldsymbol{w}) \qquad \boldsymbol{v} \in \boldsymbol{V_h}, \ \boldsymbol{w} \in \boldsymbol{\mathcal{W}}.$$

If $\mathbb{S} \in \mathbb{R}^{N\times N}$ with $N := \dim \boldsymbol{V_h}$ and $\mathbb{A}_W \in \mathbb{R}^{N_W \times N_W}$, $N_W := \dim \boldsymbol{\mathcal{W}}$, then the preconditioner (3.2) in algebraic form reads

$$\mathbb{B} = \mathbb{S}^{-1} + \mathbb{P}\mathbb{A}_W^{-1}\mathbb{P}^{\mathsf{T}} \tag{3.3}$$

where $\mathbb{P} \in \mathbb{R}^{N\times N_W}$ is the matrix representation of the transfer operator $\Pi_{\boldsymbol{\mathcal{W}}}$.

As pointed out before, the analysis of the auxiliary space preconditioner hinges on the fictitious space Theorem 3.1. Its assumptions boil down to fulfilling the conditions of the following theorem (see [62, Section 2] and [61, Lemma 2.1]).

Theorem 3.2. *With the notation and definitions introduced above, assume that the following conditions are satisfied.*

Property (F0): *The transfer operator $\Pi_{\boldsymbol{\mathcal{W}}}$ is uniformly bounded, i.e. $\exists\, c_{\boldsymbol{\mathcal{W}}} > 0$ independent of h and the parameters of the problem, and depending on the mesh only through its shape regularity constant such that*

$$a_{DG}(\Pi_{\boldsymbol{\mathcal{W}}}\boldsymbol{w}, \Pi_{\boldsymbol{\mathcal{W}}}\boldsymbol{w}) \leq c_{\boldsymbol{\mathcal{W}}}\, a_{\boldsymbol{\mathcal{W}}}(\boldsymbol{w}, \boldsymbol{w}), \qquad \forall\, \boldsymbol{w} \in \boldsymbol{\mathcal{W}}. \tag{3.4}$$

Property (F1): *The operator $\mathcal{S}^{-1}$ is continuous, namely there exists $c_s > 0$, independent of h and the parameters of the problem, and depending only on the shape regularity of the mesh such that*

$$a_{DG}(\boldsymbol{v}, \boldsymbol{v}) \leq c_s\, s(\boldsymbol{v}, \boldsymbol{v}), \qquad \forall\, \boldsymbol{v} \in \boldsymbol{V_h}.$$

Property (F2): *(Stable decomposition) For every $\boldsymbol{v} \in \boldsymbol{V_h}$ there exist $\boldsymbol{w} \in \boldsymbol{\mathcal{W}}$ and $\boldsymbol{v}_0 \in \boldsymbol{V_h}$ such that $\boldsymbol{v} = \boldsymbol{v}_0 + \Pi_{\boldsymbol{\mathcal{W}}}\boldsymbol{w}$ and there exists $C_0^2 > 0$ independent of $\boldsymbol{v}$, such that*

$$\inf_{\substack{\boldsymbol{v}_0 \in \boldsymbol{V_h}, \boldsymbol{w} \in \boldsymbol{\mathcal{W}} \\ \boldsymbol{v} = \boldsymbol{v}_0 + \Pi_{\boldsymbol{\mathcal{W}}}\boldsymbol{w}}} \{s(\boldsymbol{v}_0, \boldsymbol{v}_0) + a_{\boldsymbol{\mathcal{W}}}(\boldsymbol{w}, \boldsymbol{w})\} \leq C_0^2\, \mathrm{a}_{DG}(\boldsymbol{v}, \boldsymbol{v}), \qquad \forall\, \boldsymbol{v} = \boldsymbol{v}_0 + \Pi_{\boldsymbol{\mathcal{W}}}\boldsymbol{w}\,.$$

Then, a direct application of the fictitious space Theorem 3.1 yields $\kappa(\mathbb{B}\mathbb{A}) \leq C_0^2(c_s + c_{\boldsymbol{\mathcal{W}}})$.

3.2 Auxiliary space preconditioners for the IP-DG discretization in $\mathrm{H}_0(\mathbf{curl}, \Omega)$

In the present work, we consider the DG space $\boldsymbol{V_h}$ defined in (2.1) with local spaces $\mathcal{M}(T)$ as described in Section 2. Concerning the auxiliary space, the following choices are adopted:

(a) Let $\boldsymbol{\mathcal{W}}$ be the finite element space $\boldsymbol{\mathcal{W}} = \boldsymbol{V_h} \cap \mathrm{H}_0(\mathbf{curl}, \Omega)$, i.e.

$$\boldsymbol{\mathcal{W}} := \boldsymbol{V_h^c} = \{\boldsymbol{w} \in \mathrm{H}_0(\mathbf{curl}, \Omega) : \boldsymbol{w}|_T \in \mathcal{M}(T),\, T \in \mathcal{T}_h\}\,, \tag{3.5}$$

for any choice of the local space $\mathcal{M}(T)$ as in (2.2), (2.3) or (2.4), and endowed with the bilinear form $a_{\boldsymbol{\mathcal{W}}}(\cdot,\cdot)$ deriving from the $\mathrm{H}_0(\mathbf{curl}, \Omega)$-conforming finite element approximation of the model problem (1.1). That is,

$$a_{\boldsymbol{\mathcal{W}}}(\boldsymbol{\chi}, \boldsymbol{w}) := \sum_{T \in \mathcal{T}_h} (\nu_T \boldsymbol{\nabla} \times \boldsymbol{\chi}, \boldsymbol{\nabla} \times \boldsymbol{w})_{0,T} + \sum_{T \in \mathcal{T}_h} (\beta_T \boldsymbol{\chi}, \boldsymbol{w})_{0,T}\,, \qquad \forall\, \boldsymbol{\chi}, \boldsymbol{w} \in \boldsymbol{V_h^c}\,.$$

Note that, as observed in Section 2, $a_{\boldsymbol{\mathcal{W}}}(\cdot,\cdot)$ is nothing but the restriction of the bilinear form $\mathrm{a}_{\mathrm{DG}}(\cdot,\cdot)$ in (2.7) to the $\mathrm{H}_0(\mathbf{curl}, \Omega)$-conforming finite element space $\boldsymbol{V_h^c}$, namely

$$a_{\boldsymbol{\mathcal{W}}}(\boldsymbol{u}, \boldsymbol{v}) = \mathrm{a}_{\mathrm{DG}}(\boldsymbol{u}, \boldsymbol{v})\,, \qquad \forall\, \boldsymbol{u}, \boldsymbol{v} \in \boldsymbol{V_h^c}\,.$$

The associated operator $\mathcal{A}_{\boldsymbol{\mathcal{W}}} : \boldsymbol{V_h^c} \to (\boldsymbol{V_h^c})'$ is self-adjoint and positive definite. The transfer operator $\Pi_{\boldsymbol{\mathcal{W}}} : \boldsymbol{V_h^c} \to \boldsymbol{V_h}$ is trivially the standard inclusion.

(b) On a simplicial mesh, if $\boldsymbol{V_h}$ is the DG space (2.1) with local space $\mathcal{M}(T) = \mathcal{N}^{II}(T)$ as in (2.2), we consider a second choice for the auxiliary space. Let $\boldsymbol{\mathcal{W}}$ be the $\mathrm{H}_0(\mathbf{curl}, \Omega)$-conforming finite element space based on local polynomial spaces of type $\mathcal{N}^I(T)$ as in (2.3), i.e.

$$\boldsymbol{\mathcal{W}} := \boldsymbol{W_h^c} = \{\boldsymbol{w} \in \mathrm{H}_0(\mathbf{curl}, \Omega) : \boldsymbol{w}|_T \in \mathcal{N}^I(T),\, T \in \mathcal{T}_h\}\,. \tag{3.6}$$

Note that $\boldsymbol{W_h^c} \subset \boldsymbol{V_h^c} \subset \boldsymbol{V_h}$. The space $\boldsymbol{W_h^c}$ is endowed with the inner product $a_{\boldsymbol{\mathcal{W}}}(\cdot,\cdot)$ corresponding to the $\mathrm{H}_0(\mathbf{curl}, \Omega)$-conforming approximation based on $\boldsymbol{W_h^c}$. Hence, the corresponding induced operator $\mathcal{A}_{\boldsymbol{\mathcal{W}}} : \boldsymbol{W_h^c} \to (\boldsymbol{W_h^c})'$ is self-adjoint and positive definite, and the transfer operator $\Pi_{\boldsymbol{\mathcal{W}}} : \boldsymbol{W_h^c} \to \boldsymbol{V_h}$ is defined as the standard inclusion.

Observe that condition **(F0)** in Theorem 3.2 is trivially satisfied for both the above choices since the transfer operator $\Pi_{\boldsymbol{\mathcal{W}}}$ is the standard inclusion. Furthermore, in both cases $\boldsymbol{\mathcal{W}} = \boldsymbol{V_h^c}$ or $\boldsymbol{\mathcal{W}} = \boldsymbol{W_h^c}$, the constant in (3.4) is $c_{\boldsymbol{\mathcal{W}}} = 1$ in view of the fact that $a_{\boldsymbol{\mathcal{W}}}(\cdot,\cdot)$ is the restriction of $\mathrm{a}_{\mathrm{DG}}(\cdot,\cdot)$ to the corresponding $\mathrm{H}(\mathbf{curl}, \Omega)$-conforming spaces. Therefore, inequality (3.4) becomes an identity.

3.3 Smoothers for the auxiliary space preconditioner

To assess the performance of the proposed family of preconditioners, the choices of the auxiliary space described in Section 3.2 are combined with different possible smoothing operators $\mathcal{S} : \boldsymbol{V_h} \to \boldsymbol{V_h'}$. We now briefly introduce our choice of relaxation techniques (non-overlapping and overlapping) as subspace correction (SC) methods [90], and postpone to Section 4.2 their theoretical analysis. We focus on two main types: pointwise relaxation and patch smoothers.

Pointwise relaxation or non-overlapping SC: Since the Galerkin matrix $\mathbb{A}$ associated to the DG discretization of the model problem (2.6) is symmetric positive definite, we focus on Jacobi-type smoothers. Indeed, by virtue of [92, Lemma 3.3], the pointwise symmetric Gauss-Seidel smoother is spectrally equivalent to the corresponding Jacobi smoother, with constants independent of the problem coefficients and mesh size.

Our smoother are defined as non-overlapping additive Schwarz smoothers based on the following splittings of $\boldsymbol{V_h}$:

(i) Pointwise Jacobi smoother:

$$\boldsymbol{V_h} = \bigoplus_{T\in\mathcal{T}_h} \left(\sum_{e\in\mathcal{E}(T)} \sum_{i=1}^{N_e} \mathrm{span}\{\boldsymbol{\varphi}^i_{e,T}\} + \sum_{f\in\mathcal{F}(T)} \sum_{i=1}^{N_f} \mathrm{span}\{\boldsymbol{\varphi}^i_{f,T}\} + \sum_{i=1}^{N_b} \mathrm{span}\{\boldsymbol{\varphi}^i_{T}\} \right); \tag{3.7}$$

(ii) Block Jacobi smoother:

$$\boldsymbol{V_h} = \bigoplus_{T\in\mathcal{T}_h} \mathrm{span}\{\boldsymbol{\varphi}^1_{e,T}, \dots, \boldsymbol{\varphi}^{N_e}_{e,T}, \boldsymbol{\varphi}^1_{f,T}, \dots, \boldsymbol{\varphi}^{N_f}_{f,T}, \boldsymbol{\varphi}^1_{T}, \dots, \boldsymbol{\varphi}^{N_b}_{T}\}. \tag{3.8}$$

In Lemma 4.4 we will show that the (non-overlapping) block Jacobi smoother associated with (3.8) is spectrally equivalent to the pointwise Jacobi relaxation relative to the splitting (3.7).

Patch smoothers or overlapping SC methods: When the auxiliary space $\boldsymbol{\mathcal{W}}$ is "coarser" than $\boldsymbol{V_h^c}$, i.e., is of type (b) as in Section 3.2, a local relaxation will not be effective (see Remark 3.3 and the numerical experiments in Section 5) and one needs to resort to patch smoothers. For their description and analysis one can rely on overlapping additive Schwarz methods [48] or on the subspace correction method [90]. We consider the decomposition of $\boldsymbol{V_h}$ as a sum of spaces supported in small patches of elements. In particular, let $\mathcal{N}_h$ denote the set of all vertices of the mesh $\mathcal{T}_h$ and let y be either a vertex in $\mathcal{N}_h$, an edge in $\mathcal{E}_h$ or an element of the mesh $\mathcal{T}_h$. We denote generically by Ω_y the patch related to y, i.e.

$$\Omega_y = \{T \in \mathcal{T}_h : \text{“}y \subset T\text{”}\}, \qquad y \in \mathcal{N}_h \cup \mathcal{E}_h \cup \mathcal{T}_h ,$$

where the precise definition of the relation "$y \subset T$" is specified below in (3.9), (3.10) and (3.11) for each case. The corresponding subspace associated to each patch is defined as

$$\boldsymbol{V_h^{\Omega_y}} = \{\boldsymbol{v} \in \boldsymbol{V_h} : \mathrm{supp}(\boldsymbol{v}) \subseteq \Omega_y\}, \qquad y \in \mathcal{N}_h \cup \mathcal{E}_h \cup \mathcal{T}_h .$$

We therefore have the following (overlapping) space decompositions:

$$\boldsymbol{V_h} = \sum_{x\in\mathcal{N}_h} \boldsymbol{V_h}^{\Omega_x}, \qquad \Omega_x = \{T \in \mathcal{T}_h : x \in \partial T\}, \tag{3.9}$$

$$\boldsymbol{V_h} = \sum_{e\in\mathcal{E}_h} \boldsymbol{V_h}^{\Omega_e}, \qquad \Omega_e = \{T \in \mathcal{T}_h : e \subset \partial T\} =: \mathcal{T}(e), \tag{3.10}$$

$$\boldsymbol{V_h} = \sum_{T\in\mathcal{T}_h} \boldsymbol{V_h}^{\Omega_T}, \qquad \Omega_T = \{T' \in \mathcal{T}_h : \partial T' \cap \partial T \in \mathcal{E}_h\}. \tag{3.11}$$

Observe that

$$\Omega \subseteq \bigcup_{x\in\mathcal{N}_h} \Omega_x, \qquad \Omega \subseteq \bigcup_{e\in\mathcal{E}_h} \Omega_e, \qquad \Omega \subseteq \bigcup_{T\in\mathcal{T}_h} \Omega_T\,. \tag{3.12}$$

Moreover, since $\boldsymbol{V_h}$ is a space of piecewise discontinuous polynomials, there are no continuity constraints imposed in the above space splittings.

In order to define the additive overlapping Schwarz (or additive subspace correction method) associated to a given domain decomposition Ω_y as in (3.9), (3.10) or (3.11), we first consider the restriction of the IP-DG method (2.6) to the subspace $\boldsymbol{V_h}^{\Omega_y}$, namely the bilinear form in (2.7) becomes:

$$\begin{aligned}
\mathrm{a}_{\mathrm{DG}}^{\Omega_y}(\boldsymbol{v},\boldsymbol{v}) = &\sum_{T\in\Omega_y} \left(\nu_T\|\boldsymbol{\nabla}\times\boldsymbol{v}\|_{0,T}^2 + \beta_T\|\boldsymbol{v}\|_{0,T}^2\right) - 2\sum_{f\in\mathcal{F}_h^o\cap\Omega_y\setminus\partial\Omega_y} (\{\!\!\{\nu\boldsymbol{\nabla}\times\boldsymbol{v}\}\!\!\}_\gamma\,, [\![\,\boldsymbol{v}\,]\!]_{\boldsymbol{\tau}})_{0,f}\\
&+\sum_{T\in\Omega_y}\alpha_T(\nu)\sum_{e\in\mathcal{E}(T)}\sum_{f\in\mathcal{F}(e)\setminus\partial\Omega_y}(s_f[\![\,\boldsymbol{v}\,]\!]_{\boldsymbol{\tau}}\,,[\![\,\boldsymbol{v}\,]\!]_{\boldsymbol{\tau}})_{0,f} - \sum_{f\in\mathcal{F}_h^o\cap\partial\Omega_y}\{\!\!\{\nu\}\!\!\}_{H,f}\,(\mathbf{n}\times\boldsymbol{v},\boldsymbol{\nabla}\times\boldsymbol{v})_{0,f}\\
&+\sum_{\substack{T\in\Omega_y\\ \partial T\cap\partial\Omega_y\neq\emptyset}}\alpha_T(\nu)\sum_{e\in\mathcal{E}(T)}\sum_{f\in\mathcal{F}(e)\cap\partial\Omega_y}(s_f\,\mathbf{n}\times\boldsymbol{v}\;,\mathbf{n}\times\boldsymbol{v})_{0,f} \qquad\qquad \forall\,\boldsymbol{v}\in\boldsymbol{V_h}^{\Omega_y}\,.
\end{aligned}\tag{3.13}$$

The above bilinear form defines the local solvers for $\Omega_y\cap\partial\Omega=\emptyset$. For those patches touching the boundary of Ω, the fourth term in the above sum is modified having ν_T instead of $\{\!\!\{\nu\}\!\!\}_{H,f}$. Denoting now by J_y the cardinality of the patches required to cover the domain, the additive Schwarz smoother is defined as

$$s_O(\boldsymbol{v},\boldsymbol{v}) := \sum_{j=1}^{J_y}\mathrm{a}_{\mathrm{DG}}^{\Omega_y}(\boldsymbol{v}_j,\boldsymbol{v}_j) \qquad \text{with} \qquad \boldsymbol{v} = \sum_{j=1}^{J_y}\boldsymbol{v}_j\,, \qquad \boldsymbol{v}_j\in\boldsymbol{V_h}^{\Omega_y}\,. \tag{3.14}$$

Remark 3.3. It is worth pointing out that, as we will show in Lemma 4.19 and observe numerically, the use of a block oriented smoother in the preconditioner $\mathcal{B}$ is only essential when the auxiliary space $\boldsymbol{\mathcal{W}}$ is *coarser* than $\boldsymbol{V_h^c}$; i.e., is of the type (b). The requirement of using overlapping block-type smoothers in two-level and multi-level preconditioners for the finite element approximation of (1.1) has been observed (and illustrated numerically) in the literature by many authors and for different approaches [60, 59, 11]. The basic rigorous mathematical justification that a pointwise smoother in a two level preconditioner will not provide a convergent method, is given in [92] where a lower bound of order $1-ch^2$ on the convergence rate of such two level preconditioner is derived. More precisely, in [92, Section 4] the author provides an explicit construction of a function that *cannot be seen* by the coarse solver and cannot be damped by a pointwise relaxation. Here, as we will show in Lemma 4.19, the use of a pointwise smoother would *break* the edge bubbles (not seen by the auxiliary space) leading to a component with arbitrary high energy, that cannot be damped.

4 Asymptotic optimality of preconditioner

This section is devoted to the analysis of the preconditioners introduced in Section 3.2 and Section 3.3. We first state and discuss the main results. Then some basic auxiliary estimates required in the convergence analysis are introduced. Finally, we prove conditions **(F1)** and **(F2)** of Theorem 3.2.

Theorem 4.1. *Let $\mathbb{B}$ be the auxiliary space preconditioner as defined in* (3.3) *and associated to one of the following:*

(i) Auxiliary space $\boldsymbol{\mathcal{W}}=\boldsymbol{V_h^c}$ as in (3.5) *and Jacobi smoother relative to the splitting of $\boldsymbol{V_h}$* (3.7) *or* (3.8)*;*

(ii) Auxiliary space $\boldsymbol{\mathcal{W}} = \boldsymbol{W_h^c}$ as in (3.6) *and overlapping patch smoother as in* (3.14) *and* (3.13).

Then,

$$\kappa(\mathbb{BA}) \le c_0^2\,(1+c_s) = c_a\,(1+c_s)\max\{1,\delta(\nu,\beta)\}\,,$$

where

$$\delta(\nu,\beta) := \min\left\{ \max_{T\in\mathcal{T}_h} \frac{h_T^2\beta_T}{\nu_T},\ \max_{\substack{T,T'\in\mathcal{T}_h\\ \partial T\cap\partial T'\neq\emptyset}} \frac{\beta_T}{\beta_{T'}},\ \max_{\substack{T\in\Delta_h, T'\in\Delta_h'\\ \partial T\cap\partial T'\neq\emptyset}} \frac{\alpha_T(\nu)}{\alpha_{T'}(\nu)} \right\}\,, \tag{4.1}$$

*where Δ_h denotes the set of elements in the **curl**-dominated regime and Δ_h' denote the elements in a reaction dominated region (see* (4.37)*). The constants c_s, c_a depend only on the polynomial degree and on the shape regularity of the mesh.*

The proof of the above Theorem relies on the application of the fictitious space Theorem 3.1 and therefore boils down to the verification of conditions **(F0)**, **(F1)** and **(F2)** in Theorem 3.2. As pointed out in the description of the preconditioners in Section 3.2, condition **(F0)** is trivially satisfied in all cases, as it can be plainly seen from the definition of $a_{\boldsymbol{\mathcal{W}}}(\cdot,\cdot)$ and due to the fact that $\Pi_{\boldsymbol{\mathcal{W}}}$ is the standard inclusion. Therefore, we are left with showing Properties **(F1)** and **(F2)**.

4.1 Auxiliary results: Local estimates

In the analysis of the preconditioners some basic local estimates will be instrumental. These results are therefore collected in the next Lemma whose proof relies on standard arguments and the equivalence of all norms in finite dimensional spaces and it is therefore relegated to Appendix A. We refer the interested reader to [58, Lemma 3.12], [74, Lemma 5.43] and references therein.

Lemma 4.2. *Let $T\in\mathcal{T}_h$ be an arbitrary element and let $\widehat{T}$ be the corresponding reference element (unit tetrahedron, or unit cube) under an invertible affine map $F_T(\widehat{\mathbf{x}}) = B_T\widehat{\mathbf{x}}+c_T$. Let $\boldsymbol{v}\in\mathcal{M}(T)$ be represented as in* (2.5) *and let $\widehat{\boldsymbol{v}}$ denote the function defined through a contravariant transformation, $\widehat{\boldsymbol{v}} = B_T^T\boldsymbol{v}\circ F_T$. Then, there exists $C>0$ depending only on the polynomial degree and the shape regularity of the mesh, such that the following inequalities hold:*

$$\|\boldsymbol{v}\|_{0,T}^2 \le C h_T \|\widehat{\boldsymbol{v}}\|_{0,\widehat{T}}^2\,, \qquad \|\widehat{\boldsymbol{v}}\|_{0,\widehat{T}}^2 \le C h_T^{-1}\|\boldsymbol{v}\|_{0,T}^2\,, \tag{4.2}$$

$$\|\nabla\times\boldsymbol{v}\|_{0,T}^2 \le C h_T^{-1}\|\widehat{\nabla}\times\widehat{\boldsymbol{v}}\|_{0,\widehat{T}}^2\,, \qquad \|\widehat{\nabla}\times\widehat{\boldsymbol{v}}\|_{0,\widehat{T}}^2 \le C h_T\|\nabla\times\boldsymbol{v}\|_{0,T}^2\,, \tag{4.3}$$

and for $f\in\partial T$ image of the reference face $\widehat{f}\in\partial\widehat{T}$ under F_T,

$$\int_f |\mathbf{n}\times\boldsymbol{v}|^2\,ds \le C\int_{\widehat{f}}|\widehat{\mathbf{n}}\times\widehat{\boldsymbol{v}}|^2\,d\widehat{s}\,, \qquad \int_{\widehat{f}}|\widehat{\mathbf{n}}\times\widehat{\boldsymbol{v}}|^2\,d\widehat{s} \le C\int_f|\mathbf{n}\times\boldsymbol{v}|^2\,ds\,. \tag{4.4}$$

Moreover, there exist C_1, C_2, $C_3>0$ such that

$$C_1\|\widehat{\nabla}\times\widehat{\boldsymbol{v}}\|_{0,\widehat{T}}^2 \le C_2\|\widehat{\boldsymbol{v}}\|_{0,\widehat{T}}^2 \le \sum_{e\in\mathcal{E}(T)}\|\boldsymbol{v}_{e,T}\|_{\ell^2}^2 + \sum_{f\in\mathcal{F}(T)}\|\boldsymbol{v}_{f,T}\|_{\ell^2}^2 + \|\boldsymbol{v}_T\|_{\ell^2}^2 \le C_3\|\widehat{\boldsymbol{v}}\|_{0,\widehat{T}}^2\,, \tag{4.5}$$

where $\|\cdot\|_{\ell^2}$ denotes the standard Euclidean norm. Finally, there exist C_4, $C_5>0$ such that

$$C_4\int_{\widehat{f}}|\widehat{\mathbf{n}}\times\widehat{\boldsymbol{v}}|^2\,d\widehat{s} \le \sum_{e\in\mathcal{E}(f)}\|\boldsymbol{v}_{e,T}\|_{\ell^2}^2 + \|\boldsymbol{v}_{f,T}\|_{\ell^2}^2 \le C_5\int_{\widehat{f}}|\widehat{\mathbf{n}}\times\widehat{\boldsymbol{v}}|^2\,d\widehat{s}\,, \tag{4.6}$$

where $\mathcal{E}(f)$ denotes the set of edges of f.

Note that, as shown in [58, Equation (3.37)], the affine equivalence techniques deployed in the previous Lemma 4.2 allow to establish the L^2-stability of the local basis functions of $\boldsymbol{V_h}$. As immediate consequence of Lemma 4.2, we can derive the following:

Lemma 4.3. *Let $f = \partial T^- \cap \partial T^+$ be an interior face. There exist C_1, $C_2 > 0$ depending only on the polynomial degree and the shape regularity of the mesh such that for all $\boldsymbol{v} \in \boldsymbol{V_h}$*

$$C_1 \int_f |[\![\boldsymbol{v}]\!]_{\boldsymbol{\tau}}|^2 \, ds \leq \left\| \boldsymbol{v}_{f,T^+} - \boldsymbol{v}_{f,T^-} \right\|_{\ell^2}^2 + \sum_{e \in \mathcal{E}(f)} \left\| \boldsymbol{v}_{e,T^+} - \boldsymbol{v}_{e,T^-} \right\|_{\ell^2}^2 \leq C_2 \int_f |[\![\boldsymbol{v}]\!]_{\boldsymbol{\tau}}|^2 \, ds \,. \tag{4.7}$$

Proof. Let $\boldsymbol{v}^{\pm} \in \mathcal{M}(T^{\pm})$ denote the restrictions of $\boldsymbol{v} \in \boldsymbol{V_h}$ to $T^{\pm}$. By definition of tangential jump and normal unit vector, one has $[\![\boldsymbol{v}]\!]_{\boldsymbol{\tau}} = \mathbf{n}^+ \times \boldsymbol{v}^+ + \mathbf{n}^- \times \boldsymbol{v}^- = \mathbf{n}^+ \times (\boldsymbol{v}^+ - \boldsymbol{v}^-)$. Then, the function $\boldsymbol{w} = (\boldsymbol{v}^+ - \boldsymbol{v}^-)$ has degrees of freedom given by $\{v^i_{f,T^+} - v^i_{f,T^-}\}_{i=1}^{N_f}$ and $\{v^i_{e,T^+} - v^i_{e,T^-}\}_{i=1}^{N_e}$ for every $e \in \mathcal{E}(f)$. Using a contravariant transformation, as in Lemma 4.2, we can apply (4.6) to get the desired equivalence on the reference element

$$C_4 \int_{\widehat{f}} |\widehat{\mathbf{n}}^+ \times \widehat{\boldsymbol{w}}|^2 \, d\widehat{s} \leq \left\| \boldsymbol{v}_{f,T^+} - \boldsymbol{v}_{f,T^-} \right\|_{\ell^2}^2 + \sum_{e \in \mathcal{E}(f)} \left\| \boldsymbol{v}_{e,T^+} - \boldsymbol{v}_{e,T^-} \right\|_{\ell^2}^2 \leq C_5 \int_{\widehat{f}} |\widehat{\mathbf{n}}^+ \times \widehat{\boldsymbol{w}}|^2 \, d\widehat{s} \,.$$

Applying estimate (4.4) from Lemma 4.2 and substituting $\mathbf{n}^+ \times \boldsymbol{w} = [\![\boldsymbol{v}]\!]_{\boldsymbol{\tau}}$, results in (4.7). □

4.2 Smoothers

In this section we deal with the analysis of the smoothers introduced in Section 3.3. In particular, for each smoother, this involves not only proving that property (**F1**) is fulfilled (and therefore the smoothing operator has continuous and uniformly bounded inverse), but also determining how the operator $\mathcal{S}$ scales in relation with the identity operator. The corresponding result for the pointwise relaxation methods defined in (4.9) and (4.10) is given in the next Lemma.

Lemma 4.4. *Let $s(\cdot,\cdot)$ denote any of the bilinear forms associated to the pointwise Jacobi or block-Jacobi smoothers as defined in the splittings of $\boldsymbol{V_h}$ in (3.7) and (3.8), respectively. Then, there exists $c_s > 0$ independent of the mesh size and the coefficients of the problems but depending on the local polynomial space and on the shape regularity of the mesh such that*

$$c_s^{-1} a_{DG}(\boldsymbol{v}, \boldsymbol{v}) \leq s(\boldsymbol{v}, \boldsymbol{v}) \qquad \forall \boldsymbol{v} \in \boldsymbol{V_h} \,.$$

Moreover, $s(\cdot,\cdot)$ satisfies

$$s(\boldsymbol{v}, \boldsymbol{v}) \leq C \sum_{T \in \mathcal{T}_h} \nu_T h_T^{-2} \|\boldsymbol{v}\|_{0,T}^2 + \sum_{T \in \mathcal{T}_h} \beta_T \|\boldsymbol{v}\|_{0,T}^2 + \sum_{T \in \mathcal{T}_h} \alpha_T(\nu) h_T^{-2} \|\boldsymbol{v}\|_{0,T}^2 \,, \quad \forall \boldsymbol{v} \in \boldsymbol{V_h} \,, \tag{4.8}$$

with $C > 0$ depending on the local polynomial space and on the shape regularity of the mesh.

Proof. To define the bilinear form $s(\cdot,\cdot)$ relative to Jacobi smoother associated to the space splitting (3.7) we make use of the representation (2.5) of functions in $\boldsymbol{V_h}$ where each basis function $\{\boldsymbol{\varphi}^i_{e,T}\}_{i=1}^{N_e}$, $\{\boldsymbol{\varphi}^i_{f,T}\}_{i=1}^{N_f}$, $\{\boldsymbol{\varphi}^i_{T}\}_{i=1}^{N_b}$ is now considered as a *global* basis function on Ω extended by zero outside of its support. The pointwise Jacobi relaxation reads:

$$\begin{aligned} s_J(\boldsymbol{v}, \boldsymbol{v}) := & \sum_{T \in \mathcal{T}_h} \sum_{e \in \mathcal{E}(T)} \sum_{i=1}^{N_e} \mathrm{a_{DG}}(\boldsymbol{\varphi}^i_{e,T}, \boldsymbol{\varphi}^i_{e,T}) (v^i_{e,T})^2 \\ & + \sum_{T \in \mathcal{T}_h} \sum_{f \in \mathcal{F}(T)} \sum_{i=1}^{N_f} \mathrm{a_{DG}}(\boldsymbol{\varphi}^i_{f,T}, \boldsymbol{\varphi}^i_{f,T}) (v^i_{f,T})^2 + \sum_{T \in \mathcal{T}_h} \sum_{i=1}^{N_b} \mathrm{a_{DG}}(\boldsymbol{\varphi}^i_{T}, \boldsymbol{\varphi}^i_{T}) (v^i_{T})^2 \,, \end{aligned} \tag{4.9}$$

whilst the block Jacobi operator, using as blocks the elements $T \in \mathcal{T}_h$ of the mesh, has bilinear form

$$
\begin{aligned}
s_{Jb}(\boldsymbol{v}, \boldsymbol{v}) := & \sum_{T\in\mathcal{T}_h} \sum_{e\in\mathcal{E}(T)} \sum_{e'\in\mathcal{E}(T)} \sum_{i=1}^{N_e} \mathrm{a}_{\mathrm{DG}}(\boldsymbol{\varphi}^i_{e,T}, \boldsymbol{\varphi}^i_{e',T}) v^i_{e,T} v^i_{e',T} \\
& + \sum_{T\in\mathcal{T}_h} \sum_{f\in\mathcal{F}(T)} \sum_{f'\in\mathcal{F}(T)} \sum_{i=1}^{N_f} \mathrm{a}_{\mathrm{DG}}(\boldsymbol{\varphi}^i_{f,T}, \boldsymbol{\varphi}^i_{f',T}) v^i_{f,T} v^i_{f',T} + \sum_{T\in\mathcal{T}_h} \sum_{i=1}^{N_b} \mathrm{a}_{\mathrm{DG}}(\boldsymbol{\varphi}^i_{T}, \boldsymbol{\varphi}^i_{T}) (v^i_T)^2 .
\end{aligned}
\tag{4.10}
$$

As it will be clear from the proof, it is enough to focus on the lowest order case, namely for local degrees of freedom given by $\{v^i_{e,T}\}_{i=1}^{N_e}$ for $T \in \mathcal{T}_h$, $e \in \mathcal{E}(T)$ with $N_e \leq 2$. The general case (as given in (4.9) and (4.10)) can be shown by arguing exactly in the same way for the terms involving faces and elements degrees of freedom.

First we prove continuity of the pointwise smoother. Using the representation (2.5), Cauchy-Schwarz inequality and the arithmetic-geometric inequality yield

$$
\begin{aligned}
\mathrm{a}_{\mathrm{DG}}(\boldsymbol{v}, \boldsymbol{v}) &= \sum_{T\in\mathcal{T}_h} \sum_{e\in\mathcal{E}(T)} \sum_{\substack{T'\in\mathcal{T}_h,\\ \partial T'\cap\partial T\neq\emptyset}} \sum_{e'\in\mathcal{E}(T')} \sum_{i=1}^{N_e} \mathrm{a}_{\mathrm{DG}}(\boldsymbol{\varphi}^i_{e,T}, \boldsymbol{\varphi}^i_{e',T'}) v^i_{e,T} v^i_{e',T'} \\
&\leq \sum_{T\in\mathcal{T}_h} \sum_{e\in\mathcal{E}(T)} \sum_{\substack{T'\in\mathcal{T}_h,\\ \partial T'\cap\partial T\neq\emptyset}} \sum_{e'\in\mathcal{E}(T')} \sum_{i=1}^{N_e} \sqrt{\mathrm{a}_{\mathrm{DG}}(\boldsymbol{\varphi}^i_{e,T}, \boldsymbol{\varphi}^i_{e,T})} \sqrt{\mathrm{a}_{\mathrm{DG}}(\boldsymbol{\varphi}^i_{e',T'}, \boldsymbol{\varphi}^i_{e',T'})} v^i_{e,T} v^i_{e',T'} \\
&\leq \frac{1}{2} \sum_{T\in\mathcal{T}_h} \sum_{e\in\mathcal{E}(T)} \sum_{\substack{T'\in\mathcal{T}_h,\\ \partial T'\cap\partial T\neq\emptyset}} \sum_{e'\in\mathcal{E}(T')} \sum_{i=1}^{N_e} \left(\mathrm{a}_{\mathrm{DG}}(\boldsymbol{\varphi}^i_{e,T}, \boldsymbol{\varphi}^i_{e,T}) (v^i_{e,T})^2 + \mathrm{a}_{\mathrm{DG}}(\boldsymbol{\varphi}^i_{e',T'}, \boldsymbol{\varphi}^i_{e',T'}) (v^i_{e',T'})^2 \right) \\
&\leq C \sum_{T\in\mathcal{T}_h} \sum_{e\in\mathcal{E}(T)} \sum_{i=1}^{N_e} \mathrm{a}_{\mathrm{DG}}(\boldsymbol{\varphi}^i_{e,T}, \boldsymbol{\varphi}^i_{e,T}) (v^i_{e,T})^2 = C s_J(\boldsymbol{v}, \boldsymbol{v}) ,
\end{aligned}
$$

where the constant C depends on the shape regularity of $\mathcal{T}_h$. In order to prove (4.8), note that the continuity and stability of the bilinear form $\mathrm{a}_{\mathrm{DG}}(\cdot,\cdot)$ hold for each of the basis functions (considered as global functions). In particular, for all $i = 1, \ldots, N_e$, we have

$$
C_{\mathrm{stab}} \|\boldsymbol{\varphi}^i_{e,T}\|^2_{\mathrm{DG}} \leq \mathrm{a}_{\mathrm{DG}}(\boldsymbol{\varphi}^i_{e,T}, \boldsymbol{\varphi}^i_{e,T}) \leq C_{\mathrm{cont}} \|\boldsymbol{\varphi}^i_{e,T}\|^2_{\mathrm{DG}} ,
$$

and therefore $\mathrm{a}_{\mathrm{DG}}(\boldsymbol{\varphi}^i_{e,T}, \boldsymbol{\varphi}^i_{e,T}) \simeq C \|\boldsymbol{\varphi}^i_{e,T}\|^2_{\mathrm{DG}}$ where the constant C depends on the stability and continuity constants of $\mathrm{a}_{\mathrm{DG}}(\cdot,\cdot)$. Moreover, exploiting (4.2) and the inequalities (4.3) and (4.4), together with (4.5) and (4.6) from Lemma 4.2, results in the following standard inverse inequalities

$$
\|\boldsymbol{\nabla} \times \boldsymbol{\varphi}^i_{e,T}\|^2_{0,T} \leq C h_T^{-2} \|\boldsymbol{\varphi}^i_{e,T}\|^2_{0,T} , \qquad \|\mathbf{n} \times \boldsymbol{\varphi}^i_{e,T}\|^2_{0,f} \leq C h_T^{-1} \|\boldsymbol{\varphi}^i_{e,T}\|^2_{0,T} ,
$$

where shape regularity has been used. Hence, recalling the definition of the $\|\cdot\|_{\mathrm{DG}}$ norm (2.15), it holds

$$
\begin{aligned}
s_J(\boldsymbol{v}, \boldsymbol{v}) \simeq & \sum_{T\in\mathcal{T}_h} \sum_{e\in\mathcal{E}(T)} \sum_{i=1}^{N_e} (v^i_{e,T})^2 \left(\nu_T \|\boldsymbol{\nabla} \times \boldsymbol{\varphi}^i_{e,T}\|^2_{0,T} + \beta_T \|\boldsymbol{\varphi}^i_{e,T}\|^2_{0,T} \right) \\
& + \sum_{T\in\mathcal{T}_h} \alpha_T(\nu) \sum_{e\in\mathcal{E}(T)} \sum_{f\in\mathcal{F}(e)\cap\mathcal{F}(T)} \sum_{i=1}^{N_e} h_f^{-1} (v^i_{e,T})^2 \|\mathbf{n} \times \boldsymbol{\varphi}^i_{e,T}\|^2_{0,f}
\end{aligned}
$$

$$
\begin{aligned}
&\le C \sum_{T\in\mathcal{T}_h} \sum_{e\in\mathcal{E}(T)} \sum_{i=1}^{N_e} (v_{e,T}^i)^2 \left(\nu_T h_T^{-2} \|\boldsymbol{\varphi}_{e,T}^i\|_{0,T}^2 + \beta_T \|\boldsymbol{\varphi}_{e,T}^i\|_{0,T}^2\right) \\
&\quad + \sum_{T\in\mathcal{T}_h} \alpha_T(\nu) \sum_{e\in\mathcal{E}(T)} \sum_{i=1}^{N_e} (v_{e,T}^i)^2 \sum_{f\in\mathcal{F}(e)\cap\mathcal{F}(T)} h_f^{-1} h_T^{-1} \|\boldsymbol{\varphi}_{e,T}^i\|_{0,T}^2 \\
&\le C \sum_{T\in\mathcal{T}_h} \nu_T h_T^{-2} \|\boldsymbol{v}\|_{0,T}^2 + \sum_{T\in\mathcal{T}_h} \beta_T \|\boldsymbol{v}\|_{0,T}^2 + \sum_{T\in\mathcal{T}_h} \alpha_T(\nu) h_T^{-2} \|\boldsymbol{v}\|_{0,T}^2 \,,
\end{aligned}
$$

with $C > 0$ depending on the mesh $\mathcal{T}_h$ through its shape-regularity. For the block Jacobi smoother s_{Jb} in (4.10), using the short-hand notation $\boldsymbol{v}_i := \boldsymbol{v}|_{T_i}$, Cauchy-Schwarz inequality gives

$$
\begin{aligned}
\mathrm{a}_{\mathrm{DG}}(\boldsymbol{v},\boldsymbol{v}) &= \mathrm{a}_{\mathrm{DG}}\Bigg(\sum_{T_i\in\mathcal{T}_h} \boldsymbol{v}_i, \sum_{\substack{T_j\in\mathcal{T}_h,\\ \partial T_i\cap\partial T_j\neq\emptyset}} \boldsymbol{v}_j \Bigg) \le \sum_{T_i\in\mathcal{T}_h} \sum_{\substack{T_j\in\mathcal{T}_h,\\ \partial T_i\cap\partial T_j\neq\emptyset}} \sqrt{\mathrm{a}_{\mathrm{DG}}(\boldsymbol{v}_i,\boldsymbol{v}_i)}\sqrt{\mathrm{a}_{\mathrm{DG}}(\boldsymbol{v}_j,\boldsymbol{v}_j)} \\
&\le \frac{1}{2} \sum_{T_i\in\mathcal{T}_h} \sum_{\substack{T_j\in\mathcal{T}_h,\\ \partial T_i\cap\partial T_j\neq\emptyset}} \left(\mathrm{a}_{\mathrm{DG}}(\boldsymbol{v}_i,\boldsymbol{v}_i) + \mathrm{a}_{\mathrm{DG}}(\boldsymbol{v}_j,\boldsymbol{v}_j)\right) \le C \sum_{T_i\in\mathcal{T}_h} \mathrm{a}_{\mathrm{DG}}(\boldsymbol{v}_i,\boldsymbol{v}_i) = C s_{Jb}(\boldsymbol{v},\boldsymbol{v})\,.
\end{aligned}
$$

Moreover, the non-overlapping block Jacobi smoother enjoys the same spectral scaling of the pointwise Jacobi relaxation. Indeed,

$$
\begin{aligned}
s_{Jb}(\boldsymbol{v},\boldsymbol{v}) &= \sum_{T\in\mathcal{T}_h} \sum_{e\in\mathcal{E}(T)} \sum_{e'\in\mathcal{E}(T)} \sum_{i=1}^{N_e} \mathrm{a}_{\mathrm{DG}}(\boldsymbol{\varphi}_{e,T}^i, \boldsymbol{\varphi}_{e',T}^i) v_{e,T}^i v_{e',T}^i \\
&\le \sum_{T\in\mathcal{T}_h} \sum_{e\in\mathcal{E}(T)} \sum_{e'\in\mathcal{E}(T)} \sum_{i=1}^{N_e} \sqrt{\mathrm{a}_{\mathrm{DG}}(\boldsymbol{\varphi}_{e,T}^i, \boldsymbol{\varphi}_{e,T}^i)} \sqrt{\mathrm{a}_{\mathrm{DG}}(\boldsymbol{\varphi}_{e',T}^i, \boldsymbol{\varphi}_{e',T}^i)} v_{e,T}^i v_{e',T}^i \\
&\le \frac{1}{2} \sum_{T\in\mathcal{T}_h} \sum_{e\in\mathcal{E}(T)} \sum_{e'\in\mathcal{E}(T)} \sum_{i=1}^{N_e} \left(\mathrm{a}_{\mathrm{DG}}(\boldsymbol{\varphi}_{e,T}^i, \boldsymbol{\varphi}_{e,T}^i)(v_{e,T}^i)^2 + \mathrm{a}_{\mathrm{DG}}(\boldsymbol{\varphi}_{e',T}^i, \boldsymbol{\varphi}_{e',T}^i)(v_{e',T}^i)^2 \right) \\
&\le C \sum_{T\in\mathcal{T}_h} \sum_{e\in\mathcal{E}(T)} \sum_{i=1}^{N_e} \mathrm{a}_{\mathrm{DG}}(\boldsymbol{\varphi}_{e,T}^i, \boldsymbol{\varphi}_{e,T}^i)(v_{e,T}^i)^2 = C s_J(\boldsymbol{v},\boldsymbol{v})\,,
\end{aligned}
$$

and therefore, (4.8) follows also for $s_{Jb}(\cdot,\cdot)$. □

We now study the continuity and spectral properties of the patch smoothers defined through (3.14) and (3.13). In order to deal with all of them at once, we use a more compact notation and denote generically by: $\Omega_j = \Omega_y$ the patch related to y with $y \in \mathcal{N}_h \cup \mathcal{E}_h \cup \mathcal{T}_h$; by $\boldsymbol{V}_{\boldsymbol{h}}^j$ the corresponding subspace associated to the patch Ω_j (see (3.9), (3.10) and (3.11)); and by $\mathrm{a}_{\mathrm{DG}}^j(\cdot,\cdot) := \mathrm{a}_{\mathrm{DG}}^{\Omega_y}(\cdot,\cdot)$ the local solver defined in (3.13). Let J be the number of patches required to cover Ω (which will be different for the different splittings), then we write $\boldsymbol{V}_{\boldsymbol{h}} = \sum_{j=1}^J \boldsymbol{V}_{\boldsymbol{h}}^j$. Note that J is always a bounded and moderate constant that depends on the connectivity of the partition. From the shape regularity assumption and by construction, for each of the domain decompositions, the patches (or subdomains) Ω_j are of comparable size. Moreover, all the domain decompositions (3.12) have the *finite covering property*: that is for every $\mathbf{x} \in \Omega$, there is a finite number of patches containing $\mathbf{x}$, say $N(\mathbf{x})$. We define $N_c = \max_{\mathbf{x}\in\Omega} N(\mathbf{x})$ which is a finite (and moderate) number depending on the connectivity of the mesh. Denoting by $\mathcal{A}_j : \boldsymbol{V}_{\boldsymbol{h}}^j \to (\boldsymbol{V}_{\boldsymbol{h}}^j)'$ the local operator associated to $\mathrm{a}_{\mathrm{DG}}^j(\cdot,\cdot)$ and by $\mathcal{I}_j : \boldsymbol{V}_{\boldsymbol{h}}^j \hookrightarrow \boldsymbol{V}_{\boldsymbol{h}}$ the natural embedding, the additive Schwarz smoothing operator reads $\mathcal{S} = \sum_{j=1}^J \mathcal{I}_j \circ \mathcal{A}_j^{-1} \circ \mathcal{I}_j^*$.

The next Lemma establishes the property **(F1)** in Theorem 3.2 and provides the scaling of the smoother $s_O(\cdot,\cdot)$ in (3.14).

Lemma 4.5. *Let $\boldsymbol{V_h} = \sum_{j=1}^{J} \boldsymbol{V_h^j}$ be a space splitting with subspaces $\boldsymbol{V_h^j}$ as in* (3.9), (3.10) *or* (3.11), *and let $s_O(\cdot,\cdot)$ be the corresponding (overlapping) additive Schwarz method given in* (3.14). *Then, for every $\boldsymbol{v} \in \boldsymbol{V_h}$ there exists $c_s > 0$ depending on the local polynomial space, the shape regularity, the connectivity of the mesh and the amount of overlapping N_c in the subdomain partition, such that for any choice of $\{\boldsymbol{v}_j\}_{j=1}^J$ for which $\boldsymbol{v} = \sum_{j=1}^J \boldsymbol{v}_j$, it holds*

$$a_{DG}(\boldsymbol{v},\boldsymbol{v}) \leq c_s s_O(\boldsymbol{v},\boldsymbol{v})\,. \tag{4.11}$$

Moreover, $s_O(\cdot,\cdot)$ satisfies

$$\begin{aligned} s_O(\boldsymbol{v},\boldsymbol{v}) \simeq \sum_{j=1}^{J} \Bigg(& \sum_{T\in\Omega_j} \nu_T \,\|\boldsymbol{\nabla}\times\boldsymbol{v}_j\|_{0,T}^2 + \beta_T\,\|\boldsymbol{v}_j\|_{0,T}^2 + \sum_{T\in\Omega_j} \alpha_T(\nu) \sum_{e\in\mathcal{E}(T)} \sum_{f\in\mathcal{F}(e)\setminus\partial\Omega_j} h_f^{-1}\,\|[\![\,\boldsymbol{v}_j\,]\!]_{\boldsymbol{\tau}}\|_{0,f}^2 \\ & + \sum_{\substack{T\in\Omega_j\\ \partial T\cap\partial\Omega_j\neq\emptyset}} \alpha_T(\nu) \sum_{e\in\mathcal{E}(T)} \sum_{f\in\mathcal{F}(e)\cap\partial\Omega_j} h_f^{-1}\,\|\mathbf{n}\times\boldsymbol{v}_j\|_{0,f}^2 \Bigg)\,. \end{aligned} \tag{4.12}$$

Proof. Note that (4.11) states that in the decomposition $\boldsymbol{v} = \sum_{j=1}^J \boldsymbol{v}_j$, the energy of the parts bounds the energy of the function in $\boldsymbol{V_h}$. To measure the *overlap* of the domain splitting we introduce the constants

$$c_{jk} = \begin{cases} 1 & \text{if } \Omega_j\cap\Omega_k \neq \emptyset \\ 0 & \text{if } \Omega_j\cap\Omega_k = \emptyset \end{cases} \qquad j,k = 1,\dots,J.$$

Cauchy-Schwarz inequality, the arithmetic-geometric inequality and the fact that $c_{jk} = c_{kj}$ for all $j,k = 1,\dots,J$, gives

$$\begin{aligned} \mathrm{a}_{\mathrm{DG}}(\boldsymbol{v},\boldsymbol{v}) &= \mathrm{a}_{\mathrm{DG}}\Bigg(\sum_{j=1}^J \boldsymbol{v}_j, \sum_{k=1}^J \boldsymbol{v}_k\Bigg) = \sum_{j,k=1}^J c_{jk}\mathrm{a}_{\mathrm{DG}}(\boldsymbol{v}_j,\boldsymbol{v}_k) \leq \sum_{j,k=1}^J \sqrt{c_{jk}\mathrm{a}_{\mathrm{DG}}(\boldsymbol{v}_j,\boldsymbol{v}_j)}\sqrt{c_{kj}\mathrm{a}_{\mathrm{DG}}(\boldsymbol{v}_k,\boldsymbol{v}_k)} \\ &\leq \frac{1}{2}\sum_{j,k=1}^J \left(c_{jk}\mathrm{a}_{\mathrm{DG}}(\boldsymbol{v}_j,\boldsymbol{v}_j) + c_{kj}\mathrm{a}_{\mathrm{DG}}(\boldsymbol{v}_k,\boldsymbol{v}_k)\right) \leq \sum_{j,k=1}^J c_{jk}\mathrm{a}_{\mathrm{DG}}(\boldsymbol{v}_j,\boldsymbol{v}_j) \\ &= \sum_{j=1}^J \mathrm{a}_{\mathrm{DG}}(\boldsymbol{v}_j,\boldsymbol{v}_j)\Bigg(\sum_{k=1}^J c_{jk}\Bigg) \leq N_c \sum_{j=1}^J \mathrm{a}_{\mathrm{DG}}^j(\boldsymbol{v}_j,\boldsymbol{v}_j) = c_s s_O(\boldsymbol{v},\boldsymbol{v})\,, \end{aligned}$$

where $c_s = \max_{1\leq j\leq J}\{\sharp k : \Omega_j\cap\Omega_k\neq\emptyset\}$. The proof of (4.12) reduces to use the continuity and coercivity of $\mathrm{a}_{\mathrm{DG}}^j(\cdot,\cdot)$ on the subspace $\boldsymbol{V_h^j}$ for every $j = 1,\dots,J$. ☐

4.3 Averaging operator

Typically, in the auxiliary space framework, the proof of the stable decomposition property **(F2)** relies on the construction of an operator $\mathcal{P}_h : \boldsymbol{V_h} \to \boldsymbol{V_h} \cap \mathrm{H}(\mathbf{curl},\Omega)$ satisfying appropriate approximation and stability properties. We construct such *averaging* operator, following the ideas given in [64, 71]. In fact, our construction and approximation results could be regarded as a generalization of the result contained in [64, Appendix]. The main novelty here, is that the operator we introduce takes into account the presence of coefficients in the model problem (1.1) and is shown to provide robust approximation with respect to large variation of the coefficients. Therefore, we believe that the construction and approximation results are of independent interest, and for this reason, we present the construction of the operator and its approximation results without restricting to low order methods. It is worth stressing that the result in [64, Appendix] has been already used in the different contexts related to the DG approximation of the time harmonic Maxwell problem; in the analysis of spectral approximation [35] (see also [34] for the numerical verification of the results) and in different works related to a posteriori error estimates [65, 66].

To ease the notation, we set $\boldsymbol{\chi} := \mathcal{P}_h(\boldsymbol{v})$ and, since $\boldsymbol{\chi} \in \boldsymbol{V_h} \cap \mathrm{H}(\mathbf{curl}, \Omega)$, we can write $\boldsymbol{\chi}|_T$ in the basis of $\mathcal{M}(T)$ for all $T \in \mathcal{T}_h$. More precisely we have the following representation:

$$\boldsymbol{\chi}(\mathbf{x}) = \sum_{e\in\mathcal{E}(T)} \sum_{i=1}^{N_e} \chi_e^i \, \boldsymbol{\varphi}_{e,T}^i(\mathbf{x}) + \sum_{f\in\mathcal{F}(T)} \sum_{i=1}^{N_f} \chi_f^i \, \boldsymbol{\varphi}_{f,T}^i(\mathbf{x}) + \sum_{i=1}^{N_b} \chi_T^i \, \boldsymbol{\varphi}_T^i(\mathbf{x}) \quad \forall \mathbf{x} \in T\,. \tag{4.13}$$

Hence, in order to define $\boldsymbol{\chi}$, it is enough to specify its associated degrees of freedom $\boldsymbol{\chi}_e = \{\chi_e^i\}_{1=1}^{N_e}$, $\boldsymbol{\chi}_f = \{\chi_f^i\}_{1=1}^{N_f}$ and $\boldsymbol{\chi}_T = \{\chi_T^i\}_{1=1}^{N_b}$ in terms of those of $\boldsymbol{v}$ and ensure at the same time the $\mathrm{H}(\mathbf{curl}, \Omega)$-conformity of the global function. In order to do that, we define two sets of weights associated with faces and edges of the mesh. More precisely, let $f \in \mathcal{F}_h^o$ be an interior face such that $f = \partial T^+ \cap \partial T^-$. We define:

$$\omega_{f,T^+} := \frac{\sqrt{\nu_{T^+}}}{\sqrt{\nu_{T^+}} + \sqrt{\nu_{T^-}}} \quad \text{and} \quad \omega_{f,T^-} := 1 - \omega_{f,T^+} = \frac{\sqrt{\nu_{T^-}}}{\sqrt{\nu_{T^+}} + \sqrt{\nu_{T^-}}}\,. \tag{4.14}$$

Note that, since trivially $(a + b)^2 > a^2 + b^2$ for $a, b > 0$, we have

$$2\nu_{T^\pm}\omega_{f,T^\mp}^2 \leq \{\!\{\nu\}\!\}_{H,f} \leq \{\!\{\nu\}\!\}_{*,f} \leq \alpha_{T^+}(\nu)\,,\, \alpha_{T^-}(\nu)\,,$$

with $\{\!\{\cdot\}\!\}_{*,f}$ and $\alpha_T(\nu)$ defined as in (2.9) and $\{\!\{\cdot\}\!\}_{H,f}$ as in (2.10). In order to define the weights on the edges of the mesh, let $e \in \mathcal{E}_h^o$ be an interior edge and let $\mathcal{T}(e)$ be the set of elements sharing the edge e (as defined in Section 2.1). Note that the cardinality of the set $\mathcal{T}(e)$ is bounded by a finite constant depending on the shape regularity and the connectivity of the mesh $\mathcal{T}_h$, uniformly with respect to h. Let $\nu_j := \nu|_{T_j}$, we define

$$\omega_{e,T_\ell} := \frac{\sqrt{\nu_\ell}}{\sum\limits_{T_j\in\mathcal{T}(e)} \sqrt{\nu_j}} \qquad \forall\, T_\ell \in \mathcal{T}(e)\,. \tag{4.15}$$

We now have all ingredients to construct the averaging projection operator $\mathcal{P}_h$.

Definition 4.6. Let $\mathcal{P}_h : \boldsymbol{V_h} \to \boldsymbol{V_h^c}$ be such that $\boldsymbol{\chi} = \mathcal{P}_h(\boldsymbol{v})$, for any $\boldsymbol{v} \in \boldsymbol{V_h}$, is given by (4.13) with degrees of freedom $\boldsymbol{\chi}_e = \{\chi_e^i\}_{1=1}^{N_e}$, $\boldsymbol{\chi}_f = \{\chi_f^i\}_{1=1}^{N_f}$ and $\boldsymbol{\chi}_T = \{\chi_T^i\}_{1=1}^{N_b}$ defined as:

(i) For every $T \in \mathcal{T}_h$ the volume degrees of freedom $\boldsymbol{\chi}_T$ are set equal to those of $\boldsymbol{v}_T$:

$$\chi_T^i := v_T^i \qquad \forall i = 1, \ldots, N_b\,. \tag{4.16}$$

(ii) The face moments $\boldsymbol{\chi}_f$ are defined, for all $i = 1, \ldots, N_f$ as

$$\chi_f^i = \begin{cases} \omega_{f,T^+} v_{f,T^+}^i + \omega_{f,T^-} v_{f,T^-}^i & f \in \mathcal{F}_h^o, \quad f = \partial T^+ \cap \partial T^-, \\ 0 & f \in \mathcal{F}_h^\partial, \end{cases} \tag{4.17}$$

where the weights ω_{f,T^+}, ω_{f,T^-} are as in (4.14).

(iii) The edge moments $\boldsymbol{\chi}_e$ are defined, for all $i = 1, \dots, N_e$, as the convex combination

$$\chi_e^i = \begin{cases} \sum\limits_{T_\ell \in \mathcal{T}(e)} \omega_{e,T_\ell} v_{e,T_\ell}^i & e \in \mathcal{E}_h^o, \quad e \subset \partial T_\ell \,, \\ 0 & e \in \mathcal{E}_h^\partial, \end{cases} \tag{4.18}$$

with weights $\{\omega_{e,T_\ell}\}_\ell$ defined in (4.15).

Observe that the definition of $\mathcal{P}_h$ is completely general with respect to the distribution of the coefficient ν which is only required to be piecewise constant on $\mathcal{T}_h$ for every h. Note also that if $\nu \equiv 1$ in Ω, then the averaging operator above coincides with the projection operator proposed in [64, Appendix]. The following result provides the approximation properties of $\mathcal{P}_h$ in the local ν-weighted L^2-norm.

Lemma 4.7. *Let $\boldsymbol{v} \in \boldsymbol{V_h}$ and let $\mathcal{P}_h : \boldsymbol{V_h} \to \boldsymbol{V_h^c}$ be the averaging operator introduced in Definition 4.6. Then, there exists a constant $C > 0$ depending only on the polynomial degree and the shape regularity of the mesh such that*

$$\nu_T \|\boldsymbol{v} - \mathcal{P}_h(\boldsymbol{v})\|_{0,T}^2 \leq C\alpha_T(\nu) \sum_{f \in \mathcal{F}(T)} h_f \|[\![\, \boldsymbol{v} \,]\!]_{\boldsymbol{\tau}}\|_{0,f}^2 + C\alpha_T(\nu) \sum_{e \in \mathcal{E}(T)} \sum_{f \in \mathcal{F}(e) \setminus \mathcal{F}(T)} h_f \|[\![\, \boldsymbol{v} \,]\!]_{\boldsymbol{\tau}}\|_{0,f}^2 \,; \tag{4.19}$$

$$\alpha_T(\nu) \|\boldsymbol{v} - \mathcal{P}_h(\boldsymbol{v})\|_{0,T}^2 \leq C\alpha_T(\nu) \sum_{f \in \mathcal{F}(T)} h_f \|[\![\, \boldsymbol{v} \,]\!]_{\boldsymbol{\tau}}\|_{0,f}^2 + C\alpha_T(\nu) \sum_{e \in \mathcal{E}(T)} \sum_{f \in \mathcal{F}(e) \setminus \mathcal{F}(T)} h_f \|[\![\, \boldsymbol{v} \,]\!]_{\boldsymbol{\tau}}\|_{0,f}^2 \,; \tag{4.20}$$

Prior to give the proof of the above estimates, we present a stability result of the averaging operator $\mathcal{P}_h$ in the β-weighted L^2-norm defined in (2.14).

Corollary 4.8. *Let $\boldsymbol{v} \in \boldsymbol{V_h}$ and let $\mathcal{P}_h : \boldsymbol{V_h} \to \boldsymbol{V_h^c}$ be the averaging operator as in Definition 4.6. Then, there exists $C > 0$ depending only on the polynomial degree and the shape regularity of the mesh such that*

$$\|\boldsymbol{v} - \mathcal{P}_h(\boldsymbol{v})\|_{0,\beta,\mathcal{T}_h}^2 \leq C \max\{1, \theta(\nu,\beta)\} \|\boldsymbol{v}\|_{DG}^2 \,. \tag{4.21}$$

where $\theta(\nu,\beta)$ is defined as

$$\theta(\nu,\beta) := \min\left\{ \max_{T \in \mathcal{T}_h} \frac{h_T^2 \beta_T}{\nu_T}, \max_{\substack{T,T' \in \mathcal{T}_h \\ \partial T \cap \partial T' \neq \emptyset}} \frac{\beta_T}{\beta_{T'}} \right\}. \tag{4.22}$$

Proof. The proof boils down to showing the following estimates:

$$\|\boldsymbol{v} - \mathcal{P}_h(\boldsymbol{v})\|_{0,\beta,\mathcal{T}_h}^2 \leq C \sum_{T \in \mathcal{T}_h} h_T^2 \frac{\beta_T}{\nu_T} \sum_{e \in \mathcal{E}(T)} \sum_{f \in \mathcal{F}(e)} \alpha_T(\nu) h_f^{-1} \|[\![\, \boldsymbol{v} \,]\!]_{\boldsymbol{\tau}}\|_{0,f}^2 \,; \tag{4.23}$$

$$\|\boldsymbol{v} - \mathcal{P}_h(\boldsymbol{v})\|_{0,\beta,\mathcal{T}_h}^2 \leq C \sum_{T \in \mathcal{T}_h} \beta_T \, \|\boldsymbol{v}\|_{0,T} + \sum_{\substack{T,T' \in \mathcal{T}_h \\ \partial T \cap \partial T' \neq \emptyset}} \frac{\beta_T}{\beta_{T'}} \beta_{T'} \|\boldsymbol{v}\|_{0,T'}^2 \,. \tag{4.24}$$

To prove (4.23), we exploit the ν-weighted L^2-estimate (4.19) by multiplying and dividing by ν_T the elementwise β-weighted norms, namely

$$\begin{aligned} \sum_{T \in \mathcal{T}_h} \beta_T \|\boldsymbol{v} - \mathcal{P}_h(\boldsymbol{v})\|_{0,T}^2 &= \sum_{T \in \mathcal{T}_h} \frac{\beta_T}{\nu_T} \nu_T \|\boldsymbol{v} - \mathcal{P}_h(\boldsymbol{v})\|_{0,T}^2 \\ &\overset{(4.19)}{\leq} C \sum_{T \in \mathcal{T}_h} \frac{\beta_T}{\nu_T} \sum_{e \in \mathcal{E}(T)} \sum_{f \in \mathcal{F}(e)} \alpha_T(\nu) h_f \|[\![\, \boldsymbol{v} \,]\!]_{\boldsymbol{\tau}}\|_{0,f}^2 \\ &\leq C \sum_{T \in \mathcal{T}_h} h_T^2 \frac{\beta_T}{\nu_T} \sum_{e \in \mathcal{E}(T)} \sum_{f \in \mathcal{F}(e)} \alpha_T(\nu) h_f^{-1} \|[\![\, \boldsymbol{v} \,]\!]_{\boldsymbol{\tau}}\|_{0,f}^2 \,. \end{aligned}$$

In order to show (4.24), we use the estimate (4.20) with $\alpha_T(\nu) = 1$ for all $T \in \mathcal{T}_h$, and trace [1] and inverse inequalities [38, p. 146] to get

$$\begin{aligned}\sum_{T\in\mathcal{T}_h} \beta_T \|\boldsymbol{v} - \mathcal{P}_h(\boldsymbol{v})\|_{0,T}^2 &\leq C \sum_{T\in\mathcal{T}_h} \beta_T \Bigg(\sum_{f\in\mathcal{F}(T)} h_f \, \|[\![\boldsymbol{v}]\!]_{\boldsymbol{\tau}}\|_{0,f}^2 + \sum_{e\in\mathcal{E}(T)} \sum_{f\in\mathcal{F}(e)\setminus\mathcal{F}(T)} h_f \|[\![\boldsymbol{v}]\!]_{\boldsymbol{\tau}}\|_{0,f}^2 \Bigg) \\ &\leq C \sum_{T\in\mathcal{T}_h} \beta_T \, \|\boldsymbol{v}\|_{0,T}^2 + C \sum_{T\in\mathcal{T}_h} \sum_{\substack{T'\in\mathcal{T}_h\setminus\{T\} \\ \partial T\cap\partial T'\neq\emptyset}} \frac{\beta_T}{\beta_{T'}} \beta_{T'} \, \|\boldsymbol{v}\|_{0,T'}^2 \, .\end{aligned}$$

Taking into account the definition of the DG-norm (2.15), one can combine estimates (4.23) and (4.24) to obtain (4.21). □

Proof of Lemma 4.7. In view of the definition of the norms (2.13) and (2.14), we consider the L^2 approximation error at the element level. First, let $T \in \mathcal{T}_h$ be an arbitrary element that does not intersect the boundary $\partial\Omega$. To estimate the difference $\boldsymbol{v} - \mathcal{P}_h(\boldsymbol{v})$ we use the representations (2.5) and (4.13). The bound (4.2) together with the norm equivalence (4.5) gives

$$\nu_T \|\boldsymbol{v} - \mathcal{P}_h(\boldsymbol{v})\|_{0,T}^2 \leq C h_T \Bigg(\sum_{f\in\mathcal{F}(T)} \nu_T \left\|\boldsymbol{v}_{f,T} - \boldsymbol{\chi}_f\right\|_{\ell^2}^2 + \sum_{e\in\mathcal{E}(T)} \nu_T \left\|\boldsymbol{v}_{e,T} - \boldsymbol{\chi}_e\right\|_{\ell^2}^2 \Bigg) . \tag{4.25}$$

We estimate each of the contributions on the right hand side above separately. Let $f \in \mathcal{F}(T)$ be an interior face such that $f = \partial T' \cap \partial T$ with $T, T' \in \mathcal{T}_h$. From the definition of the averaging operator and the corresponding face degrees of freedom (4.17), together with the norm equivalence (4.7) from Lemma 4.3, we have

$$\begin{aligned}\nu_T \left\|\boldsymbol{v}_{f,T} - \boldsymbol{\chi}_f\right\|_{\ell^2}^2 &\overset{(4.17)}{=} \nu_T \left\|(1-\omega_{f,T})\boldsymbol{v}_{f,T} - \omega_{f,T'}\boldsymbol{v}_{f,T'}\right\|_{\ell^2}^2 \overset{(4.14)}{=} \nu_T (\omega_{f,T'})^2 \left\|\boldsymbol{v}_{f,T} - \boldsymbol{v}_{f,T'}\right\|_{\ell^2}^2 \\ &\leq \nu_T \left\|\boldsymbol{v}_{f,T} - \boldsymbol{v}_{f,T'}\right\|_{\ell^2}^2 \overset{(4.7)}{\leq} C\alpha_T(\nu) \int_f |[\![\boldsymbol{v}]\!]_{\boldsymbol{\tau}}|^2 \, ds \, ,\end{aligned} \tag{4.26}$$

since the face weights satisfy $\omega_{f,T'} < 1$ and $\nu_T \leq \alpha_T(\nu)$ for all $T \in \mathcal{T}_h$. Concerning the degrees of freedom on the edges, using the definition in (4.18) results in

$$\sum_{e\in\mathcal{E}(T)} \nu_T \left\|\boldsymbol{v}_{e,T} - \boldsymbol{\chi}_e\right\|_{\ell^2}^2 \leq C \sum_{e\in\mathcal{E}(T)} \sum_{\substack{T_\ell\in\mathcal{T}(e) \\ T_\ell\neq T}} \nu_T (\omega_{e,T_\ell})^2 \left\|\boldsymbol{v}_{e,T} - \boldsymbol{v}_{e,T_\ell}\right\|_{\ell^2}^2 . \tag{4.27}$$

To estimate the above term, we introduce a numbering (ordering) of the elements in the set $\mathcal{T}(e)$ for a fixed $e \in \mathcal{E}(T)$, such that $\mathcal{T}(e) = \bigcup_{j=0}^{M_e} T_j$ with $M_e := |\mathcal{T}(e)| - 1$. The ordering is such that $T_0 := T$ and

$$\begin{aligned}&\partial T_0 \cap \partial T_1 \in \mathcal{F}(T_0)\,, \quad \text{and} \quad \partial T_0 \cap \partial T_{M_e} \in \mathcal{F}(T_0)\,; \\ &\partial T_0 \cap \partial T_j \in \mathcal{E}(T_0)\,, \quad \text{but} \quad \partial T_0 \cap \partial T_j \notin \mathcal{F}(T_0) \qquad \forall j = 2, \ldots, M_e - 1\,; \\ &\partial T_j \cap \partial T_{j+1} \in \mathcal{F}(T_j) \cap \mathcal{F}(T_{j+1}) \qquad \forall j = 2, \ldots, M_e - 1\,.\end{aligned} \tag{4.28}$$

Using such numbering, by summing and subtracting suitable degrees of freedom and applying triangle inequality (see [71, Lemma 2.2] for a similar trick), results in

$$\begin{aligned}\sum_{\substack{T_\ell\in\mathcal{T}(e) \\ T_\ell\neq T_0}} \nu_{T_0} (\omega_{e,T_\ell})^2 \left\|\boldsymbol{v}_{e,T_0} - \boldsymbol{v}_{e,T_\ell}\right\|_{\ell^2}^2 &\leq \nu_{T_0} (\omega_{e,T_1})^2 \left\|\boldsymbol{v}_{e,T_0} - \boldsymbol{v}_{e,T_1}\right\|_{\ell^2}^2 \\ &\quad + \sum_{\ell=2}^{M_e-1} \nu_{T_0} (\omega_{e,T_\ell})^2 \, \ell \sum_{j=0}^{\ell-1} \left\|\boldsymbol{v}_{e,T_j} - \boldsymbol{v}_{e,T_{j+1}}\right\|_{\ell^2}^2 \\ &\quad + \nu_{T_0} (\omega_{e,T_{M_e}})^2 \left\|\boldsymbol{v}_{e,T_0} - \boldsymbol{v}_{e,T_{M_e}}\right\|_{\ell^2}^2 \, .\end{aligned}$$

Notice that trivially $\nu_{T_0}(\omega_{e,T_1})^2$, $\nu_{T_0}(\omega_{e,T_{M_e}})^2 \le \{\!\{\nu\}\!\}_{H,f} \le \{\!\{\nu\}\!\}_{*,f}$ with $f \in \mathcal{F}(T_0)$ while for the intermediate sum above (taking into account the definition in (2.9)), one has

$$\nu_{T_0}(\omega_{e,T_\ell})^2 \le \{\!\{\nu\}\!\}_{*,f} \qquad \text{with } f = \partial T_j \cap \partial T_{j+1} \quad j = 0, \dots, \ell-1, \quad \ell = 2, \dots M_e - 1\,.$$

Hence, the above estimates together with the norm equivalence (4.7) from Lemma 4.3 and the fact that ℓ is uniformly bounded ($\ell \le M_e$) yield

$$\begin{aligned}\sum_{\substack{T_\ell \in \mathcal{T}(e)\\ T_\ell \ne T_0}} \nu_{T_0}(\omega_{e,T_\ell})^2 \, \|\boldsymbol{v}_{e,T_0} - \boldsymbol{v}_{e,T_\ell}\|^2_{\ell^2} &\le C \sum_{\substack{T_\ell \in \mathcal{T}(e)\\ T_\ell \ne T_0}} \sum_{f \in \mathcal{F}(e)\cap\mathcal{F}(T_\ell)} \{\!\{\nu\}\!\}_{*,f} \|[\![\, \boldsymbol{v}\,]\!]_{\boldsymbol{\tau}}\|^2_{0,f} \\ &\le C\, \{\!\{\nu\}\!\}_{*,f} \sum_{f\in\mathcal{F}(e)} \|[\![\, \boldsymbol{v}\,]\!]_{\boldsymbol{\tau}}\|^2_{0,f}\,.\end{aligned} \tag{4.29}$$

Hence, substituting (4.29) into (4.27) for all elements that do not intersect the domain boundary $\partial\Omega$ and taking into account the definition (2.9) yields

$$\sum_{e\in\mathcal{E}(T)} \nu_T \, \|\boldsymbol{v}_{e,T} - \boldsymbol{\chi}_e\|^2_{\ell^2} \le C\alpha_T(\nu) \sum_{e\in\mathcal{E}(T)} \sum_{f\in\mathcal{F}(e)} \|[\![\, \boldsymbol{v}\,]\!]_{\boldsymbol{\tau}}\|^2_{0,f}\,, \tag{4.30}$$

where C only depends on the shape regularity and connectivity of the mesh. For elements $T \in \mathcal{T}_h$ touching the boundary $\partial T \cap \partial\Omega \ne \emptyset$ the same type of estimates can be obtained by exploiting the fact that, in view of the boundary conditions, the degrees of freedom $\boldsymbol{\chi}_{f,T}$ and $\boldsymbol{\chi}_{e,T}$ are set to zero on the boundary faces and on the boundary edges, respectively (see (4.17) and (4.18)). In particular, analogously to (4.25), it holds

$$\begin{aligned}\nu_T \|\boldsymbol{v} - \mathcal{P}(\boldsymbol{v})\|^2_{0,T} \le C h_T \Bigg(&\sum_{f\subseteq \partial T\cap\partial\Omega} \nu_T \, \|\boldsymbol{v}_{f,T}\|^2_{\ell^2} + \sum_{e\subseteq\partial T\cap\partial\Omega} \nu_T \, \|\boldsymbol{v}_{e,T}\|^2_{\ell^2} \\ &+ \sum_{\substack{f\in\mathcal{F}(T)\\ f\not\subseteq\partial\Omega}} \nu_T \, \big\|\boldsymbol{v}_{f,T} - \boldsymbol{\chi}_f\big\|^2_{\ell^2} + \sum_{\substack{e\in\mathcal{E}(T)\\ e\not\subseteq\partial\Omega}} \nu_T \, \|\boldsymbol{v}_{e,T} - \boldsymbol{\chi}_e\|^2_{\ell^2} \Bigg)\,.\end{aligned} \tag{4.31}$$

The last two contributions are estimated as in (4.26) and (4.30) respectively. The first two terms can be bounded by arguing similarly, but using equivalence (4.6) together with (4.4), namely

$$\begin{aligned}\nu_T \Bigg(\sum_{f\subseteq\partial T\cap\partial\Omega} \|\boldsymbol{v}_{f,T}\|^2_{\ell^2} + \sum_{e\subseteq\partial T\cap\partial\Omega} \|\boldsymbol{v}_{e,T}\|^2_{\ell^2} \Bigg) &\le 2\nu_T \sum_{f\subseteq\partial T\cap\partial\Omega} \Bigg(\|\boldsymbol{v}_{f,T}\|^2_{\ell^2} + \sum_{e\in\mathcal{E}(f)} \|\boldsymbol{v}_{e,T}\|^2_{\ell^2} \Bigg) \\ &\le C \sum_{f\subseteq\partial T\cap\partial\Omega} \alpha_T(\nu) \int_f |\mathbf{n}\times\boldsymbol{v}|^2 ds\,,\end{aligned} \tag{4.32}$$

and one can conclude by using the fact that the “jump” on the boundary $\partial\Omega$ reduces to the plain tangential trace. Therefore, substituting into (4.25) and (4.31) the local contributions from the interior faces (4.26), from the interior edges (4.30) and from the boundary (4.32), yields (4.19).

In order to obtain (4.20), we proceed analogously as above using $\alpha_T(\nu)$ in lieu of ν_T. The contribution from the edges can be estimated (using now the fact that $\omega_{e,T} < 1$ for all $e \in \mathcal{E}(T)$) as

$$\sum_{\substack{T_\ell\in\mathcal{T}(e)\\ T_\ell\ne T_0}} \alpha_{T_0}(\nu)(\omega_{e,T_\ell})^2 \, \|\boldsymbol{v}_{e,T_0} - \boldsymbol{v}_{e,T_\ell}\|^2_{\ell^2} \le C\alpha_{T_0}(\nu) \sum_{f\in\mathcal{F}(e)} \|[\![\, \boldsymbol{v}\,]\!]_{\boldsymbol{\tau}}\|^2_{0,f}\,, \tag{4.33}$$

and substituting (4.33) into (4.27) results in

$$\sum_{e\in\mathcal{E}(T)} \alpha_T(\nu)\,\|\boldsymbol{v}_{e,T}-\boldsymbol{\chi}_e\|_{\ell^2}^2 \le C \sum_{e\in\mathcal{E}(T)}\sum_{f\in\mathcal{F}(e)} \alpha_T(\nu)\|[\![\,\boldsymbol{v}\,]\!]_{\boldsymbol{\tau}}\|_{0,f}^2\,, \tag{4.34}$$

where C only depends on the shape regularity and connectivity of the mesh. The degrees of freedom on the faces can be evaluated as in (4.26) with $\alpha_T(\nu)$ instead of ν_T. Hence, the result follows by substituting into (4.25) and (4.31), the bounds (4.26), (4.34) and the boundary term (4.32). $\square$

4.4 Stable decomposition

By means of the approximation properties of the averaging operator derived in Section 4.3, we establish a first stability result for the splitting associated to the case (a) in Section 3.2, paying particular attention to the distribution of the coefficients ν and β.

Proposition 4.9. *Let $\mathcal{T}_h$ be shape regular and local quasi-uniform. Let $\boldsymbol{V_h}$ be defined as in* (2.1) *and let $\boldsymbol{V_h^c} = \boldsymbol{V_h}\cap H_0(\mathbf{curl},\Omega)$ be the corresponding $H(\mathbf{curl},\Omega)$-conforming finite element space. Let $s(\cdot,\cdot)$ be any of the pointwise smoothers defined in* (4.9) *and* (4.10). *Then, for any $\boldsymbol{v}\in\boldsymbol{V_h}$ there exist $\boldsymbol{v}_0\in\boldsymbol{V_h}$ and $\boldsymbol{\chi}\in\boldsymbol{V_h^c}$ such that $\boldsymbol{v}=\boldsymbol{v}_0+\boldsymbol{\chi}$ and*

$$s(\boldsymbol{v}_0,\boldsymbol{v}_0) + a_{\boldsymbol{\mathcal{W}}}(\boldsymbol{\chi},\boldsymbol{\chi}) \le c_0^2\,\max\{1,\theta(\nu,\beta)\}\,a_{DG}(\boldsymbol{v},\boldsymbol{v})\,, \tag{4.35}$$

where $\theta(\nu,\beta)$ is defined as in (4.22) *and the constant $c_0^2>0$ depends only the polynomial degree and on the shape regularity of the mesh.*

Proof. Let $\boldsymbol{v}\in\boldsymbol{V_h}$ and $\mathcal{P}_h$ be the averaging operator introduced in Definition 4.6. Since by construction, $\mathcal{P}_h(\boldsymbol{v})\in\boldsymbol{V_h^c}$, for all $\boldsymbol{v}\in\boldsymbol{V_h}$ we take $\boldsymbol{v}_0=\boldsymbol{v}-\mathcal{P}_h(\boldsymbol{v})\in\boldsymbol{V_h}$. Then, the scaling of the smoother (4.8) given in Lemma 4.4, together with the approximation estimates (4.20) and (4.21) and the fact that $\nu_T\le\alpha_T(\nu)$ for any $T\in\mathcal{T}_h$ gives

$$\begin{aligned} s(\boldsymbol{v}_0,\boldsymbol{v}_0) &\le C\sum_{T\in\mathcal{T}_h} h_T^{-2}\nu_T\|\boldsymbol{v}-\mathcal{P}_h(\boldsymbol{v})\|_{0,T}^2 + \|\boldsymbol{v}-\mathcal{P}_h(\boldsymbol{v})\|_{0,\beta,\mathcal{T}_h}^2 + \sum_{T\in\mathcal{T}_h} h_T^{-2}\alpha_T(\nu)\|\boldsymbol{v}-\mathcal{P}_h(\boldsymbol{v})\|_{0,T}^2 \\ &\le C\sum_{T\in\mathcal{T}_h}\alpha_T(\nu)\sum_{e\in\mathcal{E}(T)}\sum_{f\in\mathcal{F}(e)} h_f^{-1}\,\|[\![\,\boldsymbol{v}\,]\!]_{\boldsymbol{\tau}}\|_{0,f}^2 + C\theta(\nu,\beta)\|\boldsymbol{v}\|_{DG}^2\,. \end{aligned}$$

To conclude we need to consider $a_{\boldsymbol{\mathcal{W}}}(\mathcal{P}_h(\boldsymbol{v}),\mathcal{P}_h(\boldsymbol{v}))$. Since

$$a_{\boldsymbol{\mathcal{W}}}(\mathcal{P}_h(\boldsymbol{v}),\mathcal{P}_h(\boldsymbol{v})) \le a_{\boldsymbol{\mathcal{W}}}(\boldsymbol{v},\boldsymbol{v}) + a_{\boldsymbol{\mathcal{W}}}(\boldsymbol{v}-\mathcal{P}_h(\boldsymbol{v}),\boldsymbol{v}-\mathcal{P}_h(\boldsymbol{v})),$$

the stability proof reduces to bound the weighted H$(\mathbf{curl},\Omega)$-norm of the difference $\boldsymbol{v}-\mathcal{P}_h(\boldsymbol{v})$ (using the continuity of $a_{\boldsymbol{\mathcal{W}}}(\cdot,\cdot)$ in that norm). Hence, a standard application of inverse inequality together with (4.20) and (4.21), yields

$$\begin{aligned} a_{\boldsymbol{\mathcal{W}}}(\boldsymbol{v}-\mathcal{P}_h(\boldsymbol{v}),\boldsymbol{v}-\mathcal{P}_h(\boldsymbol{v})) &\le \|\boldsymbol{\nabla}\times(\boldsymbol{v}-\mathcal{P}_h(\boldsymbol{v}))\|_{0,\nu,\mathcal{T}_h}^2 + \|\boldsymbol{v}-\mathcal{P}_h(\boldsymbol{v})\|_{0,\beta,\mathcal{T}_h}^2 \\ &\le C\sum_{T\in\mathcal{T}_h}\alpha_T(\nu)\sum_{e\in\mathcal{E}(T)}\sum_{f\in\mathcal{F}(e)} h_f^{-1}\,\|[\![\,\boldsymbol{v}\,]\!]_{\boldsymbol{\tau}}\|_{0,f}^2 + C\theta(\nu,\beta)\|\boldsymbol{v}\|_{DG}^2\,. \end{aligned}$$

Collecting the above two estimates results in (4.35). Since the choice of $\boldsymbol{v}$ was arbitrary this concludes the proof. $\square$

Remark 4.10. The results derived in Proposition 4.9 entail that:

- If the problem is **curl**-dominated in the whole domain (i.e. $\nu_T \geq \beta_T h_T^2$ for all $T \in \mathcal{T}_h$), (4.35) guarantees that the auxiliary space preconditioner is uniformly convergent and robust with respect to jumps in the coefficients β and ν. In this case one could replace the solution operator in the auxiliary space $\mathcal{A}_{\boldsymbol{\mathcal{W}}}$ by the domain decomposition preconditioner proposed in [43], getting an optimal solver.

- If the reaction coefficient β is assumed to be of bounded variation, (4.35) ensures the uniform convergence of the auxiliary space preconditioner and the robustness with respect to possible jumps in the coefficient ν. This could be seen as in agreement with the results available in the literature for auxiliary space type preconditioners for discretizations of second order problems with only one jumping coefficient [36, 31].

- If the problem is reaction dominated in the whole domain and β is allowed to have high variations in different regions, an application of Proposition 4.9 would predict a convergence affected significantly by the size of the largest ratio $h_T^2\beta_T/\nu_T$ and the largest jump on the reaction coefficient β. However, such prediction might be pessimistic and would not endorse the results obtained in the actual computations, as we shall see in the numerical experiments (see Section 5). Also, if the problem is reaction dominated in the whole domain, one might expect that the auxiliary space solver is not required in the preconditioner (3.3). In fact, as we will show in the subsequent Proposition 4.14 and in the numerical experiments, by suitably *turning off* the auxiliary space solver in the preconditioner its convergence will not be jeopardized by the largest ratio $h_T^2\beta_T/\nu_T$ or by the largest jump on the reaction coefficient.

4.5 Localized results

To efficiently address the most general case in which the local quotient $h_T^2\beta_T/\nu_T$ can be larger than one in some parts of the domain but smaller than one in some others; that is when the problem is **curl**-dominated in some regions and reaction dominated in others, we introduce another averaging operator $\overline{\mathcal{P}}_h : \boldsymbol{V_h} \to \boldsymbol{V_h^c}$ which allows to *turn off* the auxiliary space correction in the reaction dominated regime, and to further localize the error estimates. Its definition is given in terms of the operator $\mathcal{P}_h$ (introduced in Definition 4.6) by setting it to zero in selected regions.

Definition 4.11. Let $\overline{\mathcal{P}}_h : \boldsymbol{V_h} \to \boldsymbol{V_h} \cap \mathrm{H}_0(\mathbf{curl}, \Omega)$ and let $\overline{\boldsymbol{\chi}} := \overline{\mathcal{P}}_h(\boldsymbol{v})$ be defined through the local representation (analogue of (4.13)),

$$\overline{\boldsymbol{\chi}}(\mathbf{x}) = \sum_{e\in\mathcal{E}(T)} \sum_{i=1}^{N_e} \overline{\chi}_e^i\, \boldsymbol{\varphi}_{e,T}^i(\mathbf{x}) + \sum_{f\in\mathcal{F}(T)} \sum_{i=1}^{N_f} \overline{\chi}_f^i\, \boldsymbol{\varphi}_{f,T}^i(\mathbf{x}) + \sum_{i=1}^{N_b} \overline{\boldsymbol{\chi}}_T^i\, \boldsymbol{\varphi}_T^i(\mathbf{x}) \qquad \forall \mathbf{x} \in T\,.$$

The degrees of freedom of $\overline{\boldsymbol{\chi}}$ are equal to the degrees of freedom of $\boldsymbol{\chi} := \mathcal{P}_h(\boldsymbol{v})$ (defined in (4.16), (4.17), (4.18)) or are set to zero according to the following criteria:

(i) if $T \in \mathcal{T}_h$ the volume degrees of freedom, for all $i = 1, \ldots, N_b$ are:

$$\overline{\chi}_T^i = \begin{cases} 0 & \text{if } h_T^2\beta_T \geq \alpha_T(\nu)\,, \\ \chi_T^i & \text{otherwise.} \end{cases}$$

(ii) if $f \in \mathcal{F}_h^o$ such that $f = \partial T^+ \cap \partial T^-$ the face moments, for all $i = 1, \ldots, N_f$ are:

$$\overline{\chi}_f^i = \begin{cases} 0 & \text{if } h_{T^+}^2 \beta_{T^+} \geq \alpha_{T^+}(\nu) \text{ or } h_{T^-}^2 \beta_{T^-} \geq \alpha_{T^-}(\nu)\,, \\ \chi_f^i & \text{otherwise.} \end{cases}$$

On boundary faces $f \in \mathcal{F}_h^\partial$ we set $\overline{\boldsymbol{\chi}}_f = \boldsymbol{\chi}_f$.

(iii) if $e \in \mathcal{E}_h^o$, the edge moments, for all $i = 1, \ldots, N_e$ are:

$$\overline{\chi}_e^i = \begin{cases} 0 & \text{if } \exists\, T' \in \mathcal{T}(e) :\; h_{T'}^2 \beta_{T'} \geq \alpha_{T'}(\nu)\,, \\ \chi_e^i & \text{otherwise.} \end{cases}$$

On boundary edges $e \in \mathcal{E}_h^\partial$ we set $\overline{\boldsymbol{\chi}}_e = \boldsymbol{\chi}_e$.

First, we introduce some notations and establish some preliminary results on the approximation error given by $\overline{\mathcal{P}}_h$ which will be instrumental for the subsequent analysis on the stability of the decomposition. In particular, let $T \in \mathcal{T}_h$ be fixed and such that $h_T^2 \beta_T < \alpha_T(\nu)$. We define the following sets (see Figure 4.1 for an example in a 2D schematic representation where an element is depicted as a triangle, a face is identified with an edge and an edge with a vertex):

$$\begin{aligned} \mathcal{F}'(T) &:= \{f \in \mathcal{F}(T) :\; f = \partial T \cap \partial T' \text{ for } T' \in \mathcal{T}_h \text{ such that } h_{T'}^2 \beta_{T'} \geq \alpha_{T'}(\nu)\}\,; \\ \mathcal{E}'(T) &:= \{e \in \mathcal{E}(T) :\; \exists T' \in \mathcal{T}(e) \text{ such that } h_{T'}^2 \beta_{T'} \geq \alpha_{T'}(\nu)\}\,; \\ \mathcal{T}'(T) &:= \{T' \in \mathcal{T}(e) \text{ for } e \in \mathcal{E}'(T) :\; \partial T \cap \partial T' = e \text{ and } h_{T'}^2 \beta_{T'} \geq \alpha_{T'}(\nu)\}\,. \end{aligned} \tag{4.36}$$

We will establish local bounds of the L^2-norm of the averaging projection error given by $\overline{\mathcal{P}}_h$ depending on the ratio of $\alpha_T(\nu)$ belonging to elements $T \in \mathcal{T}_h$ at the interface between a **curl**-dominated region and a subdomain in a reaction dominated regime. For this reason we need to introduce the sets of elements:

$$\Delta_h := \{T \in \mathcal{T}_h :\; h_T^2 \beta_T < \alpha_T(\nu)\}\,, \qquad \Delta_h' := \{T \in \mathcal{T}_h :\; h_T^2 \beta_T \geq \alpha_T(\nu)\}\,. \tag{4.37}$$

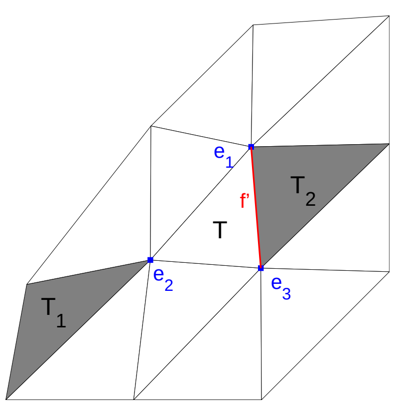

Figure 4.1: 2D sketch of the sets defined in (4.36). The elements $T' \in \{T_1, T_2\}$ in gray satisfy $h_{T'}^2 \beta_{T'} \geq \alpha_{T'}(\nu)$, while the elements in the white region satisfy $h_T^2 \beta_T < \alpha_T(\nu)$. For the element T (in the white region): $\mathcal{F}'(T)$=$\{f'\}$, $\mathcal{E}'(T)$=$\{e_1, e_2, e_3\}$, $\mathcal{T}'(T)$=$\{T_1\}$.

With this notation in mind, localized approximation estimates for the operator $\overline{\mathcal{P}}_h$ can be derived. The proofs of the following Lemmas are relegated to Appendix B and Appendix C. We refer to Figure 4.2 and Figure 4.3 for a 2D sketch of the mesh configurations covered in Lemma 4.12 and Lemma 4.13, respectively.

Lemma 4.12. *Let* $\boldsymbol{v} \in \boldsymbol{V_h}$ *and let* $\overline{\mathcal{P}}_h : \boldsymbol{V_h} \to \boldsymbol{V_h^c}$ *be the projection operator in Definition 4.11. Let* $T \in \Delta_h$ *be fixed (i.e.,* $T \in \mathcal{T}_h$ *is such that* $h_T^2\beta_T < \alpha_T(\nu)$*). Assume that the set* $\mathcal{F}'(T) \neq \emptyset$ *is non-empty. In particular, if* $\mathcal{F}(T) \setminus \mathcal{F}'(T) \neq \emptyset$*, then*

$$h_T^{-2}\alpha_T(\nu) \left\|\boldsymbol{v} - \overline{\mathcal{P}}_h(\boldsymbol{v})\right\|_{0,T}^2 \leq C\alpha_T(\nu) \sum_{e\in\mathcal{E}(T)} \sum_{f\in\mathcal{F}(e)} h_f^{-1} \left\|[\![\boldsymbol{v}]\!]_{\boldsymbol{\tau}}\right\|_{0,f}^2 + C \sum_{\substack{T'\in\mathcal{T}_h \\ \partial T\cap\partial T'\in\mathcal{F}'(T)}} \frac{\alpha_T(\nu)}{\alpha_{T'}(\nu)} \beta_{T'} \left\|\boldsymbol{v}\right\|_{0,T'}^2 . \quad (4.38)$$

If $\mathcal{F}'(T) \equiv \mathcal{F}(T)$*, then*

$$h_T^{-2}\alpha_T(\nu) \left\|\boldsymbol{v} - \overline{\mathcal{P}}_h(\boldsymbol{v})\right\|_{0,T}^2 \leq C\alpha_T(\nu) \sum_{f\in\mathcal{F}(T)} h_f^{-1} \left\|[\![\boldsymbol{v}]\!]_{\boldsymbol{\tau}}\right\|_{0,f}^2 + C \sum_{\substack{T'\in\mathcal{T}_h \\ \partial T\cap\partial T'\in\mathcal{F}(T)}} \frac{\alpha_T(\nu)}{\alpha_{T'}(\nu)} \beta_{T'} \left\|\boldsymbol{v}\right\|_{0,T'}^2 ; \quad (4.39)$$

where the constants $C > 0$ *depend only on the polynomial degree and the shape regularity of the mesh.*

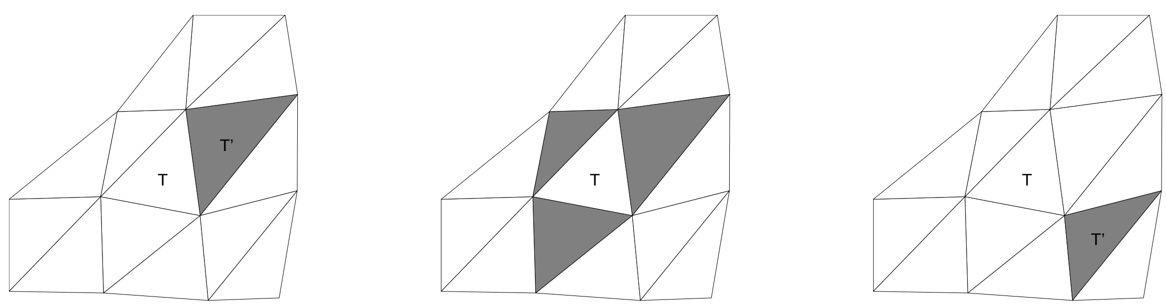

(a) Admissible configuration (b) Admissible configuration (c) Non-admissible configuration

Figure 4.2: 2D sketch of the required assumptions in Lemma 4.12. Let the cells T in white be such that $h_T^2\beta_T < \alpha_T(\nu)$, and the cells T' in gray satisfy $h_{T'}^2\beta_{T'} \geq \alpha_{T'}(\nu)$. The element T in case (a) satisfy the assumptions of the Lemma for (4.38), whereas T in (b) fulfills the hypoteses of the Lemma case (4.39) but the configuration in case (c) does not.

Lemma 4.13. *Let* $\boldsymbol{v} \in \boldsymbol{V_h}$ *and let* $\overline{\mathcal{P}}_h : \boldsymbol{V_h} \to \boldsymbol{V_h^c}$ *be the projection operator introduced in Definition 4.11. Let* $T \in \Delta_h$ *be fixed. Assume that* $\mathcal{E}'(T) \neq \emptyset$ *but* $\mathcal{F}'(T) = \emptyset$*. Then,*

$$h_T^{-2}\alpha_T(\nu) \left\|\boldsymbol{v} - \overline{\mathcal{P}}_h(\boldsymbol{v})\right\|_{0,T}^2 \leq C\,\alpha_T(\nu) \sum_{e\in\mathcal{E}(T)} \sum_{f\in\mathcal{F}(e)} h_f^{-1} \left\|[\![\boldsymbol{v}]\!]_{\boldsymbol{\tau}}\right\|_{0,f}^2 + C \sum_{T'\in\mathcal{T}'(T)} \frac{\alpha_T(\nu)}{\alpha_{T'}(\nu)} \beta_{T'} \left\|\boldsymbol{v}\right\|_{0,T'}^2 ; \quad (4.40)$$

where the constants $C > 0$ *depend only on the polynomial degree and the shape regularity of the mesh.*

We have now all the tools needed to establish the following:

Proposition 4.14. *Let* $\mathcal{T}_h$ *be shape regular and local quasi-uniform. Let* $\boldsymbol{V_h}$ *be defined as in* (2.1) *and let* $\boldsymbol{V_h^c} = \boldsymbol{V_h} \cap H_0(\boldsymbol{curl};\Omega)$ *be the corresponding* $H(\boldsymbol{curl};\Omega)$*-conforming finite element space. Let* $s(\cdot,\cdot)$ *be any of the pointwise smoothers as defined in* (4.9) *and* (4.10)*. Then, for any* $\boldsymbol{v} \in \boldsymbol{V_h}$ *there exist* $\boldsymbol{v}_0 \in \boldsymbol{V_h}$ *and* $\boldsymbol{\chi} \in \boldsymbol{V_h^c}$ *such that* $\boldsymbol{v} = \boldsymbol{v}_0 + \boldsymbol{\chi}$ *and*

$$s(\boldsymbol{v}_0, \boldsymbol{v}_0) + a_{\boldsymbol{\mathcal{W}}}(\boldsymbol{\chi}, \boldsymbol{\chi}) \leq c_0^2 \max_{\substack{T\in\Delta_h, T'\in\Delta_h' \\ \partial T\cap\partial T'\neq\emptyset}} \left\{1, \frac{\alpha_T(\nu)}{\alpha_{T'}(\nu)}\right\} a_{DG}(\boldsymbol{v}, \boldsymbol{v}) , \quad (4.41)$$

where the sets Δ_h *and* Δ_h' *are defined in* (4.37) *and the constant* c_0^2 *depends only on the polynomial degree and on the shape regularity of the mesh.*

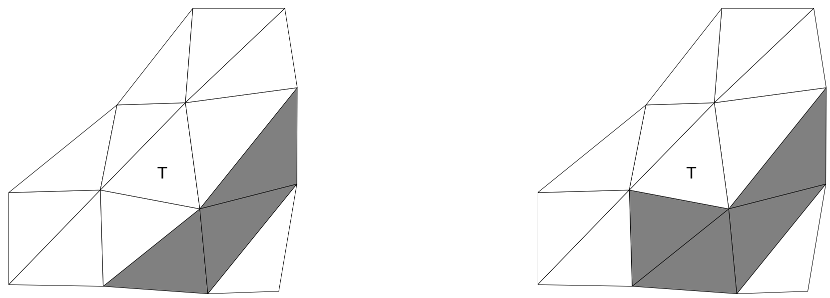

(a) Admissible configuration (b) Non-admissible configuration

Figure 4.3: 2D sketch of the required assumptions in Lemma 4.13. Let the cells T in white be such that $h_T^2\beta_T < \alpha_T(\nu)$, and the cells T' in gray satisfy $h_{T'}^2\beta_{T'} \geq \alpha_{T'}(\nu)$. The element T in case (a) satisfy the assumptions of the Lemma, whereas configuration (b) does not.

Proof. Let $\boldsymbol{v} \in \boldsymbol{V_h}$ and let $\overline{\mathcal{P}}_h$ be the averaging operator as from Definition 4.11. By construction, $\overline{\mathcal{P}}_h(\boldsymbol{v}) \in \boldsymbol{V_h^c}$. Throughout the proof we set $\boldsymbol{v}_0 = \boldsymbol{v} - \overline{\mathcal{P}}_h(\boldsymbol{v})$. We distinguish several cases depending on the regions of the domain, and proceed by local estimates. In particular, for a fixed element $T \in \mathcal{T}_h$, we distinguish four possible cases:

(i) $T \in \Delta_h'$ i.e. $h_T^2\beta_T \geq \alpha_T(\nu) \geq \nu_T$ i.e. the element is in the reaction dominated regime;

(ii) $T \in \Delta_h$ i.e. $h_T^2\beta_T < \alpha_T(\nu)$ and $\mathcal{E}'(T) = \emptyset$ (hence $\mathcal{F}'(T) = \emptyset$);

(iii) $T \in \Delta_h$ i.e. $h_T^2\beta_T < \alpha_T(\nu)$ and $\mathcal{F}'(T) \neq \emptyset$;

(iv) $T \in \Delta_h$ i.e. $h_T^2\beta_T < \alpha_T(\nu)$ and $\mathcal{F}'(T) = \emptyset$ but $\mathcal{E}'(T) \neq \emptyset$.

The last two cases refer to those elements that have a face or an edge at the interface between the reaction dominated and **curl**-dominated regime. We will typically use

$$a_{\mathcal{W}}(\overline{\mathcal{P}}_h(\boldsymbol{v}), \overline{\mathcal{P}}_h(\boldsymbol{v}))|_T \leq a_{\mathcal{W}}(\boldsymbol{v}, \boldsymbol{v})|_T + a_{\mathcal{W}}(\boldsymbol{v} - \overline{\mathcal{P}}_h(\boldsymbol{v}), \boldsymbol{v} - \overline{\mathcal{P}}_h(\boldsymbol{v}))|_T\,, \tag{4.42}$$

and therefore to bound $a_{\mathcal{W}}(\overline{\mathcal{P}}_h(\boldsymbol{v}), \overline{\mathcal{P}}_h(\boldsymbol{v}))|_T$ it will be enough to bound the last term in (4.42). Let us consider one by one the previous cases.

Case (i). In this case, T is an element in the reaction dominated region and therefore the auxiliary space solver is turned off. By definition of the operator $\overline{\mathcal{P}}_h$ (Definition 4.11), it holds $\overline{\mathcal{P}}_h(\boldsymbol{v})|_T = 0$, hence $\boldsymbol{v}_0|_T = \boldsymbol{v}|_T$. This case leaves out (locally) the correction in the auxiliary space. Hence to prove (4.41) we only need to consider the smoother. For the pointwise or block Jacobi smoother, using the scaling in (4.8) together with the fact that $h_T^{-2}\nu_T \leq h_T^{-2}\alpha_T(\nu) \leq \beta_T$, results in

$$s(\boldsymbol{v}_0, \boldsymbol{v}_0)|_T \leq C\left(h_T^{-2}\nu_T\|\boldsymbol{v}\|_{0,T}^2 + \beta_T\|\boldsymbol{v}\|_{0,T}^2 + h_T^{-2}\alpha_T(\nu)\|\boldsymbol{v}\|_{0,T}^2\right) \leq C\beta_T\|\boldsymbol{v}\|_{0,T}^2\,.$$

Case (ii). Owing to the construction of the operator $\overline{\mathcal{P}}_h$ in Definition 4.11, it holds $\overline{\mathcal{P}}_h(\boldsymbol{v})|_T = \mathcal{P}_h(\boldsymbol{v})|_T$ and hence $\boldsymbol{v}_0|_T = \boldsymbol{v}|_T - \mathcal{P}_h(\boldsymbol{v})|_T$. Therefore we can directly argue as in the proof of Proposition 4.9. Taking into account (4.42) and using inverse inequalities, the local approximation properties of $\mathcal{P}_h$ in (4.20) and the assumption $h_T^2\beta_T < \alpha_T(\nu)$ yields

$$\begin{aligned} a_{\mathcal{W}}(\boldsymbol{v} - \mathcal{P}_h(\boldsymbol{v}), \boldsymbol{v} - \mathcal{P}_h(\boldsymbol{v}))|_T &\leq \nu_T\|\boldsymbol{\nabla} \times (\boldsymbol{v} - \mathcal{P}_h(\boldsymbol{v}))\|_{0,T}^2 + \beta_T\|\boldsymbol{v} - \mathcal{P}_h(\boldsymbol{v})\|_{0,T}^2 \\ &\leq h_T^{-2}\nu_T\|\boldsymbol{v} - \mathcal{P}_h(\boldsymbol{v})\|_{0,T}^2 + h_T^{-2}\alpha_T(\nu)\|\boldsymbol{v} - \mathcal{P}_h(\boldsymbol{v})\|_{0,T}^2 \\ &\leq C\alpha_T(\nu)\sum_{e\in\mathcal{E}(T)}\sum_{f\in\mathcal{F}(e)} h_f^{-1}\,\|[\![\,\boldsymbol{v}\,]\!]_{\boldsymbol{\tau}}\|_{0,f}^2\,. \end{aligned}$$

An analogous reasoning applies to the smoothing operator $\mathcal{S}$. For the pointwise or block Jacobi smoother, the scaling in (4.8) together with (4.20), gives

$$\begin{aligned} s(\boldsymbol{v}_0,\boldsymbol{v}_0)|_T &\le C\left(h_T^{-2}\nu_T\|\boldsymbol{v}-\mathcal{P}_h(\boldsymbol{v})\|_{0,T}^2+\beta_T\|\boldsymbol{v}-\mathcal{P}_h(\boldsymbol{v})\|_{0,T}^2+h_T^{-2}\alpha_T(\nu)\|\boldsymbol{v}-\mathcal{P}_h(\boldsymbol{v})\|_{0,T}^2\right)\\ &\le C\alpha_T(\nu)\sum_{e\in\mathcal{E}(T)}\sum_{f\in\mathcal{F}(e)}h_f^{-1}\,\|[\![\,\boldsymbol{v}\,]\!]_{\boldsymbol{\tau}}\|_{0,f}^2\ . \end{aligned}$$

The last two cases cover the configuration where the current element T, in the **curl**-dominated regime, is at the interface with a reaction dominated region.
Case (iii). This situation corresponds to an element T with $h_T^2\beta_T<\alpha_T(\nu)$ sharing at least one face with an element T' having $h_{T'}^2\beta_T'\ge\alpha_{T'}(\nu)$. Under these assumptions, we can exploit the results from Lemma 4.12. Let us first assume that $\mathcal{F}(T)\setminus\mathcal{F}'(T)\neq\emptyset$. Inverse inequality together with estimate (4.38) from Lemma 4.12 gives

$$\begin{aligned} a_{\boldsymbol{\mathcal{W}}}(\boldsymbol{v}-\overline{\mathcal{P}}_h(\boldsymbol{v}),\boldsymbol{v}-\overline{\mathcal{P}}_h(\boldsymbol{v}))|_T &\le \nu_T\|\boldsymbol{\nabla}\times(\boldsymbol{v}-\overline{\mathcal{P}}_h(\boldsymbol{v}))\|_{0,T}^2+\beta_T\|\boldsymbol{v}-\overline{\mathcal{P}}_h(\boldsymbol{v})\|_{0,T}^2\\ &\le h_T^{-2}\nu_T\|\boldsymbol{v}-\overline{\mathcal{P}}_h(\boldsymbol{v})\|_{0,T}^2+h_T^{-2}\alpha_T(\nu)\|\boldsymbol{v}-\overline{\mathcal{P}}_h(\boldsymbol{v})\|_{0,T}^2\\ &\le C\alpha_T(\nu)\sum_{e\in\mathcal{E}(T)}\sum_{f\in\mathcal{F}(e)}h_f^{-1}\,\|[\![\,\boldsymbol{v}\,]\!]_{\boldsymbol{\tau}}\|_{0,f}^2+C\sum_{\substack{T'\in\mathcal{T}_h\\ \partial T\cap\partial T'\in\mathcal{F}'(T)}}\frac{\alpha_T(\nu)}{\alpha_{T'}(\nu)}\beta_{T'}\,\|\boldsymbol{v}\|_{0,T'}^2\ , \end{aligned}$$

Moreover, the same bound can be derived for the pointwise Jacobi operator introduced in (4.9) (or (4.10)) by using the scaling (4.8) and applying estimate (4.38),

$$\begin{aligned} s(\boldsymbol{v}_0,\boldsymbol{v}_0)|_T &\le C\left(h_T^{-2}\nu_T\|\boldsymbol{v}-\overline{\mathcal{P}}_h(\boldsymbol{v})\|_{0,T}^2+\beta_T\|\boldsymbol{v}-\overline{\mathcal{P}}_h(\boldsymbol{v})\|_{0,T}^2+h_T^{-2}\alpha_T(\nu)\|\boldsymbol{v}-\overline{\mathcal{P}}_h(\boldsymbol{v})\|_{0,T}^2\right)\\ &\le Ch_T^{-2}\alpha_T(\nu)\|\boldsymbol{v}-\overline{\mathcal{P}}_h(\boldsymbol{v})\|_{0,T}^2\ , \end{aligned}\tag{4.43}$$

since by assumption the current element T satisfies $h_T^2\beta_T<\alpha_T(\nu)$.

If $\mathcal{F}'(T)\equiv\mathcal{F}(T)$, we exploit the results of Lemma 4.12 in (4.39). For the $\mathrm{H}(\mathbf{curl},\Omega)$-conforming part of the decomposition (4.42), applying estimate (4.39) from that Lemma yields

$$\begin{aligned} a_{\boldsymbol{\mathcal{W}}}(\boldsymbol{v}-\overline{\mathcal{P}}_h(\boldsymbol{v}),\boldsymbol{v}-\overline{\mathcal{P}}_h(\boldsymbol{v}))|_T &\le \nu_T\|\boldsymbol{\nabla}\times(\boldsymbol{v}-\overline{\mathcal{P}}_h(\boldsymbol{v}))\|_{0,T}^2+\beta_T\|\boldsymbol{v}-\overline{\mathcal{P}}_h(\boldsymbol{v})\|_{0,T}^2\\ &\le h_T^{-2}\nu_T\|\boldsymbol{v}-\overline{\mathcal{P}}_h(\boldsymbol{v})\|_{0,T}^2+h_T^{-2}\alpha_T(\nu)\|\boldsymbol{v}-\overline{\mathcal{P}}_h(\boldsymbol{v})\|_{0,T}^2\\ &\le C\alpha_T(\nu)\sum_{f\in\mathcal{F}(T)}h_f^{-1}\,\|[\![\,\boldsymbol{v}\,]\!]_{\boldsymbol{\tau}}\|_{0,f}^2+C\sum_{\substack{T'\in\mathcal{T}_h\\ \partial T\cap\partial T'\in\mathcal{F}(T)}}\frac{\alpha_T(\nu)}{\alpha_{T'}(\nu)}\beta_{T'}\,\|\boldsymbol{v}\|_{0,T'}^2\ . \end{aligned}$$

Concerning the pointwise smoother, one can proceed as in (4.43) by applying this time estimate (4.39) from Lemma 4.12.
Case (iv). The last case fulfills the assumptions of Lemma 4.13. Since by assumption, $h_T^2\beta_T<\alpha_T(\nu)$, inverse inequality on the last term of (4.42) and estimate (4.40) give

$$\begin{aligned} a_{\boldsymbol{\mathcal{W}}}(\boldsymbol{v}-\overline{\mathcal{P}}_h(\boldsymbol{v}),\boldsymbol{v}-\overline{\mathcal{P}}_h(\boldsymbol{v}))|_T &\le \nu_T\|\boldsymbol{\nabla}\times(\boldsymbol{v}-\overline{\mathcal{P}}_h(\boldsymbol{v}))\|_{0,T}^2+\beta_T\|\boldsymbol{v}-\overline{\mathcal{P}}_h(\boldsymbol{v})\|_{0,T}^2\\ &\le h_T^{-2}\nu_T\|\boldsymbol{v}-\overline{\mathcal{P}}_h(\boldsymbol{v})\|_{0,T}^2+h_T^{-2}\alpha_T(\nu)\|\boldsymbol{v}-\overline{\mathcal{P}}_h(\boldsymbol{v})\|_{0,T}^2\\ &\le C\alpha_T(\nu)\sum_{e\in\mathcal{E}(T)}\sum_{f\in\mathcal{F}(e)}h_f^{-1}\,\|[\![\,\boldsymbol{v}\,]\!]_{\boldsymbol{\tau}}\|_{0,f}^2+C\sum_{T'\in\mathcal{T}'(T)}\frac{\alpha_T(\nu)}{\alpha_{T'}(\nu)}\beta_{T'}\,\|\boldsymbol{v}\|_{0,T'}^2\ . \end{aligned}$$

Moreover, proceeding as in case (iii) above, the pointwise Jacobi smoother scales as

$$
\begin{aligned}
s(\boldsymbol{v}_0,\boldsymbol{v}_0)|_T &\le C\left(h_T^{-2}\nu_T\|\boldsymbol{v}-\overline{\mathcal{P}}_h(\boldsymbol{v})\|_{0,T}^2+\beta_T\|\boldsymbol{v}-\overline{\mathcal{P}}_h(\boldsymbol{v})\|_{0,T}^2+h_T^{-2}\alpha_T(\nu)\|\boldsymbol{v}-\overline{\mathcal{P}}_h(\boldsymbol{v})\|_{0,T}^2\right)\\
&\le Ch_T^{-2}\alpha_T(\nu)\|\boldsymbol{v}-\overline{\mathcal{P}}_h(\boldsymbol{v})\|_{0,T}^2\,,
\end{aligned}
$$

and the conclusion follows by applying (4.40).

Collecting the local contributions from all the cases above discussed results in

$$
\begin{aligned}
s(\boldsymbol{v}_0,\boldsymbol{v}_0)+a_{\boldsymbol{\mathcal{W}}}(\boldsymbol{\chi},\boldsymbol{\chi}) &\le \|\nabla\times\boldsymbol{v}\|_{0,\nu,\mathcal{T}_h}^2+C|\boldsymbol{v}|_{*,\nu}^2\\
&\quad + C\max\left\{1,\max_{\substack{T,T'\in\mathcal{T}_h\\ T'\in\mathcal{T}'(T)}}\frac{\alpha_T(\nu)}{\alpha_{T'}(\nu)},\max_{\substack{T,T'\in\mathcal{T}_h\\ \partial T\cap\partial T'\in\mathcal{F}'(T)}}\frac{\alpha_T(\nu)}{\alpha_{T'}(\nu)}\right\}\|\boldsymbol{v}\|_{0,\beta,\mathcal{T}_h}^2\\
&\le C\max\left\{1,\max_{\substack{T\in\Delta_h,T'\in\Delta_h'\\ \partial T\cap\partial T'\neq\emptyset}}\frac{\alpha_T(\nu)}{\alpha_{T'}(\nu)}\right\}\|\boldsymbol{v}\|_{\mathrm{DG}}^2 \qquad \boldsymbol{v}=\boldsymbol{v}_0+\boldsymbol{\chi},\ \boldsymbol{v}_0\in\boldsymbol{V_h},\ \boldsymbol{\chi}\in\boldsymbol{V_h^c}\,.
\end{aligned}
$$

Coercivity of $\mathrm{a}_{\mathrm{DG}}(\cdot,\cdot)$ yields the conclusion. □

Remark 4.15. The theory presented in this paper and summarized in Theorem 4.1 encompasses the following coefficients distributions:

(i) There exists $\beta_{\max}$ and $\nu_{\min}$ such that

$$
\nu_T\ge\nu_{\min}>0\,,\qquad\text{and}\qquad 0<\beta_T\le\beta_{\max}\,,\qquad\forall T\in\mathcal{T}_h\,.
$$

(ii) $\nu>0$ is arbitrary and there exists $B>1$ such that

$$
B^{-1}\le\frac{\beta_T}{\beta_{T'}}\le B\qquad\forall T,T'\in\mathcal{T}_h\,,\quad\text{with}\quad\partial T\cap\partial T'\neq\emptyset\,.
$$

(iii) $\beta>0$ is arbitrary and there exists $\Lambda>1$ such that

$$
\Lambda^{-1}\le\frac{\alpha_T(\nu)}{\alpha_{T'}(\nu)}\le\Lambda\qquad\forall T\in\Delta_h,T'\in\Delta_h'\quad\text{with}\quad\partial T\cap\partial T'\neq\emptyset\,.
$$

The only left out case is when there exist $T\in\mathcal{T}_h$ and $T'\in\mathcal{T}_h$ such that simultaneously it holds

$$
\begin{aligned}
&\partial T\cap\partial T'\notin\mathcal{F}_h\,, &&\partial T\cap\partial T'\in\mathcal{E}_h;\\
&\nu_T\nearrow\infty \quad\text{and} &&\beta_T\searrow 0;\\
&\nu_{T'}\searrow 0 \quad\text{and} &&\beta_{T'}\nearrow\infty.
\end{aligned}
$$

In this case, since all elements sharing an edge contribute to the construction of a conforming approximation of a given function in the DG space $\boldsymbol{V_h}$, it is not possible, with the techniques presented here, to bound simultaneously the L^2-norm of the approximation error weighted by the coefficients ν and β.

Remark 4.16. The analysis presented in Section 4.5 could be carried out analogously by considering the local ratio $h_T^2\beta_T/\nu_T$ instead of $h_T^2\beta_T/\alpha_T(\nu)$. The decomposition of $\boldsymbol{v}\in\boldsymbol{V_h}$, corresponding to (4.41) would yield a bound of the form

$$
s(\boldsymbol{v}_0,\boldsymbol{v}_0)+a_{\boldsymbol{\mathcal{W}}}(\boldsymbol{\chi},\boldsymbol{\chi})\le c_0^2\max\left\{1,\max_{\substack{T\in\Delta_h,T'\in\Delta_h'\\ \partial T\cap\partial T'\neq\emptyset}}\frac{\alpha_T(\nu)}{\nu_{T'}},\max_{T\in\Delta_h'}\frac{\alpha_T(\nu)}{\nu_T}\right\}\mathrm{a}_{\mathrm{DG}}(\boldsymbol{v},\boldsymbol{v})\,,
$$

with $\boldsymbol{v}=\boldsymbol{v}_0+\boldsymbol{\chi}$, $\boldsymbol{v}_0\in\boldsymbol{V_h}$, and $\boldsymbol{\chi}\in\boldsymbol{V_h^c}$. Here the uniform bound required on the ratio $\alpha_T(\nu)/\nu_{T'}$ implies that the coefficients ν_{T_i} for elements T_i in a **curl**-dominated region and belonging to the neighborhood of T cannot be arbitrarily small within the patch. The choice of dealing with the less natural ratio $h_T^2\beta_T/\alpha_T(\nu)$ as in (4.41) is aimed at avoiding this shortcoming.

4.6 "Coarser solver" in the auxiliary space

On a simplicial mesh $\mathcal{T}_h$, one can combine a DG discretization based on the local space $\mathcal{M}(T) = \mathcal{N}^{II}(T)$ as in (2.2) and the $\mathrm{H}_0(\mathbf{curl}, \Omega)$-conforming finite element space based on the local space $\mathcal{N}^I(T)$ as in (2.3) (reproducing case (b) in Section 3.2). Using an overlapping additive smoother of the type (3.14), the stable decomposition property **(F2)** in Theorem 3.2 is fulfilled even in this case, as shown in the following:

Proposition 4.17. *Let $\mathcal{T}_h$ be a mesh of simplices, shape regular and quasi-uniform. Let $\boldsymbol{V_h}$ be the space defined in (2.1) with $\mathcal{M}(T) = \mathcal{N}^{II}(T)$. Let $\boldsymbol{W_h^c}$ be the $H(\mathbf{curl}, \Omega)$-conforming finite element space defined in (3.6). Let $s_O(\cdot, \cdot)$ be an overlapping smoother as in (3.14). Then, for any $\boldsymbol{v} \in \boldsymbol{V_h}$ there exist $\boldsymbol{v}_0 \in \boldsymbol{V_h}$ and $\boldsymbol{w} \in \boldsymbol{W_h^c}$ such that $\boldsymbol{v} = \boldsymbol{v}_0 + \boldsymbol{w}$ and*

$$s_O(\boldsymbol{v}_0, \boldsymbol{v}_0) + a_{\boldsymbol{\mathcal{W}}}(\boldsymbol{w}, \boldsymbol{w}) \leq \tilde{c}_a \max\{1, \delta(\nu, \beta)\} a_{DG}(\boldsymbol{v}, \boldsymbol{v}) \,, \tag{4.44}$$

where $\delta(\nu, \beta)$ is defined as in (4.1), namely

$$\delta(\nu, \beta) := \min \left\{ \max_{T \in \mathcal{T}_h} \frac{h_T^2 \beta_T}{\nu_T}, \max_{\substack{T, T' \in \mathcal{T}_h \\ \partial T \cap \partial T' \neq \emptyset}} \frac{\beta_T}{\beta_{T'}}, \max_{\substack{T \in \Delta_h, T' \in \Delta_h' \\ \partial T \cap \partial T' \neq \emptyset}} \frac{\alpha_T(\nu)}{\alpha_{T'}(\nu)} \right\} ,$$

and the constant $\tilde{c}_a > 0$ depends only on the polynomial degree and the shape regularity of the mesh.

Proof. Let $\boldsymbol{v} \in \boldsymbol{V_h}$, we define $\boldsymbol{\chi} := \mathcal{P}_h(\boldsymbol{v}) \in \boldsymbol{V_h^c}$, where $\mathcal{P}_h$ is the averaging operator in Definition 4.6. Let $\boldsymbol{w} := \Pi^{N,I}(\boldsymbol{\chi})$ where $\Pi^{N,I} : \boldsymbol{V_h^c} \to \boldsymbol{W_h^c}$ is the $\mathrm{H}(\mathbf{curl}, \Omega)$-conforming Nédélec interpolation operator of the second kind. Let us set

$$\boldsymbol{v}_0 = \boldsymbol{v} - \boldsymbol{w} = \boldsymbol{v} - \boldsymbol{\chi} + \boldsymbol{\chi} - \boldsymbol{w} = (\boldsymbol{v} - \mathcal{P}_h(\boldsymbol{v})) + (\boldsymbol{\chi} - \Pi^{N,I} \boldsymbol{\chi}) \,.$$

Observe that, since the mesh is made of simplices, $\mathbf{curl}(\mathcal{N}^I(T)) = \mathbf{curl}(\mathcal{N}^{II}(T))$ and therefore the difference $\boldsymbol{\chi} - \boldsymbol{w}$ is curl-free. Hence, we can rely on the following discrete Helmholtz decomposition [30],

$$\boldsymbol{\chi} = \Pi^{N,I} \boldsymbol{\chi} + \nabla q \qquad q \in \mathbb{P}_{k+1}(\mathcal{T}_h) \cap H^1(\Omega) \,. \tag{4.45}$$

Using local approximation estimates for the Nédélec interpolant (*cf.* e.g. [11]), and the definition of $\boldsymbol{\chi} = \mathcal{P}_h(\boldsymbol{v})$ results in

$$\begin{aligned} a_{\boldsymbol{\mathcal{W}}}(\boldsymbol{w}, \boldsymbol{w}) &= \sum_{T \in \mathcal{T}_h} \nu_T \|\boldsymbol{\nabla} \times \Pi^{N,I}(\boldsymbol{\chi})\|_{0,T}^2 + \sum_{T \in \mathcal{T}_h} \beta_T \|\Pi^{N,I}(\boldsymbol{\chi})\|_{0,T}^2 \\ &\leq C \sum_{T \in \mathcal{T}_h} \nu_T \|\boldsymbol{\nabla} \times \mathcal{P}_h(\boldsymbol{v})\|_{0,T}^2 + \sum_{T \in \mathcal{T}_h} \beta_T \|\mathcal{P}_h \boldsymbol{v}\|_{0,T}^2 \,. \end{aligned}$$

The estimates from Lemma 4.7 yield a bound of the form (4.44) for the $\mathrm{H}(\mathbf{curl}, \Omega)$-conforming part of the decomposition.

Concerning the patch smoother, in view of the Helmholtz decomposition (4.45), there holds

$$s_O(\boldsymbol{v}_0, \boldsymbol{v}_0) \leq s_O(\boldsymbol{v} - \mathcal{P}_h(\boldsymbol{v}), \boldsymbol{v} - \mathcal{P}_h(\boldsymbol{v})) + s_O(\nabla q, \nabla q) \,. \tag{4.46}$$

Using the scaling (4.12) derived in Lemma 4.5, the first term above can be cast as

$$\begin{aligned} s_O(\boldsymbol{v} - \mathcal{P}_h(\boldsymbol{v}), \boldsymbol{v} - \mathcal{P}_h(\boldsymbol{v})) \simeq \sum_{j=1}^{J} \Bigg(& \sum_{T \in \Omega_j} \nu_T \, \|\boldsymbol{\nabla} \times (\boldsymbol{v}_j - \mathcal{P}_h(\boldsymbol{v}_j))\|_{0,T}^2 + \beta_T \, \|\boldsymbol{v}_j - \mathcal{P}_h(\boldsymbol{v}_j)\|_{0,T}^2 \\ & + \sum_{T \in \Omega_j} \alpha_T(\nu) \sum_{e \in \mathcal{E}(T)} \sum_{f \in \mathcal{F}(e) \setminus \partial \Omega_j} h_f^{-1} \, \|[\![\boldsymbol{v}_j - \mathcal{P}_h(\boldsymbol{v}_j)]\!]_{\boldsymbol{\tau}}\|_{0,f}^2 \\ & + \sum_{\substack{T \in \Omega_j \\ \partial T \cap \partial \Omega_j \neq \emptyset}} \alpha_T(\nu) \sum_{e \in \mathcal{E}(T)} \sum_{f \in \mathcal{F}(e) \cap \partial \Omega_j} h_f^{-1} \, \|\mathbf{n} \times (\boldsymbol{v}_j - \mathcal{P}_h(\boldsymbol{v}_j))\|_{0,f}^2 \Bigg) \,. \end{aligned}$$

Let $c(\nu,\beta) := \max\{1, \delta(\nu,\beta)\}$, the estimates derived in Lemma 4.7 and Corollary 4.8 for the approximation error given by $\mathcal{P}_h$, yield

$$s_O(\boldsymbol{v}-\mathcal{P}_h(\boldsymbol{v}), \boldsymbol{v}-\mathcal{P}_h(\boldsymbol{v})) \leq Cc(\nu,\beta)\sum_{j=1}^{J}\Bigg(\sum_{T\in\Omega_j}\|\boldsymbol{v}_j\|_{0,T}^2 + \sum_{T\in\Omega_j}\alpha_T(\nu)\sum_{e\in\mathcal{E}(T)}\sum_{f\in\mathcal{F}(e)} h_f^{-1}\,\|[\![\,\boldsymbol{v}_j\,]\!]_{\boldsymbol{\tau}}\|_{0,f}^2\Bigg)\,.$$

The second term in (4.46) can be bounded as follows. Let $\nabla q_j := \boldsymbol{\chi}_j - \Pi^{N,I}\boldsymbol{\chi}_j = \mathcal{P}_h(\boldsymbol{v}_j) - \Pi^{N,I}(\mathcal{P}_h(\boldsymbol{v}_j))$ for $j = 1,\ldots,J$. Since $\nabla q \in \mathrm{Kern}(\mathbf{curl})$, the scaling (4.12) reads

$$\begin{aligned}
s_O(\nabla q, \nabla q) &\simeq \sum_{j=1}^{J}\Bigg(\sum_{T\in\Omega_j}\beta_T\,\|\nabla q_j\|_{0,T}^2 + \sum_{\substack{T\in\Omega_j\\ \partial T\cap\partial\Omega_j\neq\emptyset}}\alpha_T(\nu)\sum_{e\in\mathcal{E}(T)}\sum_{f\in\mathcal{F}(e)\cap\partial\Omega_j} h_f^{-1}\,\|\mathbf{n}\times\nabla q_j\|_{0,f}^2\Bigg)\\
&\leq C\sum_{j=1}^{J}\Bigg(\sum_{T\in\Omega_j}\beta_T\left\|\boldsymbol{\chi}_j - \Pi^{N,I}(\boldsymbol{\chi}_j)\right\|_{0,T}^2 + \sum_{\substack{T\in\Omega_j\\ \partial T\cap\partial\Omega_j\neq\emptyset}}\alpha_T(\nu)h_T^{-2}\left\|\boldsymbol{\chi}_j - \Pi^{N,I}(\boldsymbol{\chi}_j)\right\|_{0,T}^2\Bigg)\,,
\end{aligned}$$

where the inverse trace inequality has been used. The local error estimates for $\boldsymbol{\chi}_j - \Pi^{N,I}(\boldsymbol{\chi}_j)$ as in [60], [87, Lemma 10.4 and Lemma 10.8] together with the error bounds from Lemma 4.7 and Corollary 4.8, result in

$$\begin{aligned}
s_O(\nabla q, \nabla q) &\leq C\sum_{j=1}^{J}\Bigg(\sum_{T\in\Omega_j}\beta_T\,\|\mathcal{P}_h(\boldsymbol{v}_j)\|_{0,T}^2 + \sum_{\substack{T\in\Omega_j\\ \partial T\cap\partial\Omega_j\neq\emptyset}}\alpha_T(\nu)h_T^{-2}\,\|\mathcal{P}_h(\boldsymbol{v}_j)\|_{0,T}^2\Bigg)\\
&\leq Cc(\nu,\beta)\sum_{j=1}^{J}\Bigg(\sum_{T\in\Omega_j}\|\boldsymbol{v}_j\|_{0,T}^2 + \sum_{T\in\Omega_j}\alpha_T(\nu)\sum_{e\in\mathcal{E}(T)}\sum_{f\in\mathcal{F}(e)} h_f^{-1}\,\|[\![\,\boldsymbol{v}_j\,]\!]_{\boldsymbol{\tau}}\|_{0,f}^2\Bigg)\,.
\end{aligned}$$

If $\{\theta_j\}_{j=1}^{J}$ is a partition of unity relative to the decomposition $\Omega_y = \{\Omega_j\}_{j=1}^{J}$ as in e.g. [49] or [82], the conclusion (4.44) follows by

$$\begin{aligned}
&\|\boldsymbol{v}_j\|_{0,T}^2 = \|\theta_j\boldsymbol{v}\|_{0,T}^2 \leq \|\theta_j\|_{L^\infty(\Omega)}^2\,\|\boldsymbol{v}\|_{0,T}^2 \leq C\,\|\boldsymbol{v}\|_{0,T}^2 \qquad \forall\, T\in\Omega_j\,;\\
&\|[\![\,\boldsymbol{v}_j\,]\!]_{\boldsymbol{\tau}}\|_{0,f}^2 = \|[\![\,\theta_j\boldsymbol{v}\,]\!]_{\boldsymbol{\tau}}\|_{0,f}^2 \leq \|\theta_j\|_{L^\infty(\Omega)}^2\,\|[\![\,\boldsymbol{v}\,]\!]_{\boldsymbol{\tau}}\|_{0,f}^2 \leq C\,\|[\![\,\boldsymbol{v}\,]\!]_{\boldsymbol{\tau}}\|_{0,f}^2 \qquad \forall\, f\in\mathcal{F}_h\cap\Omega_j\,.
\end{aligned}$$

□

Remark 4.18. On a hexahedral mesh the stability results of Proposition 4.17 do not hold true. Indeed, as pointed out in [35, Remark 4.17] and observed numerically in [34, Section 5] (see also [55, Section 6.2] where optimal L^2-convergence is studied for the corresponding time dependent problem) the full polynomials space $\mathbb{Q}_k(T)^3$ yields a discretization which triggers spurious modes. This is confirmed by the numerical experiments in Section 6 (see in particular Figure 6.1 and Figure 6.2). Therefore, using a spectrally correct auxiliary space in the preconditioner for the DG discretization based on $\mathbb{Q}_k(T)^3$ does not seem to result in a convergent solver, independently of the type of the smoother. However, if the auxiliary space consists of full polynomials, Theorem 4.1 applies and the resulting preconditioner is uniform. Similarly, other than the choice of full polynomial space approximations and Nédélec second family auxiliary space, if the finite element DG space $\boldsymbol{V_h}$ in (2.1) is defined as $\boldsymbol{V_h} = \{\boldsymbol{v}\in L^2(\Omega)^d : \boldsymbol{v}\in\mathcal{N}_q^I(T),\, T\in\mathcal{T}_h\}$. where $\mathcal{N}_q^I(T)$ is the local space of Nédélec elements of the first family of degree k as in (2.4), the results in Theorem 4.1 carry over.

We close this section by providing a Lemma, similar to [92, Theorem 4.5], that shows that the use of an overlapping smoother in Proposition 4.17 is indeed necessary.

Lemma 4.19. *Let $\mathcal{T}_h$ be a mesh of simplices, shape regular and quasi-uniform. Let $\boldsymbol{V_h}$ be the space defined in* (2.1) *with $\mathcal{M}(T) = \mathcal{N}^{II}(T)$. Let $\boldsymbol{W_h^c}$ be the $H(\mathbf{curl},\Omega)$-conforming finite element space defined in* (3.6)*. Let $s(\cdot,\cdot)$ be any of the pointwise smoothers defined in* (4.9) *and* (4.10)*. Then, there exist $\boldsymbol{v} \in \boldsymbol{V_h}$, $\boldsymbol{w} \in \boldsymbol{W_h^c}$ and $\boldsymbol{v}_0 \in \boldsymbol{V_h}$ such that $\boldsymbol{v} = \boldsymbol{v}_0 + \boldsymbol{w}$ and*

$$s(\boldsymbol{v}_0, \boldsymbol{v}_0) + a_{\boldsymbol{\mathcal{W}}}(\boldsymbol{w}, \boldsymbol{w}) \leq C \max\left\{1, \max_{T\in\mathcal{T}_h} \frac{\alpha_T(\nu) h_T^{-2}}{\beta_T}\right\} \mathrm{a}_{DG}(\boldsymbol{v}, \boldsymbol{v}) \,,$$

where $C > 0$ depends on the shape regularity of the mesh and on the polynomial degree. As a consequence, except for the reaction dominated regime, the spectral condition number of the preconditioned system (using $\boldsymbol{W_h^c}$ and $s(\cdot,\cdot)$) would depend on the mesh size and the problem coefficients.

Proof. The proof is constructive. Let T be a fixed tetrahedron with barycentric coordinates $\lambda_1, \ldots, \lambda_4$. Let $e = e_{ij} \subset \partial T$ be a fixed edge of T with endpoints i and j and let $\boldsymbol{b}_e$ be the basis function relative to the edge e corresponding to a local shape function of the form $\boldsymbol{\nabla}(3\lambda_i\lambda_j)$ i.e. the gradient of a quadratic edge bubble. Note that $\boldsymbol{b}_e \in \mathcal{N}^{II}(T) \setminus \mathcal{N}^{I}(T)$ and $\boldsymbol{b}_e$ can be considered as a global function extended by zero outside of its support (the "macroelement" consisting of the union of the tetrahedra sharing the edge e). Then $\boldsymbol{b}_e \in \boldsymbol{V_h}$, $\boldsymbol{b}_e \in \boldsymbol{V_h^c}$ but $\boldsymbol{b}_e \notin \boldsymbol{W_h^c}$.

Observe that arguing as in the proof of Proposition 4.17, by taking $\boldsymbol{v}_h := \boldsymbol{b}_e \in \boldsymbol{V_h}$, we plainly have $\boldsymbol{\chi} := \mathcal{P}_h(\boldsymbol{b}_e) \equiv \boldsymbol{b}_e \in \boldsymbol{V_h^c}$ and $\boldsymbol{w} := \Pi^{N,I}(\boldsymbol{b}_e) \equiv \boldsymbol{0}$. Therefore, it holds

$$a_{\boldsymbol{\mathcal{W}}}(\Pi^{N,I}(\boldsymbol{b}_e), \Pi^{N,I}(\boldsymbol{b}_e)) = 0 \,,$$

and taking into account the definition of the pointwise smoother (see the proof of the scaling (4.8) given in Lemma 4.4), we have

$$\begin{aligned} s(\boldsymbol{b}_e, \boldsymbol{b}_e) &\simeq \sum_{T\in\mathcal{T}_h} \sum_{e\in\mathcal{E}(T)} \beta_T \|\boldsymbol{b}_e\|_{0,T}^2 + \sum_{T\in\mathcal{T}_h} \alpha_T(\nu) \sum_{e\in\mathcal{E}(T)} \sum_{f\in\mathcal{F}(e)} h_f^{-1} \|\boldsymbol{n} \times \boldsymbol{b}_e\|_{0,f}^2 \\ &\simeq \sum_{T\in\mathcal{T}(e)} \beta_T \|\boldsymbol{b}_e\|_{0,T}^2 + \sum_{T\in\mathcal{T}(e)} \alpha_T(\nu) h_T^{-2} \|\boldsymbol{b}_e\|_{0,T}^2 \,. \end{aligned}$$

On the other hand, since $\boldsymbol{b}_e \in \boldsymbol{V_h^c}$ its jumps $[\![\boldsymbol{b}_e]\!]_{\boldsymbol{\tau}} \equiv 0$ across the mesh faces. Hence,

$$\mathrm{a}_{\mathrm{DG}}(\boldsymbol{b}_e, \boldsymbol{b}_e) \simeq \sum_{T\in\mathcal{T}(e)} \beta_T \|\boldsymbol{b}_e\|_{0,T}^2 \,.$$

Therefore, for $\boldsymbol{v}_h := \boldsymbol{b}_e \in \boldsymbol{V_h}$, the splitting $\boldsymbol{v}_h := \boldsymbol{b}_e + \boldsymbol{0}$ gives

$$s(\boldsymbol{b}_e, \boldsymbol{b}_e) + a_{\boldsymbol{\mathcal{W}}}(\Pi^{N,I}(\boldsymbol{b}_e), \Pi^{N,I}(\boldsymbol{b}_e)) = s(\boldsymbol{b}_e, \boldsymbol{b}_e) \leq \tilde{c}_0(h_T, \beta, \nu)\, \mathrm{a}_{\mathrm{DG}}(\boldsymbol{b}_e, \boldsymbol{b}_e) \,,$$

where $\tilde{c}_0(h_T, \beta, \nu)$ is defined as

$$\tilde{c}_0(h_T, \beta, \nu) := C \max\left\{1, \max_{T\in\mathcal{T}(e)} \frac{\alpha_T(\nu) h_T^{-2}}{\beta_T}\right\} ,$$

and C depends only on the shape regularity of the mesh and on the polynomial degree of $\boldsymbol{V_h}$. The last inequality shows that unless the problem is reaction dominated (i.e. $\beta_T \geq h_T^{-2}\alpha_T(\nu)$), the smoother would not be effective in damping the function $\boldsymbol{b}_e$ (not seen by the auxiliary space) and the spectral condition number of the preconditioned system would show dependence on the mesh size, deteriorating when the mesh is refined. $\square$

5 Numerical Experiments in 2D

In the following numerical simulations we will restrict to the two dimensional problem (1.1) in the unit square $\Omega = [0,1]^2$. The numerical effort required for the validation of the theoretical results on very fine meshes where the asymptotical behavior of the proposed preconditioner emerges, deterred us from dealing with the three-dimensional case. The two dimensional operators are defined as

$$\begin{aligned} &\operatorname{curl} \boldsymbol{v} = \partial v_2/\partial x_1 - \partial v_1/\partial x_2 && \forall\, \boldsymbol{v} = (v_1, v_2) \in \mathrm{H}(\operatorname{curl}, \Omega); \\ &\mathbf{curl}\, \phi = \nabla^{\perp}\phi := (\partial\phi/\partial x_2, -\partial\phi/\partial x_1)^{\mathsf{T}} && \forall\, \phi \in \mathrm{H}(\mathbf{curl}, \Omega). \end{aligned}$$

Throughout, if not otherwise specified, the constant penalty parameter c_0 in (2.8) entering the IP-DG discretization is assumed to be $c_0 = 10$. Concerning the solver, we will compare the performances of the non-preconditioned and preconditioned conjugate gradient algorithms, with stopping criterion based on a tolerance fixed to 10^{-7}. As initial guess we will use the default one, namely the zero vector. A Lanczos procedure (see [52, Chapter 9]) within the PCG routine is used to compute the extremal eigenvalues of the preconditioned system.

To validate the theoretical results, we consider numerical experiments on both structured, locally refined and quasi-uniform triangular meshes, with continuous (the first three test cases) and strongly varying discontinuous coefficients ν and β (the last three set of experiments). Finally, we present some numerical results and considerations for the case of tensor product meshes along the lines of Remark 4.18.

As it is well known, in two dimensions, the space $\mathrm{H}(\mathbf{curl}, \Omega)$ is isomorphic to $\mathrm{H}(\mathbf{div}, \Omega)$ through a $\pi/2$ rotation. We will exploit this isomorphism in order to derive $\mathrm{H}(\mathbf{curl}, \Omega)$-conforming finite element spaces from $\mathrm{H}(\mathbf{div}, \Omega)$-conforming spaces by means of a vector rotation: The space $\mathcal{M}(T)$ in (2.3) corresponds to the *rotated* Raviart-Thomas (RT) finite element space $\mathcal{RT}_k$ [80] and similarly the space $\mathcal{M}(T)$ in (2.2) corresponds to the *rotated* Brezzi-Douglas-Marini (BDM) element space $\mathcal{BDM}_k$ [29]. With a small abuse of notation and due to space constraints, in some of the graphics and tables the term "rotated" is not explicitly specified when referring to the finite element spaces. However, the finite element spaces are always meant "rotated".

5.1 Structured triangular meshes. Constant coefficients.

As first test case, the problem with constant coefficients $\beta = \nu = 1$ is considered on a uniform structured triangular mesh. The IP-DG discretization is based on the full polynomial space (2.2) and is preconditioned with lowest order rotated BDM elements (3.5) for the auxiliary space and Jacobi pointwise smoother (4.9). As shown in Figure 5.1, the spectral condition number of the preconditioned matrix is independent of the mesh width (see also Table 5.1 for the number of iterations required for convergence).

In the same graphic and table are reported the results obtained with the preconditioner of type (b) (see Section 3) based on the lowest order rotated Raviart-Thomas elements in the discretization of the auxiliary space (3.6) combined with different pointwise and patch smoothers. Note that only in the case of a block relaxation (overlapping additive Schwarz), the condition number is independent of the mesh width. The non-efficacy of pointwise (Jacobi or block Jacobi) smoothers is in agreement with Remark 3.3 and Lemma 4.19. The efficiency of the different smoothers can be also observed in Table 5.1.

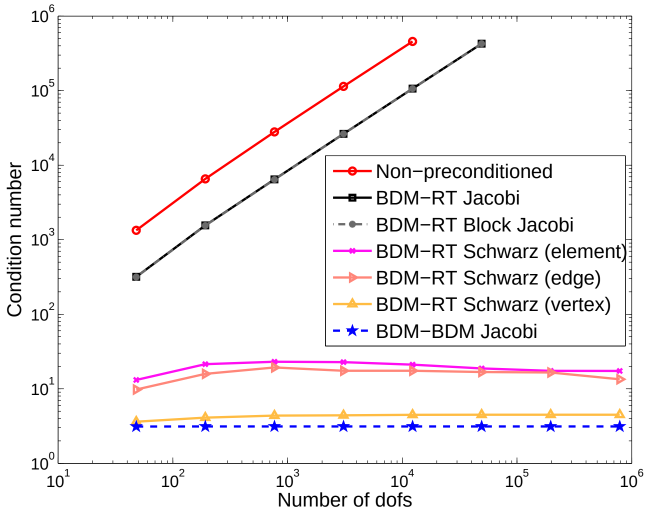

Figure 5.1: Spectral condition number vs number of dofs. The DG discretization is based on the full polynomial space (lowest order rotated BDM elements) and lowest order rotated RT elements for the auxiliary space (BDM-RT) or lowest order rotated BDM elements (BDM-BDM). Different choices of the smoother are considered.

$\boldsymbol{V_h} - \boldsymbol{\mathcal{W}}$ smoother \ $\sharp\mathcal{T}_h$	2^3	2^5	2^7	2^9	2^{11}	2^{13}	2^{15}	2^{17}
BDM Non-prec	45	190	434	889	1784	–	–	–
BDM-RT Jacobi	36	73	90	90	93	94	–	–
BDM-RT block Jacobi	32	67	78	82	85	86	–	–
BDM-RT Schwarz (element)	15	26	29	28	27	26	26	24
BDM-RT Schwarz (edge)	20	32	34	34	32	31	29	28
BDM-RT Schwarz (vertex)	12	15	16	17	17	16	16	16
BDM-BDM Jacobi	11	12	12	11	11	11	10	10

Table 5.1: Number of iterations for decreasing mesh width. Cases as in Figure 5.1.

5.2 Quasi-uniform triangular mesh. Constant coefficients.

For coefficients $\beta = \nu = 1$, the spectral condition number of the preconditioned system for an auxiliary space based on lowest order rotated BDM elements with pointwise relaxation has shown to be independent of the mesh width even on quasi-uniform triangular meshes (see Figure 5.2 and Table 5.2).

Number of dofs:	48	192	768	3072	12288
BDM Non-prec	45	238	641	1521	4455
BDM-BDM Jacobi	10	10	10	10	13

Table 5.2: Number of iterations for decreasing mesh width on quasi-uniform triangular meshes.

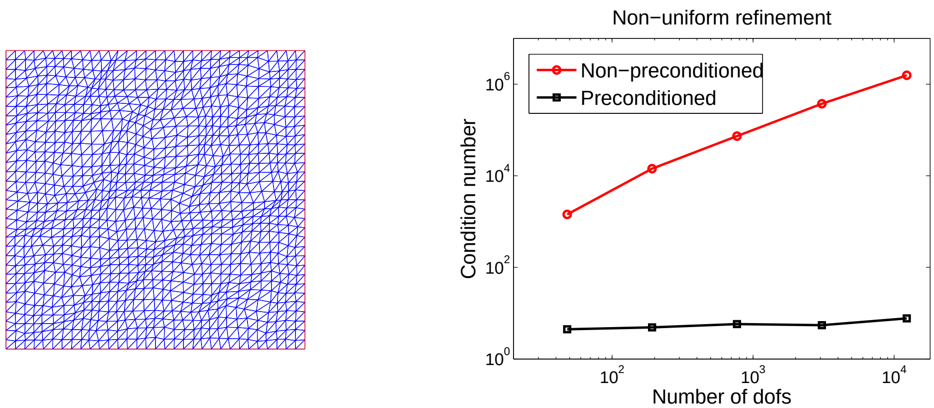

Figure 5.2: Condition number vs number of dofs for quasi-uniform meshes. Lowest order rotated BDM element for the DG space and second family edge elements on the auxiliary space. Jacobi smoother.

5.3 Triangular mesh, local refinement. Constant coefficients.

Under the same discretization as in the previous test case, with $\beta = \nu = 1$, the preconditioner proposed in Section 3.2 case (a), has proven competitive for locally refined meshes, see Figure 5.3 and Table 5.3. In particular, we consider three different test cases which often occur in applications, namely a local refinement towards a corner of the domain, towards a boundary side and towards a point/region inside the domain Ω. The refinement strategy is not driven by any error estimator. As can be easily observed, in all cases, the convergence of the preconditioner (measured from the spectral condition number or number of iterates) is uniform with respect to the mesh size.

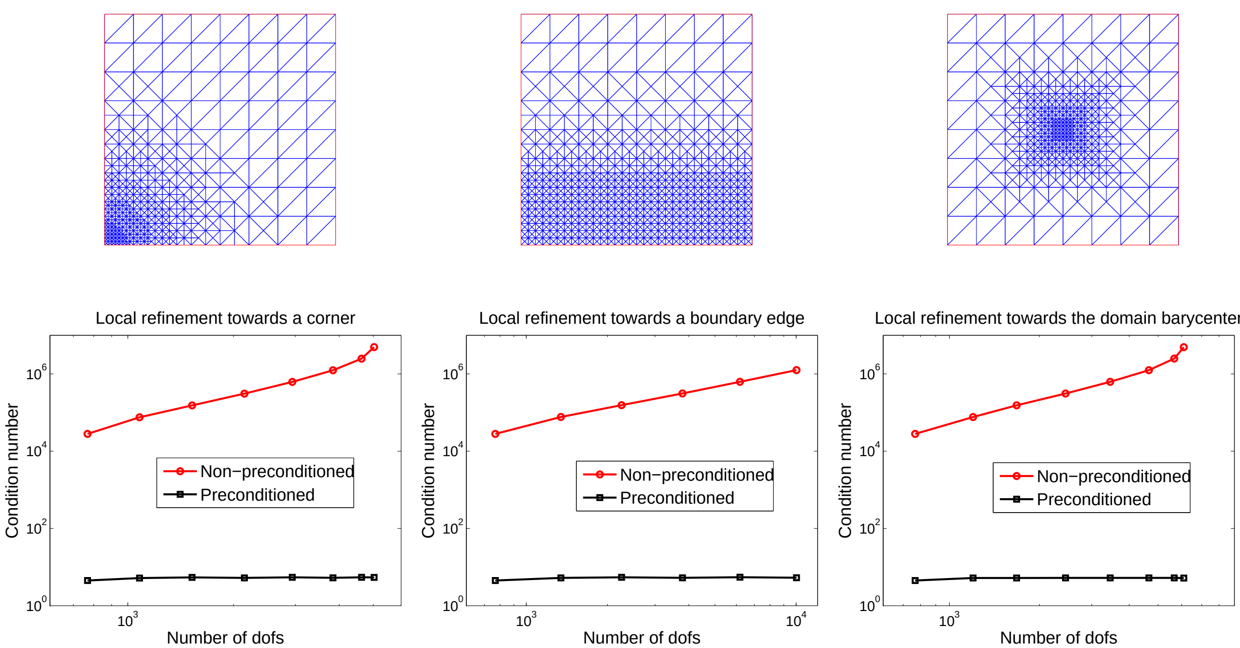

Figure 5.3: Three different local refinement strategies. Condition number vs number of dofs for a numerical discretization based on full polynomial DG spaces and second family edge elements (rotated BDM_0) for the auxiliary space. Pointwise Jacobi smoother.

Case 1, in Figure 5.3

$\sharp\mathcal{T}_h$	128	180	254	358	490	640	772	838
BDM Non-prec	434	705	1065	1488	2171	3073	4439	6024
BDM-BDM Jacobi	12	12	12	12	12	12	12	12

Case 2, in Figure 5.3

$\sharp\mathcal{T}_h$	128	224	376	632	1032	1672
BDM Non-prec	434	678	1042	1445	2123	3090
BDM-BDM Jacobi	12	12	12	12	12	12

Case 3, in Figure 5.3

$\sharp\mathcal{T}_h$	128	200	280	408	576	776	944	1016
BDM Non-prec	434	682	1046	1399	2094	3049	4324	6156
BDM-BDM Jacobi	12	12	12	12	12	12	12	12

Table 5.3: Number of iterations for decreasing mesh width.

5.4 Structured triangular mesh. Coefficients: $\beta = 1$, ν discontinuous.

Let us assume that $\beta = 1$, whilst the magnetic diffusivity ν is discontinuous and piecewise constant, namely

$$\nu(\mathbf{x}) = \begin{cases} \nu_1 & \text{if } \mathbf{x} \in \Omega_1 := [0, 0.5]^2 \cup [0.5, 1]^2 \\ \nu_2 & \text{otherwise} \end{cases}$$

The coefficient $\nu_2 = 1$ is fixed. Note that the initial uniform triangulation resolves the jump discontinuities of the coefficient ν. We compare the performances of the preconditioner as the mesh is uniformly refined and for different values of the coefficient ν_1. The discretization is based on lowest order rotated BDM elements (2.2) and preconditioned with auxiliary space as in (3.5) with pointwise Jacobi smoother (4.9).

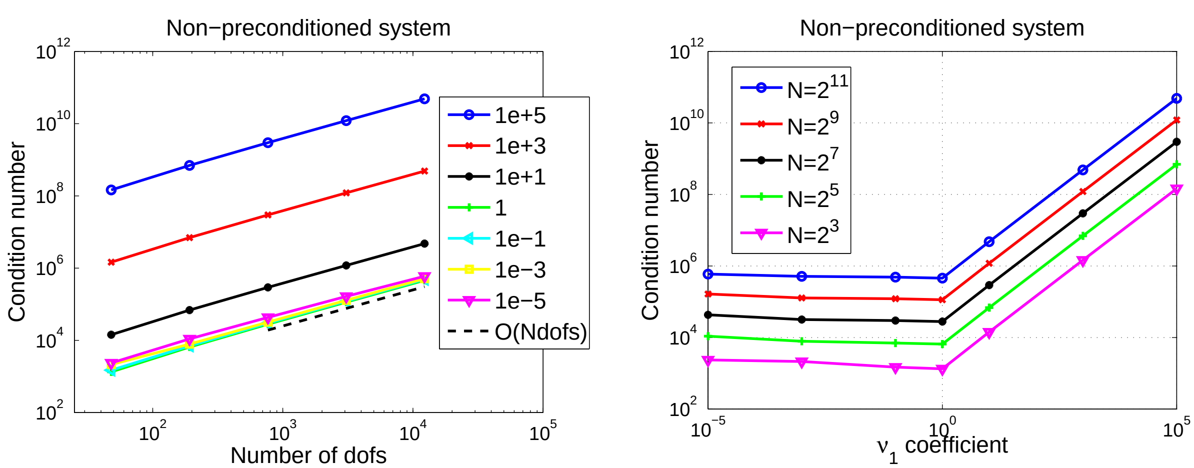

Figure 5.4: Condition number vs number of dofs for different values of the coefficient ν (left). Condition number vs values of ν for different mesh widths (right). Discretization based on full polynomial DG space. Non preconditioned system.

When the problem is solved without appealing to a preconditioner, the spectral condition number depends, as expected, on the mesh width and on the magnitude of the jump (Figure 5.4 and Table 5.4, Table 5.5). Concerning the preconditioned system, the condition number is independent of the mesh width (Figure 5.5, left) and it is asymptotically independent on the magnitude of the jump of the coefficient ν (see Figure 5.5, right). This can be readily checked also from Table 5.4 and Table 5.5, which report the condition number and number of iterations for different values of the coefficient ν_1. This is in agreement with Theorem 4.1 (see also Remark 4.10) which predicts uniform convergence when only one of the two coefficients is allowed to vary.

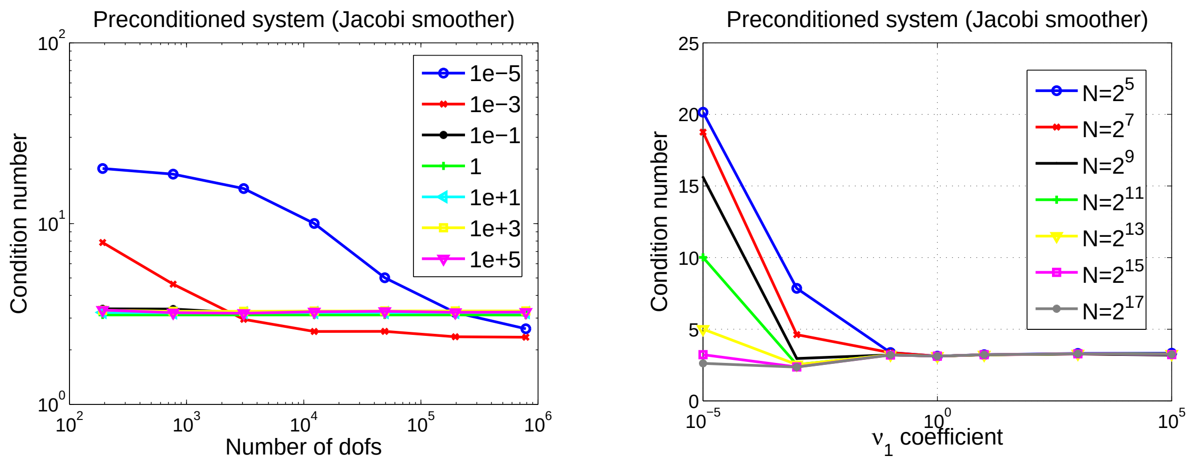

Figure 5.5: Condition number vs number of dofs for different values of the coefficient ν (left). Condition number vs values of ν for different mesh widths (right). Discretization based on full polynomial DG space and second family edge elements for the auxiliary space. Pointwise Jacobi smoother.

	Non-preconditioned system				Preconditioned system					
	$\sharp\mathcal{T}_h$				$\sharp\mathcal{T}_h$					
ν_1	2^5	2^7	2^9	2^{11}	2^7	2^9	2^{11}	2^{13}	2^{15}	2^{17}
10^{-5}	1.09e+4	4.29e+4	1.64e+5	5.93e+5	18.7612	15.6055	10.0127	5.0084	3.2176	2.6177
10^{-3}	7.86e+3	3.18e+4	1.27e+5	5.11e+5	4.6201	2.9498	2.5266	2.5303	2.3620	2.3514
10^{-1}	7.01e+3	2.98e+4	1.21e+5	4.87e+5	3.3639	3.2011	3.2118	3.2136	3.1995	3.1938
1	6.53e+3	2.79e+4	1.13e+5	4.57e+5	3.1205	3.1208	3.1202	3.1200	3.1197	3.1188
10^1	6.84e+4	2.91e+5	1.18e+6	4.76e+6	3.2055	3.2093	3.2154	3.2163	3.2171	3.2170
10^3	6.98e+6	2.97e+7	1.20e+8	4.86e+8	3.2676	3.2700	3.2760	3.2811	3.2829	3.2836
10^5	6.98e+8	2.97e+9	1.21e+10	4.86e+10	3.2124	3.1906	3.2486	3.2671	3.2284	3.2340

Table 5.4: Condition number of the preconditioned and non-preconditioned system. Coefficients: $\beta = 1$, ν discontinuous. Discretization based on full polynomial DG space and second family edge elements for the auxiliary space. Pointwise Jacobi smoother.

Non-preconditioned system

	$\sharp\mathcal{T}_h$			
ν_1	2^5	2^7	2^9	2^{11}
10^{-5}	172	424	810	1598
10^{-3}	158	465	1281	3333
10^{-1}	199	619	1405	2777
1	144	374	760	1490
10^1	280	905	2073	3807
10^3	640	3732	12324	31630
10^5	1155	7091	27563	>50000

Preconditioned system

	$\sharp\mathcal{T}_h$						
ν_1	2^5	2^7	2^9	2^{11}	2^{13}	2^{15}	2^{17}
10^{-5}	27	33	31	22	16	11	9
10^{-3}	20	16	13	12	12	11	11
10^{-1}	13	13	12	12	12	11	11
1	12	12	12	11	11	11	10
10^1	12	12	12	12	11	11	11
10^3	13	15	13	12	12	12	12
10^5	14	15	14	14	14	13	13

Table 5.5: Number of iterations. Coefficients: $\beta = 1$, ν discontinuous. Discretization based on full polynomial DG space and second family edge elements for the auxiliary space. Pointwise Jacobi smoother.

5.5 Structured triangular mesh. Coefficients: β discontinuous, $\nu = 1$.

In this experiment, we assume the magnetic diffusivity to be $\nu = 1$, while the reaction coefficient β is discontinuous and piecewise constant, namely

$$\beta(\mathbf{x}) = \begin{cases} \beta_1 & \text{if } \mathbf{x} \in \Omega_1 := [0, 0.5]^2 \cup [0.5, 1]^2 \\ \beta_2 & \text{otherwise} \end{cases}$$

The coefficient $\beta_1 = 1$ is fixed. Lowest order rotated BDM elements (2.2) are used for both the DG discretization and the auxiliary space (3.5). The auxiliary space preconditioner uses here pointwise Jacobi smoother (4.9). Table 5.6 and Table 5.7 report the condition number and number of iterations as the coefficient β_1 varies.

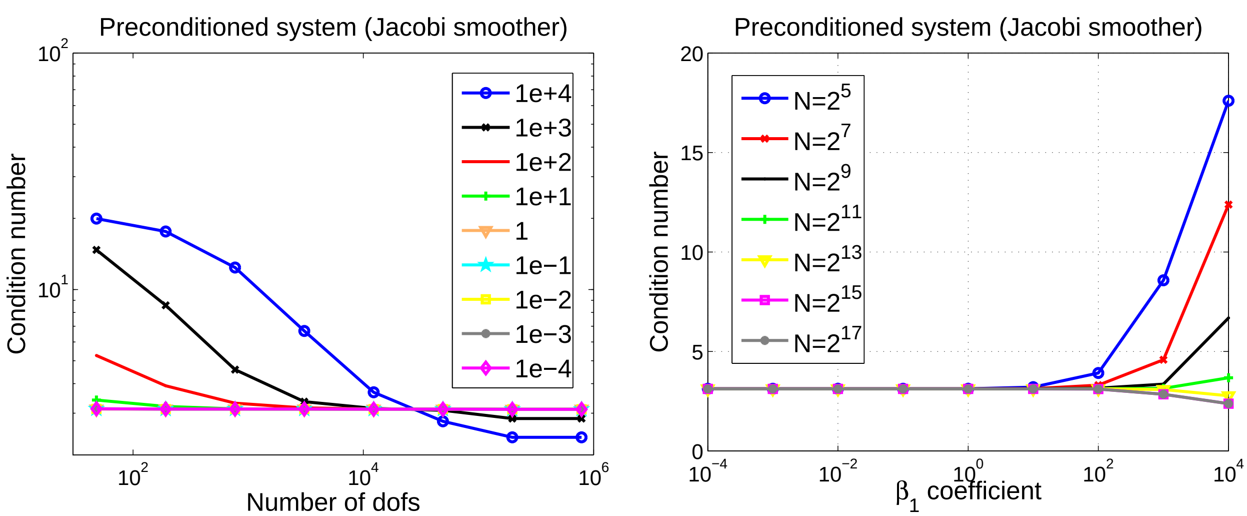

Figure 5.6: Condition number vs number of dofs for different values of the coefficient β (left). Condition number vs values of β for different mesh widths (right). Discretization based on full polynomial DG space and second family edge elements for the auxiliary space. Pointwise Jacobi smoother.

As it can be observed (see also Figure 5.6), the condition number of the preconditioned system is asymptotically independent both on the mesh width and on the magnitude of the jump of the coefficient

β. This is in agreement with Theorem 4.1 (and Remark 4.10) which predicts uniform convergence when only one of the two coefficients is allowed to vary.

Non-preconditioned system

	$\sharp\mathcal{T}_h$		
β_2	2^5	2^7	2^9
10^{-4}	5.45e+7	2.62e+8	1.11e+9
10^{-3}	5.45e+6	2.62e+7	1.11e+8
10^{-2}	5.46e+5	2.62e+6	1.11e+7
10^{-1}	5.47e+4	2.62e+5	1.12e+6
1	6.53e+3	2.79e+4	1.13e+5
10^1	5.53e+3	2.63e+4	1.12e+5
10^2	6.20e+3	2.71e+4	1.12e+5
10^3	1.58e+4	3.73e+4	1.23e+5
10^4	1.23e+5	1.62e+5	2.43e+5

Preconditioned system

	$\sharp\mathcal{T}_h$					
β_2	2^7	2^9	2^{11}	2^{13}	2^{15}	2^{17}
10^{-4}	3.1207	3.1209	3.1202	3.1200	3.1147	3.1147
10^{-3}	3.1207	3.1209	3.1202	3.1200	3.1147	3.1147
10^{-2}	3.1207	3.1209	3.1202	3.1200	3.1147	3.1147
10^{-1}	3.1207	3.1209	3.1202	3.1200	3.1147	3.1147
1	3.1205	3.1208	3.1202	3.1200	3.1197	3.1188
10^1	3.1271	3.1215	3.1201	3.1199	3.1146	3.1146
10^2	3.3061	3.1578	3.1274	3.1215	3.1115	3.1115
10^3	4.5832	3.3566	3.1415	3.0827	2.8449	2.8449
10^4	12.3839	6.6833	3.6772	2.7703	2.3719	2.3719

Table 5.6: Condition number of the preconditioned and non-preconditioned system. Coefficients: $\nu = 1$, β discontinuous. Discretization based on full polynomial DG space and second family edge elements for the auxiliary space. Pointwise Jacobi smoother.

Non-preconditioned system

	$\sharp\mathcal{T}_h$		
β_2	2^5	2^7	2^9
10^{-4}	284	2250	3685
10^{-3}	252	1980	4823
10^{-2}	305	1559	4048
10^{-1}	248	877	2003
1	144	374	760
10^1	173	570	1302
10^2	124	538	1254
10^3	116	356	751
10^4	121	340	555

Preconditioned system

	$\sharp\mathcal{T}_h$						
β_2	2^5	2^7	2^9	2^{11}	2^{13}	2^{15}	2^{17}
10^{-4}	12	12	12	11	11	10	10
10^{-3}	12	12	12	11	11	10	10
10^{-2}	12	12	12	11	11	10	10
10^{-1}	12	12	12	11	11	10	10
1	12	12	12	11	11	11	10
10^1	12	12	12	11	11	10	10
10^2	15	13	12	11	11	10	10
10^3	21	16	13	11	10	9	9
10^4	28	24	18	13	11	9	9

Table 5.7: Number of iterations. Coefficients: $\nu = 1$, β discontinuous. Discretization based on full polynomial DG space and second family edge elements for the auxiliary space. Pointwise Jacobi smoother.

5.6 Structured triangular mesh. Coefficients: β and ν discontinuous.

We now turn to the more interesting and challenging case of both β and ν discontinuous. Let $\Omega_1 := [0, 0.5]^2 \cup [0.5, 1]^2$, we define

$$\nu(\mathbf{x}) = \begin{cases} 10^{-4} & \text{if } \mathbf{x} \in \Omega_1 \\ 10^{-2} & \text{otherwise} \end{cases} \quad \text{and} \quad \beta(\mathbf{x}) = \begin{cases} 2^{\delta} \cdot 10^{-4} & \text{if } \mathbf{x} \in \Omega_1 \\ 2^{\delta} \cdot 10^{-2} & \text{otherwise} \end{cases} \tag{5.1}$$

where $\delta \in [-20, 45] \cap \mathbb{Z}$. For a given mesh with $\sharp\mathcal{T}_h = 512$ elements, we analyze the spectral condition number of the non-preconditioned and preconditioned system as the ratio

$$L(h, \nu, \beta) := h_T^2 \frac{\beta_T}{\nu_T} , \tag{5.2}$$

varies. Note that due to quasi-uniformity of the mesh and the choice of the coefficients in (5.1), the ratio $L(h, \nu, \beta)$ is constant on every $T \in \mathcal{T}_h$ and only depends on the parameter δ. For a discretization based on lowest order piecewise polynomials (2.2), we consider three different preconditioners: a single pointwise Jacobi as in (4.9), the ASM preconditioner based on the lowest order second kind edge elements for the auxiliary space (3.5) with pointwise Jacobi as smoother (4.9) and, as third case, the ASM preconditioner based on lowest order first kind edge elements for the auxiliary space (3.5) and overlapping additive Schwarz smoother (edge based) (3.14). As predicted by Proposition 4.9, when $L(h, \nu, \beta) > 1$, the auxiliary space is not needed to ensure uniform convergence with respect to both the problem coefficients and the mesh width (see Figure 5.7).

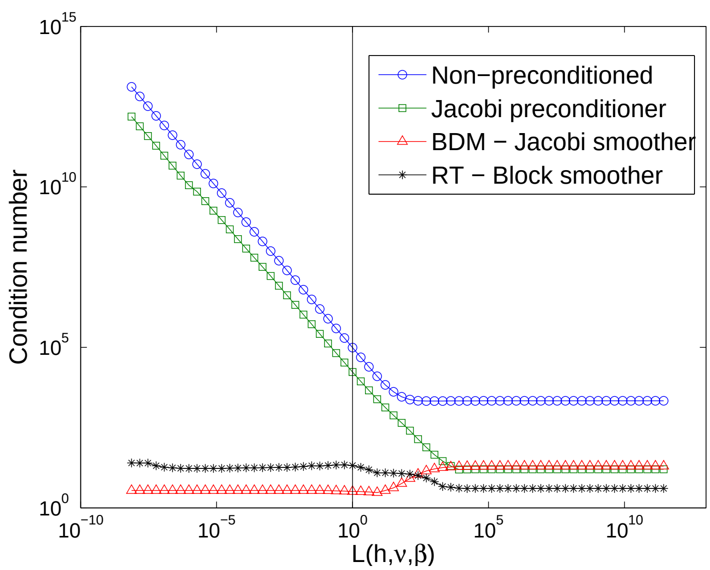

Figure 5.7: Condition number vs ratio L for a fixed mesh size h. The condition number refers to the non-preconditioned system (blue), the pointwise Jacobi preconditioner (green), the auxiliary space preconditioner based on lowest order rotated BDM elements with pointwise Jacobi smoother (red) and the auxiliary space preconditioner based on lowest order rotated RT elements with overlapping Schwarz smoother (black). Discretization: Lowest order rotated BDM elements.

5.6.1 Checkerboard Experiment

We consider an experiment where the distribution of the coefficients follows a checkerboard pattern according to the partition:

$$\Omega_1 := \bigcup_{i=0}^{3} [1/4i, 1/4(i+1)]^2 \cup \bigcup_{i=0}^{3} [1/4i, 1/4(i+1)] \times [1/4(i+2)\mathrm{mod}4, 1/4(i+2)\mathrm{mod}4 + 1/4],$$

as depicted in Figure 5.8 (white patches correspond to Ω_1). We define

$$\nu(\mathbf{x}) = \begin{cases} \nu_1 & \text{if } \mathbf{x} \in \Omega_1 \\ \nu_2 & \text{otherwise} \end{cases} \qquad \text{and} \qquad \beta(\mathbf{x}) = \begin{cases} \beta_1 & \text{if } \mathbf{x} \in \Omega_1 \\ \beta_2 & \text{otherwise} \end{cases}$$

where ν_1, ν_2, β_1 and β_2 are set to different values for the three experiments carried out; see Table 5.8.

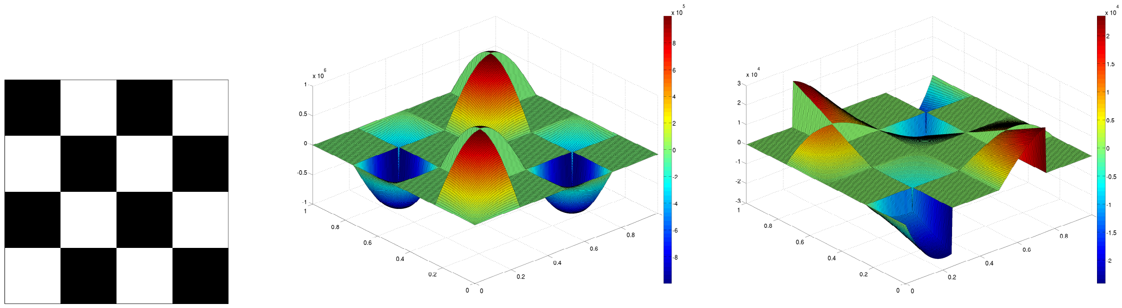

Figure 5.8: Components of the analytical vector-valued solution of the checkerboard experiment with $\nu_1 = 10^{-2}, \nu_2 = 10^4, \beta_1 = 10^3, \beta_2 = 1$.

Lowest order rotated BDM elements (2.2) are used in the DG discretization and also for the auxiliary space (3.5) in the ASM preconditioner together with a pointwise Jacobi smoother (4.9). In Figure 5.8 (center and rightmost) are represented the two components of the approximate solution. We note that the weak regularity of the solution leads to a significantly reduced convergence rate of the DG scheme. In Table 5.8 are given the estimated conditioned numbers and iterations required for convergence for the three different configurations of the coefficients. As can be observed in Table 5.8, the preconditioner significantly outperforms the non-preconditioned system even if a slight dependence of the jump of the coefficients might be recorded. Such slight dependence however seem to hinge on the possible transition from reaction dominated to curl dominated. Notice that the first and third cases reported in Table 5.8, correspond to cases where curl-dominated and reaction-dominated regimes alternate in the checkerboard pattern (for the first case the problem becomes curl-dominated in the whole domain for the two finest meshes), while the second case reported in Table 5.8 corresponds to the **curl**-dominated regime.

$\sharp\mathcal{T}_h$	2^7	2^9	2^{11}	2^{13}	2^{15}
	$\nu_1 = 10^{-2}, \quad \nu_2 = 10^4; \qquad \beta_1 = 10^3, \quad \beta_2 = 1$				
CG	2.45e+8 - (1881)	1.17e+9 - (7840)	5.00e+9 - (18899)	–	–
PCG	19.0353 - (28)	15.4283 - (30)	9.9327 - (26)	5.7309 - (19)	3.3871 - (14)
	$\nu_1 = 10^4, \quad \nu_2 = 10; \qquad \beta_1 = 10^{-2}, \quad \beta_2 = 10^{-4}$				
CG	2.45e+12 - (15275)	1.17e+13 - (>50000)	5.03e+13 - (>50000)	–	–
PCG	3.5079 - (13)	3.5062 - (13)	3.4686 - (13)	3.3397 - (13)	3.2869 - (16)
	$\nu_1 = 10^{-3}, \quad \nu_2 = 1; \qquad \beta_1 = 10^4, \quad \beta_2 = 10^2$				
CG	1.35e+3 - (148)	2.23e+3 - (228)	5.56e+3 - (363)	–	–
PCG	20.5140 - (28)	19.8753 - (30)	19.5633 - (30)	18.8764 - (29)	16.7841 - (28)

Table 5.8: Condition number and number of iterations for the checkerboard experiment. Condition number and number of iterations (in brackets). Discretization based on lowest order rotated BDM elements. Auxiliary space preconditioner based on lowest order edge element of the second family and pointwise Jacobi smoother.

6 Tensor product meshes

On tensor product meshes, we restrict to the case of continuous constant coefficients ν and β. As pointed out in Remark 4.18, on quadrilateral meshes a DG discretization of model problem (1.1) based on the full polynomial space of degree k in each variable, is not spectrally correct (see Figure 6.2). Therefore, a preconditioner built on an auxiliary space where the $\mathrm{H}_0(\mathbf{curl}, \Omega)$-conforming discretization is spectrally correct (e.g. Nédélec elements of the first family) is not effective, independently of the choice of the smoother and the amount of domain overlaps involved in its construction as it can be inferred from Figure 6.1. As alternative, piecewise polynomial approximation based on the rotated $\mathrm{H}(\mathbf{curl}, \Omega)$-conforming version of the following $\mathrm{H}(\mathbf{div}, \Omega)$-conforming elements [19, Section 2.4.2] and [9, Section 5]

$$S_{k+1} = \mathcal{RT}_k + \{\mathbf{curl} x^{k+2}y, \mathbf{curl} yx^{k+2}, \mathbf{curl} x^{k+2}, \mathbf{curl} y^{k+2}\} ;$$

$$\mathcal{ABF}_k = \mathbb{P}_{k+2,k} \times \mathbb{P}_{k,k+2} ;$$

have been implemented for $k = 0$ (recall that $\mathcal{RT}_k = \mathbb{P}_{k+1,k} \times \mathbb{P}_{k,k+1}$). Even in this case, a preconditioner based on lowest order rotated Raviart-Thomas elements on the auxiliary space performs poorly (see Table 6.1). In view of Theorem 4.1, the remedy seems to be relying on using the same local spaces for the discretization and for the $\mathrm{H}(\mathbf{curl}, \Omega)$-conforming auxiliary space. This can be easily checked in Figure 6.1 and Table 6.1 where are (also) reported the results obtained with DG discretizations based on local spaces of first family edge elements (corresponding to the elements in [19, Section 2.4.1]) and full polynomials space $\mathbb{Q}_k(T)^2$, preconditioned with auxiliary space built on the $\mathrm{H}(\mathbf{curl}, \Omega)$-conforming global elements of the same family in each case.

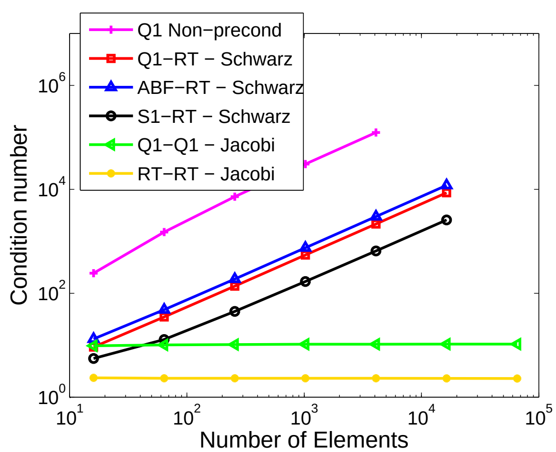

Figure 6.1: Condition number vs number of dofs for: non-preconditioned matrix from a piecewise bilinear Lagrangian elements discretization (pink), with auxiliary space preconditioner based on lowest order rotated RT elements with overlapping additive Schwarz smoother (red); same auxiliary space and smoother coupled with DG discretizations associated to $\mathcal{ABF}_0$ (blue) and S_1 (black); DG discretization with lowest order rotated RT discontinuous elements and Nédélec elements of the first family as auxiliary space with pointwise Jacobi smoother (yellow); discontinuous bilinear Lagrangian elements with $\mathrm{H}(\mathbf{curl}, \Omega)$-conforming full polynomial auxiliary space and Jacobi smoother (green).

$\sharp\mathcal{T}_h$	16×16	32×32	64×64	128×128	256×256
Q1 Non-prec	202	410	815	–	–
Q1-RT Jacobi	124	259	471	1622	2936
Q1-RT overlapping	34	61	113	202	337
ABF0-RT overlapping	32	59	116	230	458
S1-RT overlapping	19	22	28	39	57
Q1-Q1 Jacobi	22	22	21	20	19
RT-RT Jacobi	9	9	9	9	9

Table 6.1: Number of iterations for decreasing mesh width, for different discretization spaces and smoothers on a tensor product mesh.

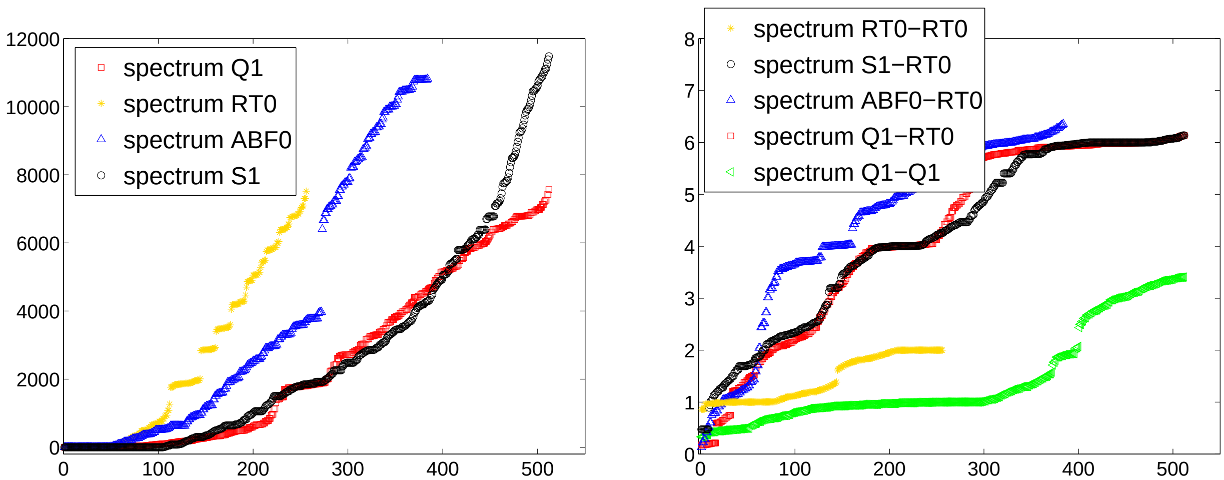

Figure 6.2: Spectrum of the non-preconditioned matrices obtained with different polynomial discretization (left) and spectrum of the corresponding preconditioning matrices (right), for different combinations as in Figure 6.1.

A Local estimates. Proof of Lemma 4.2

We first show (4.5) and (4.6). Taking into account the representation (2.5) of $\boldsymbol{v} \in \mathcal{M}(T)$ and since we use a contravariant transformation, the degrees of freedom of $\widehat{\boldsymbol{v}}$ coincide with those of $\boldsymbol{v}$ up to a sign change (see [74, pp. 79-80, Theorem 5.34]). Hence,

$$\sum_{\widehat{e}\in\mathcal{E}(\widehat{T})}\sum_{i=1}^{N_e}(\widehat{\boldsymbol{v}}^i_{\widehat{e},\widehat{T}})^2+\sum_{\widehat{f}\in\mathcal{F}(\widehat{T})}\sum_{i=1}^{N_f}(\widehat{\boldsymbol{v}}^i_{\widehat{f},\widehat{T}})^2+\sum_{i=1}^{N_b}(\widehat{\boldsymbol{v}}^i_{\widehat{T}})^2=\sum_{e\in\mathcal{E}(T)}\sum_{i=1}^{N_e}(\boldsymbol{v}^i_{e,T})^2+\sum_{f\in\mathcal{F}(T)}\sum_{i=1}^{N_f}(\boldsymbol{v}^i_{f,T})^2+\sum_{i=1}^{N_b}(\boldsymbol{v}^i_{T})^2\ . \quad (A.1)$$

On the other hand, a straightforward computation on the reference element $\widehat{T}$ and the above identity give

$$\begin{aligned}\|\widehat{\boldsymbol{v}}\|^2_{0,\widehat{T}} &\simeq \sum_{\widehat{e}\in\mathcal{E}(\widehat{T})}\sum_{i=1}^{N_e}(\widehat{\boldsymbol{v}}^i_{\widehat{e},\widehat{T}})^2\|\widehat{\boldsymbol{\varphi}}^i_{\widehat{e},\widehat{T}}\|^2_{0,\widehat{T}}+\sum_{\widehat{f}\in\mathcal{F}(\widehat{T})}\sum_{i=1}^{N_f}(\widehat{\boldsymbol{v}}^i_{\widehat{f},\widehat{T}})^2\|\widehat{\boldsymbol{\varphi}}^i_{\widehat{f},\widehat{T}}\|^2_{0,\widehat{T}}+\sum_{i=1}^{N_b}(\widehat{\boldsymbol{v}}^i_{\widehat{T}})^2\|\widehat{\boldsymbol{\varphi}}^i_{\widehat{T}}\|^2_{0,\widehat{T}}\\ &= \sum_{e\in\mathcal{E}(T)}\sum_{i=1}^{N_e}(\boldsymbol{v}^i_{e,T})^2+\sum_{f\in\mathcal{F}(T)}\sum_{i=1}^{N_f}(\boldsymbol{v}^i_{f,T})^2+\sum_{i=1}^{N_b}(\boldsymbol{v}^i_{T})^2\,.\end{aligned}$$

Furthermore, since on $\widehat{T}$ it holds $\|\widehat{\nabla}\times\widehat{\boldsymbol{v}}\|^2_{0,\widehat{T}}\le C\|\widehat{\boldsymbol{v}}\|^2_{0,\widehat{T}}$, then (4.5) follows.
In order to prove (4.6), we recall that, from the definition of the local spaces $\mathcal{M}(T)$, the tangential trace $\mathbf{n}\times\boldsymbol{v}$ on $f\subset\partial T$ is fully determined by the degrees of freedom of $\boldsymbol{v}$ on the edges and on the faces (see [74, Lemma 5.35]). Then, arguing as before and using (A.1) (with no volume degrees of freedom in the sums) yields (4.6) on the reference element.

The estimates in (4.2) and the inequalities (4.3) can be found in [19, Lemma 2.10] and [74, Section 3.9]. In particular, (4.3) ensues from

$$\boldsymbol{\nabla}\times\boldsymbol{v}(\mathbf{x}) = B_T^{-\mathsf{T}}\widehat{\boldsymbol{\nabla}}\times\widehat{\boldsymbol{v}}(F_T^{-1}(\mathbf{x}))B_T^{-1}$$

and the fact that the affine transformation F_T satisfies $\det(DF_T)=\det(B_T)\le Ch^3$ and $\|B_T^{-1}\|\le Ch_T^{-1}$ where $\|B_T^{-1}\|$ stands for the Euclidean matrix norm. The proof of the estimate (4.4) relies on scaling arguments, using that by means of the (affine) contravariant transformation F_T the unit normal $\widehat{\mathbf{n}}$ vector to $\widehat{f}$ is mapped to the unit normal $\mathbf{n}$ through $\mathbf{n}\circ F_T = B_T^{-\mathsf{T}}\widehat{\mathbf{n}}/|B_T^{-\mathsf{T}}\widehat{\mathbf{n}}|$.

B Proof of Lemma 4.12

Without loss of generality we can assume that T is an interior element, since the degrees of freedom on the boundaries of the domain can be bounded exactly as in Lemma 4.7. We proceed as in the proof of Lemma 4.7 but locally. Two cases have to be considered: first assume that $\mathcal{F}'(T) \neq \emptyset$ and $\mathcal{F}(T)\backslash\mathcal{F}'(T) \neq \emptyset$. In view of the Definition 4.11 of the operator $\overline{\mathcal{P}}_h$, by the inequalities (4.2) and (4.5),

$$\begin{aligned}
h_T^{-2}\alpha_T(\nu)\|\boldsymbol{v}-\overline{\mathcal{P}}_h(\boldsymbol{v})\|_{0,T}^2 &\leq C h_T h_T^{-2}\alpha_T(\nu)\Big(\sum_{f\in\mathcal{F}(T)}\left\|\boldsymbol{v}_{f,T}-\overline{\boldsymbol{\chi}}_f\right\|_{\ell^2}^2+\sum_{e\in\mathcal{E}(T)}\|\boldsymbol{v}_{e,T}-\overline{\boldsymbol{\chi}}_e\|_{\ell^2}^2\Big)\\
&\leq C h_T^{-1}\Big(\sum_{f\in\mathcal{F}(T)\backslash\mathcal{F}'(T)}\alpha_T(\nu)\left\|\boldsymbol{v}_{f,T}-\boldsymbol{\chi}_f\right\|_{\ell^2}^2+\sum_{f\in\mathcal{F}'(T)}\alpha_T(\nu)\left\|\boldsymbol{v}_{f,T}\right\|_{\ell^2}^2\\
&\quad+\sum_{f\in\mathcal{F}(T)\backslash\mathcal{F}'(T)}\sum_{e\in\mathcal{E}(f)}\alpha_T(\nu)\left\|\boldsymbol{v}_{e,T}-\boldsymbol{\chi}_e\right\|_{\ell^2}^2+\sum_{f\in\mathcal{F}'(T)}\sum_{e\in\mathcal{E}(f)}\alpha_T(\nu)\left\|\boldsymbol{v}_{e,T}\right\|_{\ell^2}^2\Big)\,.
\end{aligned}$$

We now estimate each of the contributions on the right hand side above separately. The degrees of freedom on the faces can be bounded as in (4.26) from Lemma 4.7:

$$\begin{aligned}
\sum_{f\in\mathcal{F}(T)\backslash\mathcal{F}'(T)}\alpha_T(\nu)\left\|\boldsymbol{v}_{f,T}-\boldsymbol{\chi}_f\right\|_{\ell^2}^2 &\leq \sum_{\substack{f\in\mathcal{F}(T)\backslash\mathcal{F}'(T)\\ f=\partial T\cap\partial T'}}\alpha_T(\nu)(\omega_{f,T'})^2\left\|\boldsymbol{v}_{f,T}-\boldsymbol{v}_{f,T'}\right\|_{\ell^2}^2\\
&\leq C\sum_{f\in\mathcal{F}(T)\backslash\mathcal{F}'(T)}\alpha_T(\nu)\left\|[\![\,\boldsymbol{v}\,]\!]_{\boldsymbol{\tau}}\right\|_{0,f}^2\,. \qquad \text{(B.1)}
\end{aligned}$$

The degrees of freedom corresponding to faces where the dofs of the conforming approximation have been set to zero are estimated by means of (4.7), (4.2) and (4.5) as

$$\begin{aligned}
\sum_{f\in\mathcal{F}'(T)}\alpha_T(\nu)\left\|\boldsymbol{v}_{f,T}\right\|_{\ell^2}^2 &\leq \sum_{\substack{f\in\mathcal{F}'(T)\\ f=\partial T\cap\partial T'}}2\alpha_T(\nu)\left\|\boldsymbol{v}_{f,T}-\boldsymbol{v}_{f,T'}\right\|_{\ell^2}^2+2\alpha_T(\nu)\left\|\boldsymbol{v}_{f,T'}\right\|_{\ell^2}^2\\
&\leq C\sum_{f\in\mathcal{F}'(T)}\alpha_T(\nu)\left\|[\![\,\boldsymbol{v}\,]\!]_{\boldsymbol{\tau}}\right\|_{0,f}^2+C\sum_{\substack{T'\in\mathcal{T}_h\\ \partial T\cap\partial T'\in\mathcal{F}'(T)}}\alpha_T(\nu)h_T^{-1}\left\|\boldsymbol{v}\right\|_{0,T'}^2\,. \qquad \text{(B.2)}
\end{aligned}$$

Analogously, the degrees of freedom corresponding to edges belonging to faces in $\mathcal{F}'(T)$ can be bounded as

$$\begin{aligned}
\sum_{f\in\mathcal{F}'(T)}\sum_{e\in\mathcal{E}(f)}\alpha_T(\nu)\left\|\boldsymbol{v}_{e,T}\right\|_{\ell^2}^2 &\leq \sum_{\substack{f\in\mathcal{F}'(T)\\ f=\partial T\cap\partial T'}}\sum_{e\in\mathcal{E}(f)}2\alpha_T(\nu)\left\|\boldsymbol{v}_{e,T}-\boldsymbol{v}_{e,T'}\right\|_{\ell^2}^2+2\alpha_T(\nu)\left\|\boldsymbol{v}_{e,T'}\right\|_{\ell^2}^2\\
&\leq C\sum_{f\in\mathcal{F}'(T)}\alpha_T(\nu)\left\|[\![\,\boldsymbol{v}\,]\!]_{\boldsymbol{\tau}}\right\|_{0,f}^2+C\sum_{\substack{T'\in\mathcal{T}_h\\ \partial T\cap\partial T'\in\mathcal{F}'(T)}}\alpha_T(\nu)h_T^{-1}\left\|\boldsymbol{v}\right\|_{0,T'}^2\,. \qquad \text{(B.3)}
\end{aligned}$$

Finally, the bound on the remaining edges can be derived as in (4.29) from Lemma 4.7,

$$\begin{aligned}
\sum_{f\in\mathcal{F}(T)\backslash\mathcal{F}'(T)}\sum_{e\in\mathcal{E}(f)}\alpha_T(\nu)\left\|\boldsymbol{v}_{e,T}-\boldsymbol{\chi}_e\right\|_{\ell^2}^2 &\leq \sum_{f\in\mathcal{F}(T)\backslash\mathcal{F}'(T)}\sum_{e\in\mathcal{E}(f)}\sum_{T_\ell\in\mathcal{T}(e)\backslash\{T\}}\alpha_T(\nu)(\omega_{e,T_\ell})^2\left\|\boldsymbol{v}_{e,T}-\boldsymbol{v}_{e,T_\ell}\right\|_{\ell^2}^2\\
&\leq C\sum_{f\in\mathcal{F}(T)\backslash\mathcal{F}'(T)}\sum_{e\in\mathcal{E}(f)}\sum_{f\in\mathcal{F}(e)}\alpha_T(\nu)\left\|[\![\,\boldsymbol{v}\,]\!]_{\boldsymbol{\tau}}\right\|_{0,f}^2\\
&\leq C\sum_{e\in\mathcal{E}(T)}\sum_{f\in\mathcal{F}(e)}\alpha_T(\nu)\left\|[\![\,\boldsymbol{v}\,]\!]_{\boldsymbol{\tau}}\right\|_{0,f}^2\,. \qquad \text{(B.4)}
\end{aligned}$$

Combining the estimates (B.1), (B.2), (B.3) and (B.4) results in

$$
\begin{aligned}
h_T^{-2}\alpha_T(\nu)\|\boldsymbol{v}-\overline{\mathcal{P}}_h(\boldsymbol{v})\|_{0,T}^2 \le C & \sum_{f\in\mathcal{F}(T)\setminus\mathcal{F}'(T)} \alpha_T(\nu)h_T^{-1}\,\|[\![\,\boldsymbol{v}\,]\!]_{\boldsymbol{\tau}}\|_{0,f}^2 + \sum_{f\in\mathcal{F}'(T)} \alpha_T(\nu)h_T^{-1}\,\|[\![\,\boldsymbol{v}\,]\!]_{\boldsymbol{\tau}}\|_{0,f}^2 \\
& + \sum_{\substack{T'\in\mathcal{T}_h\\ \partial T\cap\partial T'\in\mathcal{F}'(T)}} \alpha_T(\nu)h_T^{-2}\,\|\boldsymbol{v}\|_{0,T'}^2 + \sum_{e\in\mathcal{E}(T)}\sum_{f\in\mathcal{F}(e)} \alpha_T(\nu)h_T^{-1}\,\|[\![\,\boldsymbol{v}\,]\!]_{\boldsymbol{\tau}}\|_{0,f}^2 \\
\le C & \sum_{\substack{T'\in\mathcal{T}_h\\ \partial T\cap\partial T'\in\mathcal{F}'(T)}} \frac{\alpha_T(\nu)}{\alpha_{T'}(\nu)}\alpha_{T'}(\nu)h_T^{-2}\,\|\boldsymbol{v}\|_{0,T'}^2 + \sum_{e\in\mathcal{E}(T)}\sum_{f\in\mathcal{F}(e)} \alpha_T(\nu)h_T^{-1}\,\|[\![\,\boldsymbol{v}\,]\!]_{\boldsymbol{\tau}}\|_{0,f}^2 \,.
\end{aligned}
$$

Using the shape regularity of the mesh and the fact that $h_{T'}^{-2}\alpha_{T'}(\nu) < \beta_{T'}$ for all $T' \in \mathcal{T}_h$ with $\partial T\cap\partial T' \in \mathcal{F}'(T)$, yields (4.38).

For the case $\mathcal{F}'(T) \equiv \mathcal{F}(T)$, by Definition 4.11 of $\overline{\mathcal{P}}_h$, one has $\overline{\boldsymbol{\chi}}_e = 0$ for every $e \in \mathcal{E}(T)$, $\overline{\boldsymbol{\chi}}_f = 0$ for every $f \in \mathcal{F}(T)$ and $\overline{\boldsymbol{\chi}}_T = \boldsymbol{\chi}_T$. Therefore, the approximation error can be estimated as

$$
h_T^{-2}\alpha_T(\nu)\|\boldsymbol{v}-\overline{\mathcal{P}}_h(\boldsymbol{v})\|_{0,T}^2 \le Ch_T^{-1}\Bigg(\sum_{f\in\mathcal{F}(T)} \alpha_T(\nu)\,\|\boldsymbol{v}_{f,T}\|_{\ell^2}^2 + \sum_{e\in\mathcal{E}(T)} \alpha_T(\nu)\,\|\boldsymbol{v}_{e,T}\|_{\ell^2}^2\Bigg).
$$

For the degrees of freedom on the faces we use (B.2) whereas the degrees of freedom on the edges can be estimated through (B.3) with $\mathcal{F}'(T) \equiv \mathcal{F}(T)$. This results in

$$
\begin{aligned}
h_T^{-2}\alpha_T(\nu)\|\boldsymbol{v}-\overline{\mathcal{P}}_h(\boldsymbol{v})\|_{0,T}^2 &\le C \sum_{f\in\mathcal{F}(T)} \alpha_T(\nu)h_f^{-1}\,\|[\![\,\boldsymbol{v}\,]\!]_{\boldsymbol{\tau}}\|_{0,f}^2 + \sum_{\substack{T'\in\mathcal{T}_h\\ \partial T\cap\partial T'\in\mathcal{F}(T)}} h_T^{-2}\alpha_T(\nu)\,\|\boldsymbol{v}\|_{0,T'}^2 \\
&\le C \sum_{f\in\mathcal{F}(T)} \alpha_T(\nu)h_f^{-1}\,\|[\![\,\boldsymbol{v}\,]\!]_{\boldsymbol{\tau}}\|_{0,f}^2 + \sum_{\substack{T'\in\mathcal{T}_h\\ \partial T\cap\partial T'\in\mathcal{F}(T)}} \frac{\alpha_T(\nu)}{\alpha_{T'}(\nu)}h_T^{-2}\alpha_{T'}(\nu)\,\|\boldsymbol{v}\|_{0,T'}^2 \\
&\le C \sum_{f\in\mathcal{F}(T)} \alpha_T(\nu)h_f^{-1}\,\|[\![\,\boldsymbol{v}\,]\!]_{\boldsymbol{\tau}}\|_{0,f}^2 + \sum_{\substack{T'\in\mathcal{T}_h\\ \partial T\cap\partial T'\in\mathcal{F}(T)}} \frac{\alpha_T(\nu)}{\alpha_{T'}(\nu)}\beta_{T'}\,\|\boldsymbol{v}\|_{0,T'}^2 \,,
\end{aligned}
$$

where we have used again the fact that for all $T' \in \mathcal{T}_h$, $\partial T\cap\partial T' \in \mathcal{F}'(T)$, it holds $h_{T'}^{-2}\alpha_{T'}(\nu) < \beta_{T'}$.

C Proof of Lemma 4.13

Using the Definition 4.11 of the operator $\overline{\mathcal{P}}_h$, since $\mathcal{F}'(T) = \emptyset$, we have $\overline{\boldsymbol{\chi}}_f = \boldsymbol{\chi}_f$ for all $f \in \mathcal{F}(T)$. Therefore, using the representation in terms of degrees of freedom (2.5) together with (4.2) and (4.5) results in

$$
\begin{aligned}
h_T^{-2}\alpha_T(\nu)\|\boldsymbol{v}-\overline{\mathcal{P}}_h\boldsymbol{v}\|_{0,T}^2 &\le Ch_T^{-1}\Bigg(\sum_{f\in\mathcal{F}(T)} \alpha_T(\nu)\,\big\|\boldsymbol{v}_{f,T}-\overline{\boldsymbol{\chi}}_f\big\|_{\ell^2}^2 + \sum_{e\in\mathcal{E}(T)} \alpha_T(\nu)\,\|\boldsymbol{v}_{e,T}-\overline{\boldsymbol{\chi}}_e\|_{\ell^2}^2\Bigg) \\
&\le Ch_T^{-1}\Bigg(\sum_{f\in\mathcal{F}(T)} \alpha_T(\nu)\,\big\|\boldsymbol{v}_{f,T}-\boldsymbol{\chi}_f\big\|_{\ell^2}^2 + \sum_{e\in\mathcal{E}'(T)} \alpha_T(\nu)\,\|\boldsymbol{v}_{e,T}\|_{\ell^2}^2 \\
&\quad + \sum_{e\in\mathcal{E}(T)\setminus\mathcal{E}'(T)} \alpha_T(\nu)\,\|\boldsymbol{v}_{e,T}-\boldsymbol{\chi}_e\|_{\ell^2}^2\Bigg).
\end{aligned}
$$

Hence, the degrees of freedom on the faces can be bounded as in (4.26) in Lemma 4.7:

$$\sum_{f\in\mathcal{F}(T)} \alpha_T(\nu)\left\|\boldsymbol{v}_{f,T}-\boldsymbol{\chi}_f\right\|_{\ell^2}^2 \leq \sum_{\substack{f\in\mathcal{F}(T)\\ f=\partial T\cap\partial T'}} \alpha_T(\nu)(\omega_{f,T'})^2\left\|\boldsymbol{v}_{f,T}-\boldsymbol{v}_{f,T'}\right\|_{\ell^2}^2 \leq C\sum_{f\in\mathcal{F}(T)} \alpha_T(\nu)\left\|[\![\,\boldsymbol{v}\,]\!]_{\boldsymbol{\tau}}\right\|_{0,f}^2 . \tag{C.1}$$

Concerning the edges, the estimate (4.29) in Lemma 4.7 gives

$$\sum_{e\in\mathcal{E}(T)\backslash\mathcal{E}'(T)} \alpha_T(\nu)\left\|\boldsymbol{v}_{e,T}-\boldsymbol{\chi}_e\right\|_{\ell^2}^2 \leq C\sum_{e\in\mathcal{E}(T)\backslash\mathcal{E}'(T)}\sum_{f\in\mathcal{F}(e)} \alpha_T(\nu)\left\|[\![\,\boldsymbol{v}\,]\!]_{\boldsymbol{\tau}}\right\|_{0,f}^2 . \tag{C.2}$$

The degrees of freedom on the edges in $\mathcal{E}'(T)$ can be bounded using triangle inequality as follows. Let $e\in\mathcal{E}'(T)$ be fixed and let $T_k\in\mathcal{T}'(T)\cap\mathcal{T}(e)$. Let $\mathcal{T}(e)=\bigcup_{j=0}^{M_e}T_j$ be as in (4.28), with $T_0:=T$. Then,

$$\alpha_{T_0}(\nu)\left\|\boldsymbol{v}_{e,T_0}\right\|_{\ell^2}^2 \leq C\,\alpha_{T_0}(\nu)\left(\left\|\boldsymbol{v}_{e,T_0}-\boldsymbol{v}_{e,T_1}\right\|_{\ell^2}^2+\sum_{1\leq j<k}\left\|\boldsymbol{v}_{e,T_j}-\boldsymbol{v}_{e,T_{j+1}}\right\|_{\ell^2}^2+\left\|\boldsymbol{v}_{e,T_k}\right\|_{\ell^2}^2\right).$$

Hence,

$$\begin{aligned}\sum_{e\in\mathcal{E}'(T)} \alpha_T(\nu)\left\|\boldsymbol{v}_{e,T}\right\|_{\ell^2}^2 \leq C &\sum_{f\in\mathcal{F}(T)} \alpha_T(\nu)\left\|[\![\,\boldsymbol{v}\,]\!]_{\boldsymbol{\tau}}\right\|_{0,f}^2+\sum_{T'\in\mathcal{T}'(T)}\alpha_T(\nu)h_T^{-1}\left\|\boldsymbol{v}\right\|_{0,T'}^2\\ &+\sum_{e\in\mathcal{E}'(T)}\sum_{f\in\mathcal{F}(e)\backslash\mathcal{F}(T)}\alpha_T(\nu)\left\|[\![\,\boldsymbol{v}\,]\!]_{\boldsymbol{\tau}}\right\|_{0,f}^2 .\end{aligned} \tag{C.3}$$

Coupling (C.1), (C.2) and (C.3) yields

$$h_T^{-2}\alpha_T(\nu)\|\boldsymbol{v}-\overline{\mathcal{P}}_h\boldsymbol{v}\|_{0,T}^2 \leq C\sum_{T'\in\mathcal{T}'(T)}\frac{\alpha_T(\nu)}{\alpha_{T'}(\nu)}\alpha_{T'}(\nu)h_T^{-2}\left\|\boldsymbol{v}\right\|_{0,T'}^2+\sum_{e\in\mathcal{E}(T)}\sum_{f\in\mathcal{F}(e)}\alpha_T(\nu)h_T^{-1}\left\|[\![\,\boldsymbol{v}\,]\!]_{\boldsymbol{\tau}}\right\|_{0,f}^2 .$$

Using the fact that $h_{T'}^{-2}\alpha_{T'}(\nu)<\beta_{T'}$ for all $T'\in\mathcal{T}'(T)$ yields (4.40) and concludes the proof.

Acknowledgment. The first author was partially supported by KAUST grants BAS/1/1636 − 01 − 01 and Pocket ID 1000000193.

References

[1] S. Agmon. *Lectures on elliptic boundary value problems.* AMS Chelsea Publishing, Providence, RI, 2010.

[2] P. F. Antonietti and B. Ayuso. Schwarz domain decomposition preconditioners for discontinuous Galerkin approximations of elliptic problems: non-overlapping case. *Math. Model. Numer. Anal.*, 41(1):21–54, 2007.

[3] P. F. Antonietti and B. Ayuso. Multiplicative Schwarz methods for discontinuous Galerkin approximations of elliptic problems. *Math. Model. Numer. Anal.*, 42(3):443–469, 2008.

[4] P. F. Antonietti, B. Ayuso de Dios, S. Bertoluzza, and M. Penacchio. Substructuring preconditioners for an *h-p* domain decomposition method with Interior Penalty mortaring. *Calcolo*, to appear.

[5] P. F. Antonietti, B. Ayuso de Dios, S. C. Brenner, and L.-Y. Sung. Schwarz methods for a preconditioned WOPSIP method for elliptic problems. *Comput. Methods Appl. Math.*, 12(3):241–272, 2012.

[6] P. F. Antonietti and P. Houston. A class of domain decomposition preconditioners for *hp*-discontinuous Galerkin finite element methods. *J. Sci. Comput.*, 46(1):124–149, 2011.

[7] P. F. Antonietti, M. Sarti, and M. Verani. Multigrid algorithms for *hp*-discontinuous Galerkin discretizations of elliptic problems. *SIAM J. Numer. Anal.*, 53(1):598–618, 2015.

[8] D. N. Arnold. An interior penalty finite element method with discontinuous elements. *SIAM J. Numer. Anal.*, 19(4):742–760, 1982.

[9] D. N. Arnold, D. Boffi, and R. S. Falk. Quadrilateral $H(\mathrm{div})$ finite elements. *SIAM J. Numer. Anal.*, 42(6):2429–2451, 2005.

[10] D. N. Arnold, F. Brezzi, B. Cockburn, and L. D. Marini. Unified analysis of discontinuous Galerkin methods for elliptic problems. *SIAM J. Numer. Anal.*, 39(5):1749–1779, 2001/02.

[11] D. N. Arnold, R. S. Falk, and R. Winther. Multigrid in $H(\mathrm{div})$ and $H(\mathrm{curl})$. *Numer. Math.*, 85(2):197–217, 2000.

[12] B. Ayuso de Dios, F. Brezzi, L. D. Marini, J. Xu, and L. Zikatanov. A simple preconditioner for a discontinuous Galerkin method for the Stokes problem. *J. Sci. Comput.*, 58(3):517–547, 2014.

[13] B. Ayuso de Dios, I. Georgiev, J. Kraus, and L. Zikatanov. A subspace correction method for discontinuous Galerkin discretizations of linear elasticity equations. *ESAIM Math. Model. Numer. Anal.*, 47(5):1315–1333, 2013.

[14] B. Ayuso de Dios, M. Holst, Y. Zhu, and L. Zikatanov. Multilevel preconditioners for discontinuous, Galerkin approximations of elliptic problems, with jump coefficients. *Math. Comp.*, 83(287):1083–1120, 2014.

[15] B. Ayuso de Dios, A. Lombardi, P. Pietra, and L. Zikatanov. A block solver for the exponentially fitted IIPG-0 method. In *Domain decomposition methods in science and engineering XX*, volume 91 of *Lect. Notes Comput. Sci. Eng.*, pages 239–246. Springer, Heidelberg, 2013.

[16] B. Ayuso de Dios and L. Zikatanov. Uniformly convergent iterative methods for discontinuous Galerkin discretizations. *J. Sci. Comput.*, 40(1-3):4–36, 2009.

[17] G. A. Baker. Finite element methods for elliptic equations using nonconforming elements. *Math. Comp.*, 31(137):45–59, 1977.

[18] A. T. Barker, S. C. Brenner, E.-H. Park, and L.-Y. Sung. Two-level additive Schwarz preconditioners for a weakly over-penalized symmetric interior penalty method. *J. Sci. Comput.*, 47(1):27–49, 2011.

[19] D. Boffi, F. Brezzi, and M. Fortin. *Mixed finite element methods and applications*, volume 44 of *Springer Series in Computational Mathematics*. Springer, Heidelberg, 2013.

[20] D. Braess and W. Hackbusch. A new convergence proof for the multigrid method including the V-cycle. *SIAM J. Numer. Anal.*, 20(5):967–975, 1983.

[21] J. H. Bramble, J. E. Pasciak, and J. Xu. The analysis of multigrid algorithms with nonnested spaces or noninherited quadratic forms. *Math. Comp.*, 56(193):1–34, 1991.

[22] S. C. Brenner. Convergence of the multigrid V-cycle algorithm for second-order boundary value problems without full elliptic regularity. *Math. Comp.*, 71(238):507–525, 2002.

[23] S. C. Brenner, J. Cui, T. Gudi, and L.-Y. Sung. Multigrid algorithms for symmetric discontinuous Galerkin methods on graded meshes. *Numer. Math.*, 119(1):21–47, 2011.

[24] S. C. Brenner and L. Owens. A W-cycle algorithm for a weakly over-penalized interior penalty method. *Comput. Methods Appl. Mech. Engrg.*, 196(37-40):3823–3832, 2007.

[25] S. C. Brenner, E.-H. Park, and L.-Y. Sung. A balancing domain decomposition by constraints preconditioner for a weakly over-penalized symmetric interior penalty method. *Numer. Linear Algebra Appl.*, 20(3):472–491, 2013.

[26] S. C. Brenner and L.-Y. Sung. Multigrid algorithms for C^0 interior penalty methods. *SIAM J. Numer. Anal.*, 44(1):199–223, 2006.

[27] S. C. Brenner and K. Wang. Two-level additive Schwarz preconditioners for C^0 interior penalty methods. *Numer. Math.*, 102(2):231–255, 2005.

[28] S. C. Brenner and J. Zhao. Convergence of multigrid algorithms for interior penalty methods. *Appl. Numer. Anal. Comput. Math.*, 2(1):3–18, 2005.

[29] F. Brezzi, J. Douglas, Jr., and L. D. Marini. Two families of mixed finite elements for second order elliptic problems. *Numer. Math.*, 47(2):217–235, 1985.

[30] F. Brezzi, M. Fortin, and R. Stenberg. Error analysis of mixed-interpolated elements for Reissner-Mindlin plates. *Math. Models Methods Appl. Sci.*, 1(2):125–151, 1991.

[31] K. Brix, M. Campos Pinto, C. Canuto, and W. Dahmen. Multilevel preconditioning of discontinuous Galerkin spectral element methods. Part I: Geometrically conforming meshes. *IMA J. Numer. Anal.*, to appear.

[32] K. Brix, M. Campos Pinto, and W. Dahmen. A multilevel preconditioner for the interior penalty discontinuous Galerkin method. *SIAM J. Numer. Anal.*, 46(5):2742–2768, 2008.

[33] K. Brix, M. Campos Pinto, W. Dahmen, and R. Massjung. Multilevel preconditioners for the interior penalty discontinuous Galerkin method. II. Quantitative studies. *Commun. Comput. Phys.*, 5(2-4):296–325, 2009.

[34] A. Buffa, P. Houston, and I. Perugia. Discontinuous Galerkin computation of the Maxwell eigenvalues on simplicial meshes. *J. Comput. Appl. Math.*, 204(2):317–333, 2007.

[35] A. Buffa and I. Perugia. Discontinuous Galerkin approximation of the Maxwell eigenproblem. *SIAM J. Numer. Anal.*, 44(5):2198–2226 (electronic), 2006.

[36] C. Canuto, L. F. Pavarino, and A. B. Pieri. BDDC preconditioners for continuous and discontinuous Galerkin methods using spectral/*hp* elements with variable local polynomial degree. *IMA J. Numer. Anal.*, 34(3):879–903, 2014.

[37] E. T. Chung, H. H. Kim, and O. B. Widlund. Two-level overlapping Schwarz algorithms for a staggered discontinuous Galerkin method. *SIAM J. Numer. Anal.*, 51(1):47–67, 2013.

[38] P. G. Ciarlet. *The finite element method for elliptic problems.* North-Holland Publishing Co., Amsterdam, 1978. Studies in Mathematics and its Applications, Vol. 4.

[39] P. G. Ciarlet. Basic error estimates for elliptic problems. In *Handbook of numerical analysis, Vol. II*, Handb. Numer. Anal., II, pages 17–351. North-Holland, Amsterdam, 1991.

[40] B. Cockburn, O. Dubois, J. Gopalakrishnan, and S. Tan. Multigrid for an HDG method. *IMA J. Numer. Anal.*, 34(4):1386–1425, 2014.

[41] V. A. Dobrev, R. D. Lazarov, P. S. Vassilevski, and L. T. Zikatanov. Two-level preconditioning of discontinuous Galerkin approximations of second-order elliptic equations. *Numer. Linear Algebra Appl.*, 13(9):753–770, 2006.

[42] C. R. Dohrmann and O. B. Widlund. An iterative substructuring algorithm for two-dimensional problems in $H(\text{curl})$. *SIAM J. Numer. Anal.*, 50(3):1004–1028, 2012.

[43] C. R. Dohrmann and O. B. Widlund. FETI-DP method for DG discretization of elliptic problems with discontinuous coefficients. Technical report, Courant Institute, New York, 2014. Tech. Report submitted.

[44] M. Dryja. On discontinuous Galerkin methods for elliptic problems with discontinuous coefficients. *Comput. Methods Appl. Math.*, 3(1):76–85 (electronic), 2003.

[45] M. Dryja, J. Galvis, and M. Sarkis. BDDC methods for discontinuous Galerkin discretization of elliptic problems. *J. Complexity*, 23(4-6):715–739, 2007.

[46] M. Dryja, J. Galvis, and M. Sarkis. Neumann-Neumann methods for a DG discretization of elliptic problems with discontinuous coefficients on geometrically nonconforming substructures. *Numer. Methods Partial Differential Equations*, 28(4):1194–1226, 2012.

[47] M. Dryja, J. Galvis, and M. Sarkis. A FETI-DP preconditioner for a composite finite element and discontinuous Galerkin method. *SIAM J. Numer. Anal.*, 51(1):400–422, 2013.

[48] M. Dryja and O. B. Widlund. An additive variant of the Schwarz alternating method in the case of many subregions. Technical Report 339, Department of Computer Science, Courant Institute, New York, 1987.

[49] M. Dryja and O. B. Widlund. Domain decomposition algorithms with small overlap. *SIAM J. Sci. Comput.*, 15(3):604–620, 1994.

[50] X. Feng and O. A. Karakashian. Two-level additive Schwarz methods for a discontinuous Galerkin approximation of second order elliptic problems. *SIAM J. Numer. Anal.*, 39(4):1343–1365 (electronic), 2001.

[51] X. Feng and O. A. Karakashian. Two-level non-overlapping Schwarz preconditioners for a discontinuous Galerkin approximation of the biharmonic equation. *J. Sci. Comput.*, 22/23:289–314, 2005.

[52] G. H. Golub and C. F. Van Loan. *Matrix computations.* Johns Hopkins Studies in the Mathematical Sciences. Johns Hopkins University Press, Baltimore, MD, third edition, 1996.

[53] J. Gopalakrishnan and G. Kanschat. A multilevel discontinuous Galerkin method. *Numer. Math.*, 95(3):527–550, 2003.

[54] M. J. Grote, A. Schneebeli, and D. Schötzau. Interior penalty discontinuous Galerkin method for Maxwell's equations: energy norm error estimates. *J. Comput. Appl. Math.*, 204(2):375–386, 2007.

[55] M. J. Grote, A. Schneebeli, and D. Schötzau. Interior penalty discontinuous Galerkin method for Maxwell's equations: optimal L^2-norm error estimates. *IMA J. Numer. Anal.*, 28(3):440–468, 2008.

[56] H. Heumann, R. Hiptmair, and C. Pagliantini. Stabilized Galerkin for transient advection of differential forms. Technical Report 2015-06, Seminar for Applied Mathematics, ETH Zürich, Switzerland, 2015.

[57] R. Hiptmair. Multigrid method for Maxwell's equations. *SIAM J. Numer. Anal.*, 36(1):204–225, 1999.

[58] R. Hiptmair. Finite elements in computational electromagnetism. *Acta Numer.*, 11:237–339, 2002.

[59] R. Hiptmair. Analysis of multilevel methods for eddy current problems. *Math. Comp.*, 72(243):1281–1303, 2003.

[60] R. Hiptmair and A. Toselli. Overlapping and multilevel Schwarz methods for vector valued elliptic problems in three dimensions. In *Parallel solution of partial differential equations (Minneapolis, MN, 1997)*, volume 120 of *IMA Vol. Math. Appl.*, pages 181–208. Springer, New York, 2000.

[61] R. Hiptmair, G. Widmer, and J. Zou. Auxiliary space preconditioning in $H_0(\mathrm{curl};\ \Omega)$. *Numer. Math.*, 103(3):435–459, 2006.

[62] R. Hiptmair and J. Xu. Nodal auxiliary space preconditioning in $\mathbf{H}(\mathbf{curl})$ and $\mathbf{H}(\mathrm{div})$ spaces. *SIAM J. Numer. Anal.*, 45(6):2483–2509 (electronic), 2007.

[63] R. Hiptmair and W.-Y. Zheng. Local multigrid in $\mathbf{H}(\mathbf{curl})$. *J. Comput. Math.*, 27(5):573–603, 2009.

[64] P. Houston, I. Perugia, A. Schneebeli, and D. Schötzau. Interior penalty method for the indefinite time-harmonic Maxwell equations. *Numer. Math.*, 100(3):485–518, 2005.

[65] P. Houston, I. Perugia, and D. Schötzau. Energy norm a posteriori error estimation for mixed discontinuous Galerkin approximations of the Maxwell operator. *Comput. Methods Appl. Mech. Engrg.*, 194(2-5):499–510, 2005.

[66] P. Houston, I. Perugia, and D. Schötzau. An a posteriori error indicator for discontinuous Galerkin discretizations of $H(\mathrm{curl})$-elliptic partial differential equations. *IMA J. Numer. Anal.*, 27(1):122–150, 2007.

[67] Q. Hu, S. Shu, and J. Zou. A mortar edge element method with nearly optimal convergence for three-dimensional Maxwell's equations. *Math. Comp.*, 77(263):1333–1353, 2008.

[68] Q. Hu, S. Shu, and J. Zou. A discrete weighted Helmholtz decomposition and its application. *Numer. Math.*, 125(1):153–189, 2013.

[69] Q. Hu and J. Zou. A nonoverlapping domain decomposition method for Maxwell's equations in three dimensions. *SIAM J. Numer. Anal.*, 41(5):1682–1708, 2003.

[70] Q. Hu and J. Zou. Substructuring preconditioners for saddle-point problems arising from Maxwell's equations in three dimensions. *Math. Comp.*, 73(245):35–61, 2004.

[71] O. A. Karakashian and F. Pascal. A posteriori error estimates for a discontinuous Galerkin approximation of second-order elliptic problems. *SIAM J. Numer. Anal.*, 41(6):2374–2399 (electronic), 2003.

[72] T. V. Kolev, J. Xu, and Y. Zhu. Multilevel preconditioners for reaction-diffusion problems with discontinuous coefficients. Technical report, 2014. arXiv:1411.7092.

[73] J. K. Kraus and S. K. Tomar. Multilevel preconditioning of two-dimensional elliptic problems discretized by a class of discontinuous Galerkin methods. *SIAM J. Sci. Comput.*, 30(2):684–706, 2008.

[74] P. Monk. *Finite element methods for Maxwell's equations*. Numerical Mathematics and Scientific Computation. Oxford University Press, New York, 2003.

[75] J.-C. Nédélec. Mixed finite elements in $\mathbf{R}^3$. *Numer. Math.*, 35(3):315–341, 1980.

[76] S. V. Nepomnyaschikh. Mesh theorems on traces, normalizations of function traces and their inversion. *Soviet J. Numer. Anal. Math. Modelling*, 6(3):223–242, 1991.

[77] P. Oswald. Preconditioners for nonconforming discretizations. *Math. Comp.*, 65(215):923–941, 1996.

[78] I. Perugia and D. Schötzau. The *hp*-local discontinuous Galerkin method for low-frequency time-harmonic Maxwell equations. *Math. Comp.*, 72(243):1179–1214, 2003.

[79] F. Rapetti and A. Toselli. A FETI preconditioner for two-dimensional edge element approximations of Maxwell's equations on nonmatching grids. *SIAM J. Sci. Comput.*, 23(1):92–108, 2001.

[80] P.-A. Raviart and J. M. Thomas. A mixed finite element method for 2nd order elliptic problems. In *Mathematical aspects of finite element methods*, pages 292–315. Lecture Notes in Math., Vol. 606. Springer, Berlin, 1977.

[81] J. Schöberl and Ch. Lehrenfeld. Domain decomposition preconditioning for high order hybrid discontinuous Galerkin methods on tetrahedral meshes. In *Advanced finite element methods and applications*, volume 66 of *Lect. Notes Appl. Comput. Mech.*, pages 27–56. Springer, Heidelberg, 2013.

[82] B. F. Smith, P. E. Bjørstad, and W. D. Gropp. *Domain decomposition*. Cambridge University Press, Cambridge, 1996.

[83] A. Toselli. Neumann-Neumann methods for vector field problems. *Electron. Trans. Numer. Anal.*, 11:1–24, 2000.

[84] A. Toselli. Overlapping Schwarz methods for Maxwell's equations in three dimensions. *Numer. Math.*, 86(4):733–752, 2000.

[85] A. Toselli. Dual-primal FETI algorithms for edge finite-element approximations in 3D. *IMA J. Numer. Anal.*, 26(1):96–130, 2006.

[86] A. Toselli and X. Vasseur. Dual-primal FETI algorithms for edge element approximations: two-dimensional H and P finite elements on shape-regular meshes. *SIAM J. Numer. Anal.*, 42(6):2590–2611, 2005.

[87] A. Toselli and O. B. Widlund. *Domain decomposition methods—algorithms and theory*, volume 34 of *Springer Series in Computational Mathematics*. Springer-Verlag, Berlin, 2005.

[88] A. Toselli, O. B. Widlund, and B. I. Wohlmuth. An iterative substructuring method for Maxwell's equations in two dimensions. *Math. Comp.*, 70(235):935–949, 2001.

[89] M. F. Wheeler. An elliptic collocation-finite element method with interior penalties. *SIAM J. Numer. Anal.*, 15(1):152–161, 1978.

[90] J. Xu. Iterative methods by space decomposition and subspace correction. *SIAM Rev.*, 34(4):581–613, 1992.

[91] J. Xu. The auxiliary space method and optimal multigrid preconditioning techniques for unstructured grids. *Computing*, 56(3):215–235, 1996. International GAMM-Workshop on Multi-level Methods (Meisdorf, 1994).

[92] L. T. Zikatanov. Two-sided bounds on the convergence rate of two-level methods. *Numer. Linear Algebra Appl.*, 15(5):439–454, 2008.